Model Based Design of Functional Polymer Materials by Initiators for Continuous Activator Regeneration Atom Transfer Radical Polymerization (ICAR ATRP)

Modelgebaseerd ontwerp van functionele polymeermaterialen via initiatoren-voor-continue-activatorregeneratie-atoomtransfer-radicalaire-polymerisatie (ICAR ATRP)

Carolina de los Angeles Toloza Porras

Promotoren: prof. dr. ir. G. B. Marin, prof. dr. M.-F. Reyniers
Proefschrift ingediend tot het behalen van de graad van
Doctor in de Ingenieurswetenschappen: Chemische Technologie

Vakgroep Chemische Proceskunde en Technische Chemie
Voorzitter: prof. dr. ir. G. B. Marin
Faculteit Ingenieurswetenschappen en Architectuur
Academiejaar 2012 - 2013

UNIVERSITEIT GENT

ISBN 978-90-8578-578-1
NUR 952
Wettelijk depot: D/2013/10.500/11

BEGELEIDINGSCOMMISSIE

Promotoren

prof. dr. Marie-Françoise Reyniers
Laboratorium voor Chemische Technologie
Vakgroep Chemische Proceskunde en Technische Chemie
Universiteit Gent

prof. dr. ir. Guy B. Marin
Laboratorium voor Chemische Technologie
Vakgroep Chemische Proceskunde en Technische Chemie
Universiteit Gent

Universiteit Gent
Vakgroep Chemische Proceskunde en Technische Chemie
Laboratorium voor Chemische Technologie

Technologiepark 918/Krijgslaan 281 S5
9000 Gent
België

De auteur genoot tijdens de onderzoeksactiviteiten de steun van de langdurige en structurele *Methusalem* financiering van de Vlaamse Overheid [BOF09/01M00409] en dit onderzoek werd uitgevoerd in het kader van het project “Modelgebaseerde optimalisatie en controle voor procesintensificatie in chemische en biofarmaceutische systemen (*OPTICO*/ G.A. No. 280813) gefinancierd door de Europese Commissie.

EXAMENCOMMISSIE

Leescommissie

prof. dr. Richard Hoogenboom
Supramolecular Chemistry Group
Vakgroep Organische Chemie
Universiteit Gent

prof. dr. Robin A. Hutchinson
Department of Chemical Engineering
Faculty of Engineering and Applied Science
Queen's University

dr. ir. Dagmar D'hooge [secretaris]
Laboratorium voor Chemische Technologie
Vakgroep Chemische Proceskunde en Technische Chemie
Universiteit Gent

Andere leden

prof. dr. ir. Guy B. Marin [promotor]
Laboratorium voor Chemische Technologie
Vakgroep Chemische Proceskunde en Technische Chemie
Universiteit Gent

prof. dr. Marie-Françoise Reyniers [promotor]
Laboratorium voor Chemische Technologie
Vakgroep Chemische Proceskunde en Technische Chemie
Universiteit Gent

prof. dr. Olivier Coulembier
Laboratory of Polymeric and Composite Materials
University of Mons

prof. dr. Thomas Junkers
Instituut voor Materiaalonderzoek
Universiteit Hasselt

prof. dr. ir. Hendrik Van Landeghem [voorzitter]
Vakgroep Technische Bedrijfsvoering
Universiteit Gent

Contents

Preface

I would like to thank:

Prof. M.-F. Reyniers and Prof. G.B. Marin, my supervisors, for their excellent guidance,

Prof. R. Hoogenboom, Prof. R. A. Hutchinson, Prof. O. Coulembier, Prof. T. Junkers, Dr. D. D'hooge, and Prof. H.Van Landeghem as jury members,

Dr. D. D'hooge for his excellent guidance, greatly appreciated help, and unforgettable discussions,

all LCT colleagues, specially:

Paul Van Steenberge for being an excellent colleague and contributing substantially to my research,

Pieter Derboven for remarkable discussions and significant collaboration,

Gaoping Xue for being my brother in Belgium,

William Scott, Unmesh Menon, Evgeniy Redekop, Ionel Craciun, Chetan Shreedhar Raghuveer, Luis Lozano Guerra and all the colleagues at LCT, for creating a perfect atmosphere in Belgium and for their support,

Marcel Vervust, Hans Heene, Petra Vereecken, Kim Verbeeck, Georges Verenghen, for his greatly appreciated help and technical support,

all members of the IAP/UAP/PAI network,

the 'Long Term Structural Methusalem Funding by the Flemish Government' (BOF09/01M00409) and the project 'Model-Based Optimization & Control for Process-Intensification in Chemical and Biopharmaceutical Systems' (OPTICO/ G.A. No. 280813) funded by the European Commission, for financial support,

Stefaan and Yolanda Vandewalle for supporting me and welcoming me in Belgium,

Jhon Muñoz for being my better half,

Jose Raul Toloza and Maria Stella Porras, my parents, for their support and love,

Nidia Toloza, Jason Toloza, Javier Toloza, my sister and brothers for not allowing me to abandon the boat in the middle of the storm,

Milton Guerrero, Jenny Morales and Milena Gómez, as a very special part of my family

my nephews and nieces for being my continuous inspiration,

my dearest friends and you for reading this.

Carolina Toloza Porras

February 2012

Nederlandse samenvatting

Eén van de meest belangrijke polymerisatieprocessen is conventionele radicalaire polymerisatie (FRP) wat momenteel wordt aangewend voor de industriële productie van verscheidene (co)polymeren die toegepast worden voor de productie van filmen, vezels, verf, elastomeren en huishoudproducten, … Verschillende nieuwe toepassingen, zoals deklagen, adhesieven, thermoplastische elastomeren, elektronica, zouden echter kunnen verkregen worden indienen de microstructuur van het polymeer beter zou kunnen worden gemodificeerd. Deze gemodificeerde polymeren, die gekarakteriseerd zijn door unieke eigenschappen en een complexe architectuur, kunnen worden gesynthetiseerd met behulp van zogenaamde gecontroleerde radicalaire polymerisatie (CRP).

In CRP, wordt een controlerend agens toegevoegd dat macroradicalen kan vangen en in een “slapende” toestand kan brengen. Deze “slapende” toestand is gekenmerkt door de aanwezigheid van eindgroepfunctionaliteit in de polymeerketen. Daar dit vangproces dominant is, kan de radicaalconcentratie significant worden verminderd wat een gecontroleerde groei toelaat en het minimaliseren van terminatiereacties die aanleiding geven tot de ongewenste vorming van dode polymeermoleculen. Eén van de meest belangrijke en meest verspreide CRP-technieken is atoom-transfer radicalaire polymerisatie (ATRP), wat het onderwerp is van dit proefschrift.

De ATRP-techniek kan worden toegepast om een breed bereik aan monomeren te polymeriseren met een gecontroleerde ketenlengte en functionaliteit. ATPR is een katalytisch proces waarin een transitiemetaalcomplex in twee oxidatietoestanden (activator/deactivator) en een alkyl halogenide as ATRP initiator optreden. Typisch werd één katalysatormolecule aangewend per ATRP initiator molecule zodat alle (slapende) polymeerketens gelijkmatig kunnen deelnemen aan activering-groei-deactivering cycli en controle over ketenlengte en functionaliteit kan worden verkregen. In de praktijk resulteert dit in ATRP katalysatorhoeveelheden in de orde

van 10000 ppm (met betrekking met monomeer) wat belangrijke nadelen impliceert voor de ATRP-techniek in vergelijking met andere CRP's.

In de laatste jaren werd een belangrijke voortuitgang geboekt in ATRP-onderzoek met betrekking tot zogenaamde ATRP-gemodificeerde technieken waarin een substantiële reductie van de hoeveelheid katalysator wordt verkregen dankzij een continue in-situ (re)generatie. Tot op heden werd aangetoond dat waarden zo laag als 50 ppm kunnen worden gehanteerd zonder dat de controle over de ATRP wordt beïnvloed. Daarenboven kan de polymerisatie uitgevoerd worden onder de aanwezigheid van een beperkte hoeveelheid aan zuurstof gezien deze technieken initieel enkel deactivator toevoegen aan het reactiemengsel in tegenstelling tot normale ATRP-processen, waarin de polymerisatie wordt aangevangen met activator. Tevens resulteert een veel snellere polymerisatie wat de industriële aantrekkelijkheid van ICAR ATRP verder aangeeft.

Initiatoren voor continue activator regeneratie atoom-transfer radicalaire polymerisatie (ICAR ATRP) is naar voren getreden als een van deze gemodificeerde ATRP-technieken. In ICAR ATRP, wordt een conventionele radicalaire initiator aangewend als bron voor radicalen die deactivatormoleculen kunnen reduceren zodat activatormoleculen kunnen worden gegenereerd. Deze radicalen nemen ook deel aan propagatie zodat de polymerisatie versneld wordt. In dit proefschrift, wordt het potentieel van ICAR ATRP onderzocht voor homo- (Hoofdstuk 2-3) en blokcopolymerisatie (Hoofdstuk 4) van styreen en acrylaatmonomeren. Verder wordt aangetoond dat deze techniek geschikt is voor het bepalen van relevante intrinsiek kinetische parameters voor het activering/deactivering-proces (Hoofdstuk 2-3).

De ICAR ATRP van styreen (Hoofdstuk 2) met $CuBr_2$/TPMA (TPMA: tris(2-pyridylmethyl)amine) als deactivator is experimenteel geëvalueerd uitgaand van een significant bereik aan beoogde gemiddelde ketenlengtes bij finale conversie (50-500), koper-gebaseerde deactivator hoeveelheden (5-250 ppm) en polymerisatietemperaturen (60-80°C). Daarnaast wordt een deterministisch kinetisch model aangewend voor het beschrijven van de experimentele data en dit enkel voor conversies lager dan 50% zodanig dat diffusielimiteringen enkel op terminatie dienen

in rekening te worden gebracht. Een goede beschrijving van de experimentele trends is verkregen wat toelaat relevante Arrheniusparameters te bepalen voor het activering/deactivering-proces in ATRP. De simulaties bevestigen de relatief hoge activiteit van de geselecteerde katalysator en tonen aan dat koperhoeveelheden lager dan 10 ppm dienen vermeden te worden indien een goed controle over de ketenlengte dient verkregen te worden.

In Hoofdstuk 3, wordt de polymerisatie van *n*-butyl acrylaat, waarbij secondaire en tertiaire species betrokken zijn via intramoleculaire waterstof-abstractie, grondig geanalyseerd gebruik makend van zowel normale als ICAR ATRP en $CuBr_2$/PMDETA (PMDETA: N,N,N′,N″,N″-pentamethyldiethyleentriamine) als deactivator. Eerst worden activering/deactivering intrinsieke snelheidscoëfficiënten voor secondaire en tertiaire species bepaald uitgaand van data verkregen bij 105°C, zoals gerapporteerd in de literatuur voor normale ATRP inclusief metingen van de hoeveelheid aan korte keten vertakkingen. De simulatieresultaten verkregen voor het ICAR ATRP proces laten het in kaart brengen van de correlatie tussen polymerisatietijd, control over ketenlengte en levend karakter toe als een functie van de hoeveelheid koper en de beoogde ketenlengte bij een welbepaalde conversie. De simulatieresultaten bevestigen de hogere stabiliteit van tertiaire macrospecies daar zij sneller gevormd worden door activering en minder snel verdwijnen door deactivering. Eveneens wordt aangetoond dat acrylaten toelaten ATRPs uit te voeren met een beperkt verlies aan eindgroepfunctionaliteit wat belangrijk is voor de synthese van meer complexe architecturen. Voor voldoende hoge ketenlengtes (>500) kan een succesvolle ICAR ATRPs uitgevoerd worden met ppm waarden zo laag als 50 ppm.

Gebaseerd op de inzichten verkregen voor de homopolymerisaties in Hoofdstuk 2 en 3, wordt in Hoofdstuk 4 the productie van blokcopolymeren bestaande uit isobornyl acrylaat en styreen theoretisch bestudeerd met de ICAR ATRP-techniek gebruik makend van $CuBr_2$/PMDETA als deactivator. Zowel “één-pot” als “twee-pot” procedures worden beschouwd. De invloed van de polymerisatietemperatuur en de initiële hoeveelheid koperhoeveelheid is geanalyseerd in detail. Arrheniusparameters uit de literatuur worden gebruikt voor deze studie en een kinetisch Monte Carlo model

is aangewend voor het berekenen van de expliciete samenstelling van de polymeerketens. Deze expliciete berekening laat in het bijzonder een uitgebreide vergelijking toe van de beide procedures in het licht van de optimalisatie van ICAR ATRP voor de synthese van goed gedefinieerde blokcopolymeren. De simulaties tonen aan dat het zorgvuldig kiezen van de polymerisatiecondities toelaat het belang van ongewenste homopolymeerketens bestaande uit het tweede monomeer en triblokcopolymeerketens te onderdrukken. Er wordt eveneens aangetoond dat de “een-pot” procedure meer geschikt is voor een zelfde globaal gehalte aan koper daar het een snellere polymerisatie toelaat en de diblokkwaliteit van de verkregen structuren even hoog is. Tevens kunnen met deze procedure lagere gehaltes aan koper aangewend worden alvorens een significant verlies aan control optreedt.

Finaal worden in Hoofdstuk 5 de meest belangrijke conclusies van de voorbije hoofdstukken hernomen en toekomstige perspectieven voor onderzoek geformuleerd. Aandacht wordt zowel besteed aan de ICAR ATRP als andere CRP technieken.

English summary

One of the most important polymerization processes is conventional free radical polymerization (FRP), which is currently used for the industrial production of several (co)polymers employed in the fabrication of plastic films, fibers, paints, elastomers, and household goods. However, several new applications, such as coatings, adhesives, thermoplastic elastomers, electronics, and drug delivery could benefit from an appropriate tuning of the polymer microstructure. These “manipulated polymers”, which are characterized by unique properties and complex architectures, can be synthesized via so-called controlled radical polymerization (CRP) techniques.

In CRP, a mediating agent is utilized in order to trap macroradicals into a dormant state, which is characterized by end-group functionality being present in the polymer chain. Since this trapping process is dominant, the macroradical concentration is significantly diminished allowing the controlled growth of the polymer chains and the minimization of termination reactions that lead to unwanted dead polymer. One of the most important and widely used CRPs is atom transfer radical polymerization (ATRP), which is the subject of this PhD thesis.

The ATRP technique has been applied to (co)polymerize a broad range of monomers with controlled chain length and functionality. ATRP is a catalytic process involving a transition metal complex in two oxidation states (activator/deactivator) and an alkyl halide as ATRP initiator. Commonly, one molecule of catalyst is employed per molecule of ATRP initiator, so that all the dormant polymer/macroradical chains can be effectively activated/deactivated and control over chain length and functionality can be achieved. In practice, this means ATRP catalyst concentrations in the order of 10000 ppm (with respect to the monomer), which implies important disadvantages for the ATRP technique, as compared with other CRPs.

In the last years, important advances in ATRP research have led to the development of ATRP modified techniques, in which a substantial reduction of the catalyst

concentration is possible thanks to its continuous in-situ (re)generation. Up to now, it has been demonstrated that values as low as 50 ppm can be employed without affecting significantly the control provided by ATRP. Moreover, due to the low concentration of deactivator that is employed in these modified ATRP techniques and because of the initial absence of activator, the polymerization can be performed in the presence of limited amounts of oxygen, in contrast to the normal ATRP process in which the low oxidation state of the transition metal complex (activator) is used as starting material. Moreover, for ICAR ATRP the polymerization rate is much higher making this technique more suitable for industrial application.

Initiators for continuous activator regeneration atom transfer radical polymerization (ICAR ATRP) has recently emerged as one of the mentioned modified ATRP techniques. In ICAR ATRP, a conventional radical initiator is employed as source of radical species that can reduce deactivator molecules to (re)generate activator molecules. These radicals participate also in propagation steps, enhancing therefore the rate of polymerization. In this PhD thesis, the potential of the ICAR ATRP technique is explored for homo- (Chapter 2-3) and block copolymerizations (Chapter 4) of styrene and acrylate monomers. Furthermore, it is demonstrated that this technique is suitable for the determination of relevant intrinsic kinetic parameters related to the activation/deactivation process in ATRP (Chapter 2-3). It is shown that to ensure a good control over chain length ppm levels higher than 10 should be selected.

The ICAR ATRP of styrene using $CuBr_2$/TPMA (TPMA: tris(2-pyridylmethyl)amine) as deactivator (Chapter 2) is experimentally evaluated covering a significant range of targeted chain lengths (50-500), Cu-based deactivator concentrations (5-250 ppm) and polymerization temperatures(60-80°C). Next to that, a deterministic kinetic model is applied to describe the experimental findings. The trends are well-captured by the kinetic model, facilitating an initial assessment of the relevant Arrhenius parameters for the activation/deactivation determining steps in the ATRP. It is confirmed that the selected catalyst can be seen as moderately active.

In Chapter 3, the polymerization of *n*-butyl acrylate (*n*BuA), which involves secondary and tertiary species formed via backbiting reactions, is thoroughly analyzed using

normal and ICAR ATRP techniques and $CuBr_2$/PMDETA (PMDETA: N,N,N′,N″,N″-pentamethyldiethylenetriamine) as deactivator. First, an initial assessment of the activation/deactivation intrinsic parameters for secondary and tertiary species is performed based on the description of a set of experimental data at 105 °C. These data were taken from a study of normal ATRP reported in literature, which included measurement of the branching content via proton nuclear magnetic resonance spectroscopy, ^{1}H NMR. The simulation results obtained for the ICAR ATRP permit an interesting mapping of polymerization time and the control over chain length and livingness as a function of the Cu ppm levels and the selected TCL. It is shown that ATRPs conducted with acrylates allow to obtain a high livingness which is required for the successful synthesis of more complex molecular architectures, such as gradient, star, graft, and block copolymers. In addition, it is demonstrated that for sufficiently high targeted chain lengths (> 500) Cu ppm levels as low as 50 can be used while obtaining a good control over the ICAR ATRP process.

Based on the insights obtained for the homopolymerizations shown in Chapter 2 and 3, the production of block copolymers made from isobornyl acrylate and styrene by ICAR ATRP is theoretically explored considering two different polymerization approaches, i.e. one-pot semi-batch and two-pot batch (Chapter 4). The influence of temperature and initial Cu concentration is analyzed in detail. Arrhenius parameters reported in literature are used for this study and a kinetic Monte Carlo model is employed to track the explicit composition of the polymer chains. This, next to the simulated conversion profile and polymer properties, allow a detailed comparison of the two approaches in view of an optimization of ICAR ATRP for the synthesis of tailored block copolymers. It shown that for a fixed overall Cu level the one-pot procedure is more suited than the two-pot procedure since it allows a fast polymerization while achieving a good diblock copolymer quality.

Finally, in Chapter 5 the most important conclusions of the previous chapters are summarized and future prospects for research are suggested. For the future prospects, both the ICAR ATRP technique and other CRP techniques are considered.

List of symbols

Roman symbols

a	activation [-]
A	monomer A [-]
A	pre-exponential factor in Arrhenius expression [L $mol^{-1}s^{-1}$] or [s^{-1}]
B	monomer B [-]
Br	bromine [-]
C_l	concentration of the reactant l [mol L^{-1}]
$Cu^{(0)}$	metallic copper [-]
Cu(I)	copper with oxidation number 1 [-]
Cu(II)	copper with oxidation number 2 [-]
da	deactivation [-]
dis	dissociation [-]
E_a	energy in Arrhenius expression [kJ·mol^{-1}]
f^{chem}	conventional radical initiator intrinsic efficiency [-]
hp	homopolymer [-]
i	chain lenght [-]
I	initiator fragment derived from the conventional radical initiator dissociation [-]
I_2	conventional radical initiator [-]

IX	dormant conventional radical initiator species [-]
j	chain lenght [-]
k_a	rate coefficient of activation for macrospecies [L mol^{-1} s^{-1}]
k_a^*	rate coefficient of activation involving Cu^0 [L mol^{-1} s^{-1}]
k_{a0}	rate coefficient of activation for ATRP initiator [L mol^{-1} s^{-1}]
k_{add}	rate coefficient of addition [L mol^{-1} s^{-1}]
k_{aIX}	rate coefficient of activation for dormant conventional radical initiator species [L mol^{-1} s^{-1}]
K_{ATRP}	equilibrium coefficient for ATRP [-]
$k_{\beta C\text{-}sc}$	rate coefficient of βC-scission [s^{-1}]
k_{comp}	rate coefficient of comproportionation [L mol^{-1} s^{-1}]
k_{da}	rate coefficient of deactivation for macroradicals [L mol^{-1} s^{-1}]
k_{da}^*	rate coefficient of deactivation for macroradicals involving Cu^0 [L mol^{-1} s^{-1}]
k_{da0}	rate coefficient of deactivation for ATRP initiating radical [L mol^{-1} s^{-1}]
k_{daI}	rate coefficient of deactivation for conventional radical initiator fragments [L mol^{-1} s^{-1}]
k_{dis}	rate coefficient of dissociation for conventional radical initiator [s^{-1}]
k_{disp}	rate coefficient of disproportionation [L mol^{-1} s^{-1}]
K_{eq}	equilibrium coefficient [-]
K_{eq}^s	equilibrium coefficient for secondary species [-]

K_{eq}^{t}	equilibrium coefficient for tertiary species [-]
k_{frag}	rate coefficient of fragmentation [L mol^{-1} s^{-1}]
k_{l}^{app}	apparent rate coefficient of reaction step *l* [L mol^{-1} s^{-1}] or [s^{-1}]
k_{l}^{chem}	intrinsic rate coefficient of reaction step *l* [L mol^{-1} s^{-1}] or [s^{-1}]
k_{MC}	apparent “Monte Carlo rate coefficient” [s^{-1}]
k_{pi}	rate coefficient of propagation of macroradicals [L mol^{-1} s^{-1}]
k_{p0}	rate coefficient of propagation of ATRP initiating radical [L mol^{-1} s^{-1}]
k_{pI}	rate coefficient of propagation of conventional radical initiator fragments [L mol^{-1} s^{-1}]
k_{t0}	rate coefficient of termination of ATRP initiating radicals [L mol^{-1} s^{-1}]
k_{tij}	rate coefficient of termination of macroradicals [L mol^{-1} s^{-1}]
l	reaction step [-]
L	ligand [-]
Mo	Molybdenum [-]
$M_t^{n+1}X_2$/L	deactivator in ATRP [-]
$M_t^{n}X$/L	activator in ATRP [-]
n	oxidation number [-]
n_A	number of molecules of molecule A [-]
N_A	Avogadro constant [mol^{-1}]
Ni	Nickel [-]

p	propagation [-]
P_i	dead polymer [-]
P_l	reaction probability towards reaction *l* [-]
r_1	Random number [-]
R_0X	ATRP initiator [-]
r_A	monomer reactivity ratio [-]
R_i	macroradical [-]
$R_{i,s}$	secondary macroradical [-]
R_i^sX	secondary dormant macrospecies [-]
$R_{i,t}$	tertiary macroradical [-]
R_i^sX	tertiary dormant macrospecies [-]
R_l	reaction rate of reaction *l*
S'(k,l)	cumulative (with respect to *l*) amount of monomer units evaluated from right to left [-]
S(k,l)	cumulative (with respect to *l*) amount of monomer units evaluated from left to right [-]
Sn	Tin
t	termination [-]
T	temperature [°C]
tc	termination by recombination [-]
Te	Tellurium [-]
T_g	glass transition temperature [°C]

Ti	Titanium [-]
trM	transfer to monomer [-]
V	Volume [L]
X	halogen atom [-]
x_n	number-averaged chain length [-]
x_s	moments of the CLD [-]
y	monomer position in a polymer chain (l=1, …, i) [-]
z	number of chains [-]

Greek symbols

α,ω	end positions in a polymer chain [-]
βC-sc	βC-scission reaction of a tertiary macroradical [s^{-1}]
σ_{max}	value of standard deviation at the highest measured monomer conversion [-]
μ	selected reaction channel [-]
τ	time between two reactions used in kinetic Monte Carlo [s]

Abbreviations

AIBN	2,2'-azobis(2-methylpropionitrile)
^{13}C NMR	carbon nuclear magnetic resonance
^{1}H NMR	proton nuclear magnetic resonance
ARGET	activator regenerated by electron transfer

ATRP	atom transfer radical polymerization
BD	block deviation (of a single polymer chain), ranging from 0 to 1
BD*	number block deviation, ranging from 0 to 0.25
BD_1	first block evaluation method
BD_2	second block evaluation method
BD_3	third block evaluation method
BD_4	fourth block evaluation method
BD_5	fifth block evaluation method
Bpy	2 ,2'-bipyridine
CLD	chain length distribution
CRP	controlled radical polymerization
CuBr	copper (I) bromide
$CuBr_2$	copper (II) bromide
CYCLAM-B	1,4,8,11-tetraazacyclotetradecane
DCM	dichloromethane
DMAEA	dimethylaminoethyl acrylate
DMF	dimethylformamide
eATRP	electrochemically mediated atom transfer radical polymerization
EtBriB	ethyl 2-bromo isobutyrate

EGF	end-group functionality
FID	flame ionization detector
FRP	free radical polymerization
GC	gas chromatography
GD	gradient deviation
GPC	gel permeation chromatography
HMTETA	1,1,4,7,10,10-hexamethyltriethylenetetramine
iBoA	isobornyl acrylate
ICAR	initiators for continuous activator regeneration
kMC	kinetic Monte Carlo
LCB	long chain branch
LPO	lauryl peroxide
M	Monomer
MA	methyl acrylate
MBrP	methyl 2-bromopropionate
Me_6TREN	tris[2-(dimethylamino)ethyl]amine
MM	macromonomer
MMA	methyl methacrylate
*n*BuA	*n*-butyl acrylate
NMP	nitroxide mediated polymerization
Ox	oxidized agent

PDI	polydispersity index
PID	proportional–integral–derivative
PMDETA	N,N,N',N'',N''- pentamethyldiethylenetriamine
ppm	parts per million
RAFT	reversible addition fragmentation chain transfer
RAFT-CLD-T	reversible addition fragmentation chain transfer-chain length dependent-termination
RDRP	reversible deactivation radical polymerization
Red	reducing agent
RI	refractive index
RP	radical polymerization
Sty	styrene
SARA	supplemental activator and reducing agent
SCB	short chain branch
SEC	size exclusion chromatography
SET-LRP	single electron transfer living radical polymerization
*t*BuA	*tert*-butyl acrylate
TCL	target chain length
THF	tetrahydrofuran
TPMA	tris(2-pyridylmethyl)amine)
UV-VIS	Ultra Violet-visual

Chapter 1: Introduction

Polymers are used as raw materials for the manufacturing of numerous products used in everyday life, such as plastic films, fibers, paints, elastomers, and household goods. In particular, chain-growth polymerization,[1] in which macrospecies containing an active center react with monomer units, has been extensively applied for the production of a wide variety of high average chain length polymers characterized by a broad chain length distribution (CLD).[2] High chain lengths are necessary for polymer strength, whereas low chain lengths are important for plasticity and thus processability. The most frequently applied chain-growth polymerization techniques are coordination and free radical polymerization (FRP). In the former, chain growth takes place at a catalytic site via an insertion mechanism while in the latter macroradicals increase their chain length by addition to monomer generally in the absence of a catalyst.[1]

Although chain-growth polymerizations are currently selected for the industrial production of polymers for a vast number of applications, several new applications would be accessible in case the polymer microstructure could be appropriately tuned, i.e. more complex polymer architectures, such as well-defined star, gradient, graft and block copolymers (see Figure 1.1) could be synthesized.[3, 4] These “microstructure controlled polymers” are characterized by unique properties, broadening the polymer market to high-tech applications, such as coatings, adhesives, thermoplastic elastomers, electronics, and biomedical applications.[5-7]

Interestingly, these complex polymer anatomies are possible via so-called controlled(/living) radical polymerization (C(/L)RP) techniques,[8-14] in which control over chain length, functionality and composition is possible mainly due to the minimization of termination reactions occurring in conventional free radical polymerization processes.

One of the most important and widely used CRP’s is atom transfer radical polymerization (ATRP),[12, 15] which is the subject of this PhD thesis. The success of

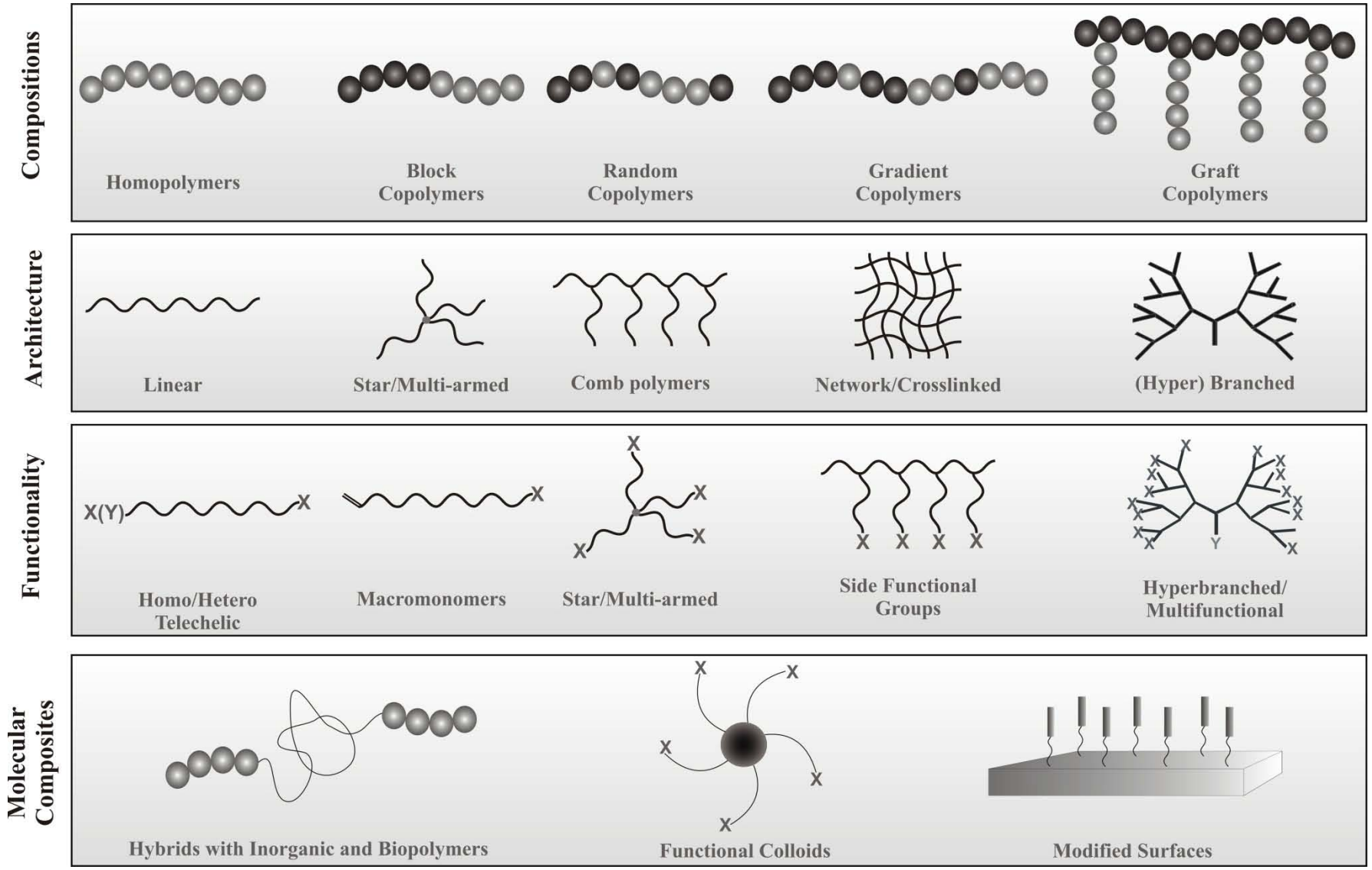

Figure 1.1: Examples of macromolecular architectures attainable with controlled radical polymerization (CRP).[3]

the ATRP technique can be related to its versatility to (co)polymerize a broad range of monomers with controlled chain length and functionality. As will be explained further, in ATRP a catalyst is added as a mediating or controlling agent to tune the polymeric microstructure. Although normal ATRP is inherently a powerful CRP technique, its industrial application has been hampered by the excessive catalyst concentrations that are necessary to successfully carry out the polymerization under fast and controlled conditions.[10] In the last years, ATRP-research has therefore been mainly focused on the development of mechanistic modifications in order to diminish the ATRP catalyst concentration.[16] For this purpose, initiators for continuous activator regeneration atom transfer radical polymerization (ICAR ATRP) has particularly emerged as an ATRP-modified technique in which catalyst concentrations as low as 50 ppm (with respect to monomer) can be used without sacrificing the level of control over the polymer properties.[17]

In this chapter, the ATRP technique as such is introduced and compared with the other main CRP techniques, followed by a general overview of the currently developed modified ATRP techniques targeting a significant reduction of the catalyst concentration. In particular, a more detailed description of the ICAR ATRP technique, which is the main ATRP technique studied in this PhD thesis, is given. Finally, the objectives and outline of the PhD thesis are presented.

1.1 Main controlled radical polymerization techniques

One of the most fascinating advances in polymer science began with the discovery of anionic living polymerization (anionic LP) by Michael Szwarc in 1956,[18, 19] since elimination of termination and chain transfer reactions in this process constituted the departure point for the evolution of research and development of CRP, also known as reversible deactivation radical polymerization (RDRP).[20]

In CRP, a fast and adjustable (pseudo-)equilibrium involving macroradical and dormant macrospecies can be accomplished through the presence of an extra component leading to the occurrence of activation/deactivation reactions, additional to the basic FRP reactions, i.e. initiation, propagation and termination (Figure 1.2). This

new component is called a mediating or controlling agent and it is capable of temporarily trapping propagating chains into a dormant state to control their unrestrained propagation in the time scale of milliseconds, minimizing termination. Reactivation only takes place in the time scale of minutes. In contrast, in FRP dead polymer chains are rapidly formed in the time scale of seconds, and no such activation-growth-deactivation cycles are possible. The presence of a mediating agent implies a reduction of the polymerization rate and, in case the CRP initiation is fast, the production of polymers with a narrow CLD. Moreover, due to the nature of the mediating agents and initiators used in CRP, functionality can be incorporated in the polymer chains permitting the construction of complex macromolecular compositions and topologies (Figure 1.1).

Reaction	FRP	CRP (NMP)
Conventional radical initiation:	$I_2 \xrightarrow{f k_d} 2\,I$	———
CRP initiation:	———	$R_0X \underset{k_{da0}}{\overset{k_{a0}}{\rightleftharpoons}} R_0 + X$
Propagation:	$I + M \xrightarrow{k_{p0}} R_1$ ——— $R_i + M \xrightarrow{k_{pi}} R_{i+1}$	——— $R_0 + M \xrightarrow{k_{p0}} R_1$ $R_i + M \xrightarrow{k_{pi}} R_{i+1}$
Activation/ deactivation:	———	$R_iX \underset{k_{da}}{\overset{k_a}{\rightleftharpoons}} R_i + X$
Chain Transfer to Monomer:	$R_i + M \xrightarrow{k_{trM}} P_i + R_1$	$R_i + M \xrightarrow{k_{trM}} P_i + R_1$
Termination:	$R_i + R_j \xrightarrow{k_{tij}} P_{i+j}$	$R_i + R_j \xrightarrow{k_{tij}} P_{i+j}$

Figure 1.2: General mechanism of free radical polymerization (FRP) and controlled radical polymerization (CRP) illustrated for nitroxide-mediated polymerization (NMP); X represents the mediating agent; shown for termination by recombination

Historically, the four most frequently considered CRP techniques are reversible-addition fragmentation chain transfer polymerization polymerization[21] (RAFT

polymerization; Figure 1.3 top), nitroxide-mediated polymerization[22] (NMP; Figure 1.3 second row), atom transfer radical polymerization[12, 15] (ATRP; Figure 1.3 third row) and single-electron transfer living radical polymerization[13, 14] (SET-LRP) (Figure 1.3 bottom).

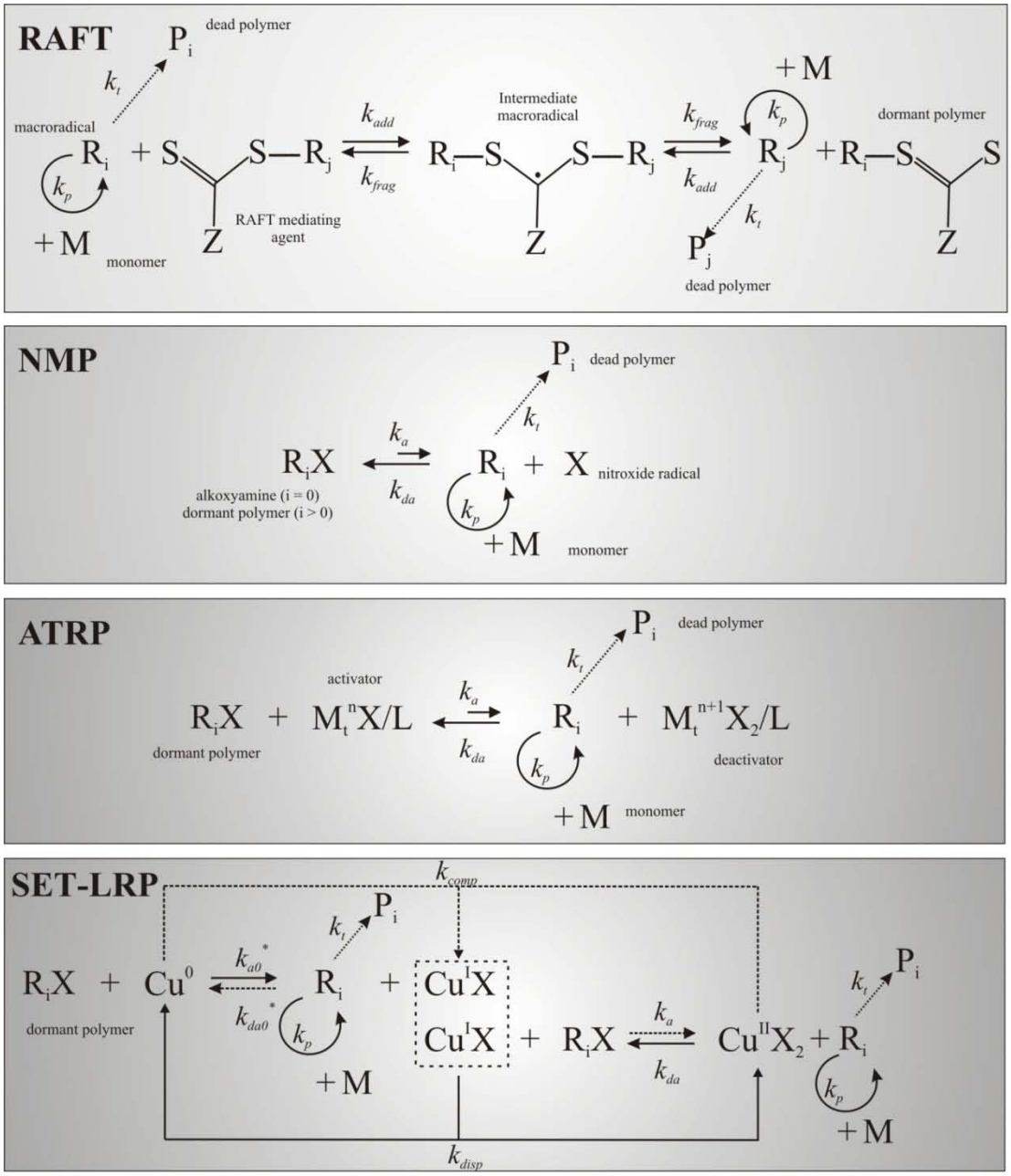

Figure 1.3: Principle of RAFT polymerization, NMP, ATRP and SET-LRP; k_{add}, k_{frag}, k_a, k_{da}, k_p, k_t, k_{disp}, k_{comp}: rate coefficient of addition, fragmentation, activation, deactivation, propagation, termination, disproportionation and comproportionation;(*): refers to the activation/deactivation process involving Cu^0 species; in SET-LRP the ligand is omitted for clarity; n(+1): oxidation number; *i*,*j* : chain length; in RAFT polymerization the conventional radical initiation step is also not shown for simplicity; with *i*=0, R_0X corresponds to the CRP initiator, except for RAFT polymerization (RAFT agent).

As illustrated in Figure 1.3 (top), the first technique utilizes a RAFT mediating agent containing a thiocarbonylthio group, which is responsible for the living character of the polymerization. Contrary to ATRP, no catalyst is required and the transfer of end-group functionality (EGF) involves two different macromolecules. As initial radical source a conventional radical initiator is used generating radicals, which after a few propagation steps can undergo a reversible addition/fragmentation process with the RAFT agent in case they survive termination. Importantly, RAFT polymerization is suitable for a wide variety of monomers (styrenes, (meth)acrylates, vinyl chloride, (meth)acrylamides, …) under FRP polymerization rates using a relatively low polymerization temperature. However, the resulting polymers can be characterized by a relatively low stability and the process can be less interesting due to the ill-scenting RAFT mediating agent.

In NMP (Figure 1.3, second row), on the other hand, a relatively high polymerization temperature is typically needed for the activation of dormant species toward macroradicals and persistent nitroxide species, starting from an alkoxyamine NMP initiator (R_0X, $i=0$). Unfortunately, this technique is mainly limited to styrenes and acrylates. Note that, as in ATRP, one macroradical is involved per activation/deactivation process. However, the activation is not bimolecular, but unimolecular, and similarly to RAFT polymerization, no catalyst is required. Contrary to RAFT polymerization, in NMP a persistent radical effect [22, 23] takes place since initial termination reactions lead to an excess of nitroxide species, which strongly favors deactivation reactions and thus lowers the radical concentration. This in turn, reduces the occurrence of termination reactions as desired for a good CRP.

Furthermore, as can be derived from Figure 1.3 (third row) and shown in detail in Figure 1.4, ATRP is a catalytic process that employs as catalyst a transition metal complex, which can exist in two different oxidation states during the polymerization. The lower oxidation state transition metal complex (M_t^nX/L), which is named the activator, is responsible for the homolytic cleavage of the alkyl halogen bond of the ATRP initiator (R_0X; $i=0$). From this activation reaction that proceeds with a rate coefficient k_{a0}, an initiating radical (R_0; $i=0$) and a higher oxidation state transition

metal complex ($M_t^{n+1}X/L$), i.e. deactivator, are generated. As in the case of NMP and RAFT polymerization, this initiating radical ideally undergoes limited propagation before it is trapped via the deactivation reaction (k_{da}) that takes place thanks to the presence of deactivator molecules. Similarly as in NMP, a persistent radical effect leads to a low radical concentration, since the deactivator molecules are persistent species.

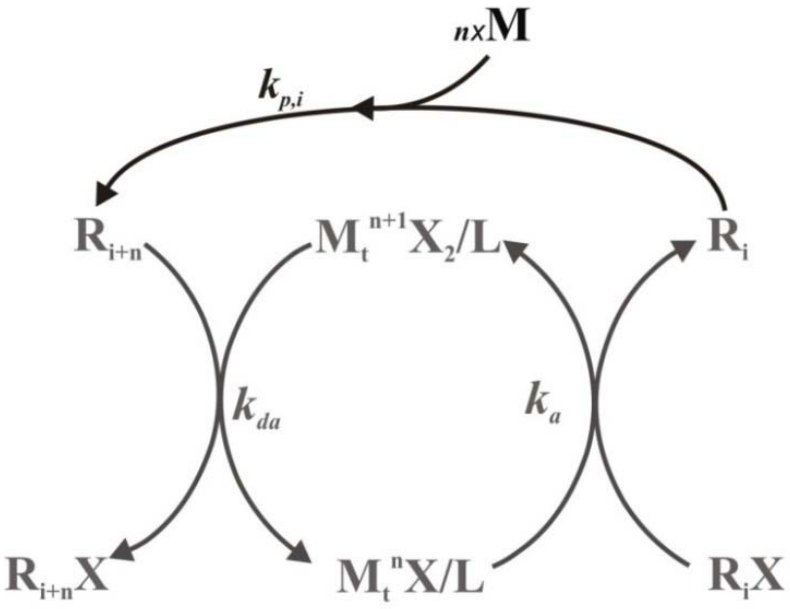

Figure 1.4: Illustration of the ATRP catalytic cycle; for *i*=0 ATRP initiator and replace $k_{a/da}$ by $k_{a0/da0}$

ATRP has been successfully applied for the polymerization of an extensive variety of monomers (styrenes, (meth)acrylates, (meth)acrylamides, …) using a diversity of transition metals, including Titanium (Ti),[24] Molybdenum (Mo),[25, 26] Rhenium (Re),[27, 28] Iron (Fe),[29-33] Nickel (Ni)[34, 35] and Copper (Cu).[36-38] Currently, copper has proven to be the most efficient transition metal and has been employed in conjunction with a broad variety of typically nitrogen-based ligands including linear tetradentate,[39] tripodal/branched tetradentate,[17] macrocyclic,[40] bidentate[41] and tridentate ligands.[36, 42] The most frequently used catalysts are complexes made out of copper bromide or/and copper chloride with N,N,N',N'',N''-pentamethyldiethylenetriamine (PMDETA), tris(2-pyridylmethyl)amine) (TPMA) and tris[2-(dimethylamino)ethyl]amine (Me_6TREN).

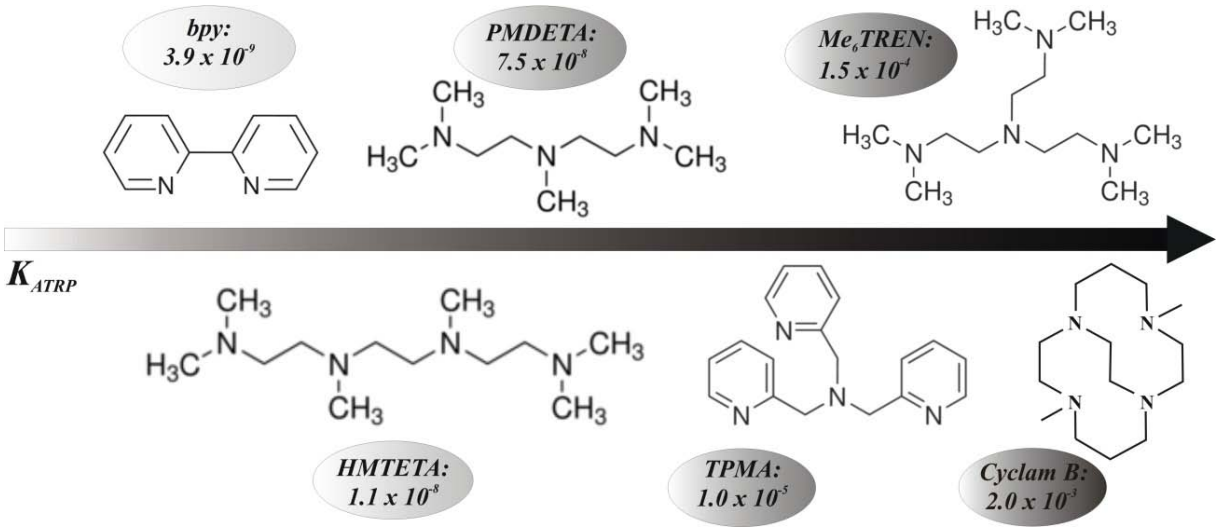

Figure 1.5: Illustration of ATRP equilibrium coefficient for some of the commonly used nitrogen-based ligands with ethyl 2-bromo isobutyrate as initiator and CuBr as copper salt. Values determined at 22°C in acetonitrile.[43]

Crucial for the success of ATRP is the selection of catalyst with a sufficiently low ATRP equilibrium coefficient (k_a/k_{da}) (Figure 1.5; different ligands with CuBr). Also, a high concentration of ATRP catalyst was originally required in order to maintain the control over chain length and livingness.[44, 45] Usually an equal concentration of ATRP initiator and ATRP catalyst was employed in order to shift the composition towards the dormant state. For instance, for a targeted chain length (TCL) of 100, 10000 ppm (with respect to monomer) of Cu species were employed to carry out the ATRP. However, due to product specifications, expensive and rigorous post-purification processes are indispensable to ensure the quality of the final polymeric material.

Finally, Figure 1.3(bottom) shows that in the presence of Cu^0 (and excess of ligand) in an appropriate solvent, an ATRP-related process can be obtained, i.e. SET-LRP. In this process, the activation/deactivation occurs with Cu^0 as major species since the 'activator' of ATRP is in principle immediately converted via disproprotionation into Cu^0 and deactivator. However, as discussed below, in case comproportionation is dominant again an ATRP technique is obtained.

1.2 Modified ATRP techniques

In the last years, four different modified techniques have been developed in order to reduce the catalyst concentration in ATRP processes.[16] It has been demonstrated that in principle catalyst concentrations as low as 50 ppm can be used with these techniques, while obtaining good control over chain length and livingness. For some applications, such as biomedical and electronics, removal of Cu down to 1 ppm is even required. As normal ATRP, these modified processes allow the synthesis of tailored block copolymers with high EGF and narrow CLD. Additionally, since these processes are started with deactivator and not with the air-sensitive activator the polymerization demands less stringent procedures than those currently employed in normal ATRP. Nevertheless, it should be noted that due to the low concentrations of catalyst, only relatively active catalysts such as CuBr ligated with TPMA, Me_6TREN or PMDETA are suitable to successfully perform these processes.

Figure 1.6 illustrates the principle of the main modified ATRP techniques, i.e. initiators for continuous activator regeneration (ICAR) ATRP,[17] activators regenerated by electron transfer (ARGET) ATRP,[17, 46] electrochemically mediated atom transfer radical polymerization *e*ATRP[47] and supplemental activator and reducing agent atom transfer radical polymerization (SARA) ATRP.[48] In ICAR ATRP the reaction is started with ATRP initiator, deactivator, monomer and conventional radical initiator molecules. For sufficiently high temperatures, the latter species create radicals, which can participate in propagation reactions and react with deactivator molecules to (re)generate activator species. When termination occurs, the deactivator is not accumulated but reduced, in case enough conventional radical initiator fragments are present in the mixture. However, as will be discussed in this PhD thesis, a too high conventional radical initiator concentration leads to a deterioration of the balance of activator/deactivator species and a reduction of the control over the ATRP.

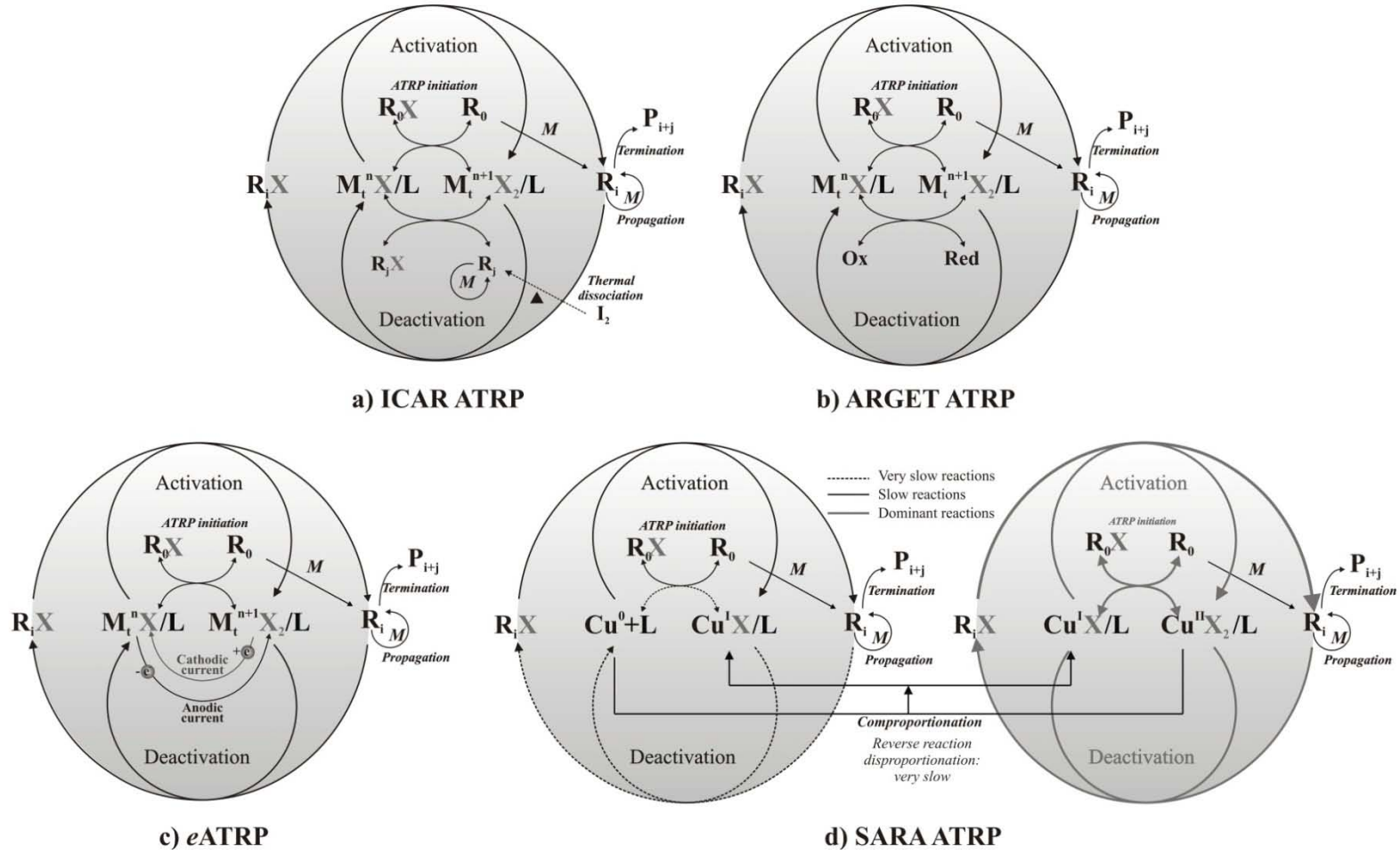

Figure 1.6: Overview of modified ATRP techniques; M: monomer; M_t^nX/L: activator and $M_t^{n+1}X_2/L$: deactivator; R_0X: ATRP initiator; *i, j*; chain length; R_iX: dormant polymer molecule; P_{i+j}: dead polymer molecule; polymerization starts with a) R_0X, M, $M_t^{n+1}X_2/L$ and I_2 (conventional radical initiator), b) R_0X, M, $M_t^{n+1}X_2/L$ and Red (reducing agent), c) R_0X, M and $M_t^{n+1}X_2/L$ in the presence of an electrode, d) R_0X, M, Cu^0 as wire or powder, excess of ligand and $Cu^{II}X_2/L$; SARA is shown for Cu transition metal, it can shift to a SET-LRP (Figure 1.3 bottom row) in case disproportionation is dominant over comproportionation and activation with Cu^0 is very important.

Similar to ICAR ATRP, in ARGET ATRP the polymerization is started from ATRP initiator, deactivator, monomer and a reducing agent¸ such as a tin (*Sn*) complex or a hydrazine compound. In contrast to ICAR ATRP, in these reduction steps no extra radicals are involved and thus no additional propagation path is possible. On the other hand, in *e*ATRP, a current is used to drive the polymerization, i.e. to convert deactivator into activator species. This conversion method constitutes an advantage over other modified ATRP techniques since the polymerization rate can be manipulated via the applied current and potential in a more environmentally friendly manner. However, its actual application represents an interesting challenge due to its more rigorous experimental procedure.

Finally, SARA ATRP has emerged as a new modification of ATRP using Cu^0 species. As illustrated in Figure 1.6d, in SARA ATRP, elemental Cu^0 (powder or wire) is employed in the presence of ligand as a supplemental source of activator while reducing a fraction of deactivator species, i.e. comproportionation constitutes the dominant mechanism in SARA ATRP and the Cu(I) species are the major catalytic species. On the other hand, in case disproportionation of the Cu(I) species becomes dominant a so-called SET-LRP results, in which Cu^0 is the major species, as explained above (Figure 1.3; bottom).[48]

1.3 Objectives and outline

In the following chapters it is demonstrated how kinetic modeling can be applied to optimize ICAR ATRP processes involving styrene and acrylate monomers at laboratory scale. Both homo- and block copolymerizations are considered while providing guidelines for the selection of optimal polymerization conditions, which lead to a controlled and fast ICAR ATRP using ppm levels of catalyst. Intrinsic kinetic parameters are determined based on new experimental and/or literature data. It should be stressed that the followed modeling strategy can be extended to other modified ATRP techniques and different combinations of (co)monomer and ATRP catalyst, allowing a profound evaluation of the industrial potential of ATRP processes, which is currently very difficult.

In Chapter 2, an extensive set of experimental data covering a significant variation of the reaction conditions is reported for the ICAR ATRP of styrene mediated by $CuBr_2$/TPMA and using ethyl 2-bromo isobutyrate (EtBriB) and 2,2′-azobis(2-methylpropionitrile) (AIBN) respectively as ATRP and conventional radical initiator. Measurements of monomer conversion, ATRP initiator conversion, molar mass, and polydispersity (PDI) over a broad range of conditions allow, for the first time, the determination of Arrhenius parameters for (de)activation involving both ATRP initiator and macroinitiator species. A deterministic kinetic model is selected and it is particularly confirmed that CuBr/TPMA is a relatively active catalyst but that Cu ppm levels lower than 10 lead to a reduced control over chain length.

In Chapter 3, a similar deterministic kinetic model is employed for the (ICAR) ATRP of *n*-butyl acrylate (*n*BuA) mediated by $CuBr_2$/PMDETA using methyl 2-bromo propionate (MBrP) and *tert*-butyl peroxy-2-ethylhexanoate, respectively, as ATRP and conventional radical initiator at 105 °C. The influence of backbiting leading to the formation of tertiary macroradicals is analyzed in detail and kinetic parameters for activation/deactivation of secondary and tertiary macroradicals are tuned based on a set of experimental data reported in literature for the corresponding normal ATRP. These data include branching content measurements obtained by ^{1}H NMR. The obtained kinetic parameters are used to obtain for the first time insights into the influence of the initial Cu concentration and targeted chain length (TCL) on the polymerization rate and the control over chain length and livingness. Based on an analysis of the ICAR ATRP for a significant range of Cu levels and TCLs, simulations allow to propose guidelines for the selection of appropriate conditions for the industrial application of the ICAR ATRP homopolymerization process with *n*BuA, i.e. to conduct a fast and controlled polymerization with low levels of Cu-catalyst.

In Chapter 4, the capability of ICAR ATRP for the synthesis of complex macromolecular structures is further explored for the case of block copolymerization. Based on the insights obtained for the ICAR ATRP of styrene in Chapter 2 and *n*BuA in Chapter 3, the ICAR ATRP is studied by means of simulations for the synthesis of well-defined diblock(-like) copolymers. In particular, the preparation of poly(isobornyl

acrylate-*b*-styrene) diblocks by ICAR ATRP using $CuBr_2$/PMDETA as catalyst, and MBrP and lauryl peroxide (LPO) respectively as ATRP and conventional radical initiator is investigated. In this case a stochastic kinetic model, which permits the individual tracking of the macromolecular composition, is used. A block deviation value, <BD>, to evaluate the diblock quality of the copolymer is introduced. Additionally, the results of the so-called one-pot semibatch and two-pot batch approach are compared at different temperatures and initial concentrations of Cu-catalyst in order to define optimal conditions for the synthesis of tailored diblock copolymers containing styrene and acrylate blocks.

Finally, in Chapter 5 a summary of the general conclusions of this PhD thesis and the prospects for future work on ICAR ATRP and related CRP techniques are presented.

References

[1] G. Odian, *Principles of polymerization*. Wiley-Interscience: USA, **1981**.

[2] K. Matyjaszewski; T. P. Davis, *Handbook of Radical Polymerization*. Wiley-Interscience: Hoboken, **2002**.

[3] K. Matyjaszewski; J. Spanswick, *Materials Today* **2005,** *8,* 26-33.

[4] J. Spanswick; B. Pike, Opportunities in Controlled Radical Polymerization. In *Controlled/Living Radical Polymerization: Progress in ATRP*, American Chemical Society: **2009**; Vol. 1023, pp 385-396.

[5] C. Fei; J. Frieder, New Architectures and Applications of Organoboron Polymers Prepared via Controlled Radical Polymerization. In *Progress in Controlled Radical Polymerization: Materials and Applications*, American Chemical Society: **2012**; Vol. 1101, pp 27-38.

[6] Z. Mirela; L. Jean-François, Controlling Polymer Primary Structure Using CRP: Synthesis of Sequence-Controlled and Sequence-Defined Polymers. In *Progress in Controlled Radical Polymerization: Materials and Applications*, American Chemical Society: **2012**; Vol. 1101, pp 1-12.

[7] A. O. Patil; H. Dong; A. H. Tsou; S. Bodige, Polymer?Inorganic Hybrid Materials Using Controlled Radical Polymerization. In *Progress in Controlled Radical*

Polymerization: Materials and Applications, American Chemical Society: **2012**; Vol. 1101, pp 163-182.

[8] W. A. Braunecker; K. Matyjaszewski, *Progress in Polymer Science* **2008,** *33*, 165.

[9] S. Gaynor; D. Greszta; D. Mardare; M. Teodorescu; K. Matyjaszewski, *J Macromol Sci-Pure Appl Chem* **1994,** *A31*, 1561.

[10] D. F. Grishin; I. D. Grishin, *Russian Journal of Applied Chemistry* **2011,** *84*, 2021.

[11] K. Matyjaszewski, *Controlled/Living Radical Polymerization: Progress in ATRP, NMP and RAFT*. ACS: Washington, **2000**.

[12] J. S. Wang; K. Matyjaszewski, *J Am Chem Soc* **1995,** *117*, 5614.

[13] M. J. Monteiro; T. Guliashvili; V. Percec, *J Polym Sci Pol Chem* **2007,** *45*, 1835-1847.

[14] B. M. Rosen; V. Percec, *Chem Rev* **2009,** *109*, 5069-5119.

[15] M. Kato; M. Kamigaito; M. Sawamoto; T. Higashimura, *Macromolecules* **1995,** *28*, 1721.

[16] D. R. D'Hooge; D. Konkolewicz; M. F. Reyniers; G. B. Marin; K. Matyjaszewski, *Macromolecular Theory and Simulations* **2012,** *21*, 52.

[17] K. Matyjaszewski; W. Jakubowski; K. Min; W. Tang; J. Y. Huang; W. A. Braunecker; N. V. Tsarevsky, *Proceedings of the National Academy of Sciences of the United States of America* **2006,** *103*, 15309.

[18] M. Szwarc, *Nature* **1956,** *178*, 1168-1169.

[19] M. Szwarc; M. Levy; R. Milkovich, *Journal of the American Chemical Society* **1956,** *78*, 2656-2657.

[20] A. D. Jenkins; R. G. Jones; G. Moad, *Pure and Applied Chemistry* **2010,** *82*, 483-491.

[21] G. Moad; S. H. Thang, *Australian Journal of Chemistry* **2009,** *62*, 1379-1381.

[22] D. Bertin; D. Gigmes; S. R. A. Marque; P. Tordo, *Chem Soc Rev* **2011,** *40*, 2189-2198.

[23] H. Fischer, *Macromolecules* **1997,** *30*, 5666-5672.

[24] Y. A. Kabachii; S. Y. Kochev; L. M. Bronstein; I. B. Blagodatskikh; P. M. Valetsky, *Polymer Bulletin* **2003,** *50*, 271-278.

[25] E. Le Grognec; R. Claverie; R. Poli, *Journal of the American Chemical Society* **2001,** *123*, 9513-9524.

[26] J. A. M. Brandts; P. van de Geijn; E. E. van Faassen; J. Boersma; G. van Koten, *Journal of Organometallic Chemistry* **1999,** *584*, 246-253.

[27] Y. Kotani; M. Kamigaito; M. Sawamoto, *Macromolecules* **1999,** *32*, 2420-2424.

[28] S. Komiya; T. Chigira; T. Suzuki; M. Hirano, *Chemistry Letters* **1999**, 347-348.

[29] K. Matyjaszewski; M. L. Wei; J. H. Xia; N. E. McDermott, *Macromolecules* **1997,** *30*, 8161-8164.

[30] R. K. O'Reilly; V. C. Gibson; A. J. P. White; D. J. Williams, *Polyhedron* **2004,** *23*, 2921-2928.

[31] M. Teodorescu; S. G. Gaynor; K. Matyjaszewski, *Macromolecules* **2000,** *33*, 2335-2339.

[32] Y. H. Ng; F. di Lena; C. L. L. Chai, *Macromolecular Research* **2012,** *20*, 552-558.

[33] W. W. He; L. F. Zhang; J. Miao; Z. P. Cheng; X. L. Zhu, *Macrom Rapid Commun* **2012,** *33*, 1067-1073.

[34] C. Granel; P. Dubois; R. Jerome; P. Teyssie, *Macromolecules* **1996,** *29*, 8576-8582.

[35] H. Uegaki; Y. Kotani; M. Kamigaito; M. Sawamoto, *Macromolecules* **1997,** *30*, 2249-2253.

[36] S. A. Turner; Z. D. Remillard; D. T. Gijima; E. Gao; R. D. Pike; C. Goh, *Inorganic Chemistry* **2012,** *51*, 10762-10773.

[37] X. H. Liu; J. Wang; F. J. Zhang; S. L. An; Y. L. Ren; Y. H. Yu; P. Chen; S. Xie, *J Pol Sci, Part A: Polym Chem* **2012,** *50*, 4358-4364.

[38] N. V. Tsarevsky, *Israel Journal of Chemistry* **2012,** *52*, 276-287.

[39] S. J. Ding; Y. Q. Shen; M. Radosz, *J Polym Sci Pol Chem* **2004,** *42*, 3553-3562.

[40] N. V. Tsarevsky; W. A. Braunecker; W. Tang; S. J. Brooks; K. Matyjaszewski; G. R. Weisman; E. H. Wong, *Journal of Molecular Catalysis a-Chemical* **2006,** *257*, 132-140.

[41] R. Ferro; S. Milione; T. Caruso; A. Grassi, *Journal of Molecular Catalysis a-Chemical* **2009,** *307*, 128-133.

[42] K. Matyjaszewski; B. Gobelt; H. J. Paik; C. P. Horwitz, *Macromolecules* **2001,** *34*, 430-440.

[43] W. Tang; Y. Kwak; W. Braunecker; N. V. Tsarevsky; M. L. Coote; K. Matyjaszewski, *Journal of the American Chemical Society* **2008,** *130*, 10702-10713.

[44] N. V. Tsarevsky; K. Matyjaszewski, *Chemical Reviews* **2007,** *107*, 2270-2299.

[45] Y. Q. Shen; H. D. Tang; S. J. Ding, *Progress in Polymer Science* **2004,** *29*, 1053-1078.

[46] Y. Kwak; A. J. D. Magenau; K. Matyjaszewski, *Macromolecules* **2011,** *44*, 811-819.

[47] A. J. D. Magenau; N. C. Strandwitz; A. Gennaro; K. Matyjaszewski, *Science* **2011,** *332*, 81.

[48] Y. Z. Zhang; Y. Wang; C. H. Peng; M. J. Zhong; W. P. Zhu; D. Konkolewicz; K. Matyjaszewski, *Macromolecules* **2012,** *45*, 78-86.

Chapter 2: Kinetic modeling as a tool to retrieve activation and deactivation Arrhenius parameters for the ICAR ATRP of styrene mediated by CuBr/TPMA

Summary

An experimental study of the initiators for continuous activator regeneration atom transfer radical polymerization (ICAR ATRP) of styrene with $CuBr_2$/TPMA (TPMA: tris(2-pyridylmethyl)amine) as deactivator is coupled with kinetic modeling to determine the key activation/deactivation Arrhenius parameters. The study covers a variation of the ppm level of ATRP catalyst from 10 to 50ppm, the initial molar ratio of monomer to ATRP initiator (ethyl 2-bromo isobutyrate) from 50 to 500, the initial ratio of conventional radical initiator to ATRP initiator (2,2′-azobis(2-methylpropionitrile)) from 0.2 to 2 and the polymerization temperature from 60 to 80°C. Modeling is limited to conversions below 0.50 to avoid interference of side phenomena, such as diffusional limitations on the activation/deactivation process. Values of 1.2 10 and 8.0 10^6 L mol^{-1} s^{-1} are obtained at 70 °C, respectively, for activation and deactivation involving macrospecies, which confirms the relatively high activity of CuBr/TPMA as ATRP catalyst. Cu ppm levels higher than 10 ppm are required for the control over chain length.

2.1 Introduction

Atom transfer radical polymerization (ATRP) has become one of the most important polymerization techniques for the synthesis of well-defined polymers with predetermined chain length, narrow molar mass distribution and high livingness.[1-3] ATRP is a radical process applicable to an extensive variety of monomers and has been used as a tool to build complex macromolecular architectures covering a broad spectrum of properties.[4, 5] As in other controlled radical polymerization (CRP) processes,[6-11] the presence of a mediating agent allows to establish and maintain a

dynamic equilibrium between dormant (*RX*; Figure 2.1a) and radical species (*R*) favoring the dormant state, and thus to diminish the radical concentration and the occurrence of inevitable termination reactions which lead to the formation of dead polymer (*P*).

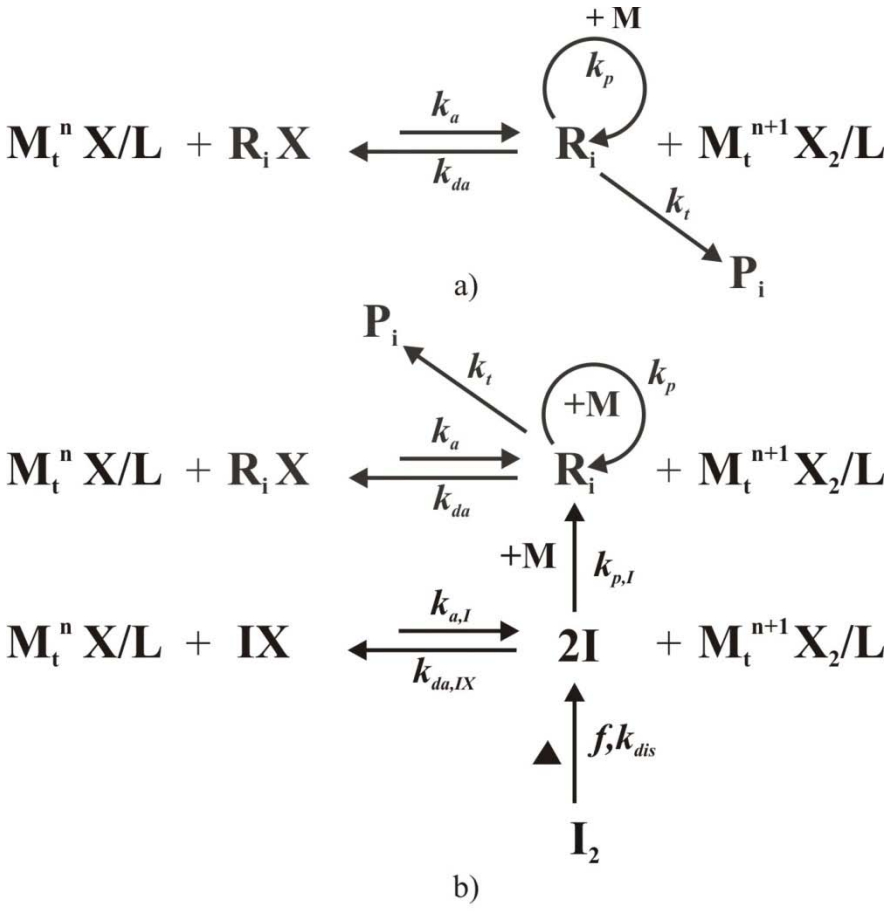

Figure 2.1: a) Principle of normal ATRP and b) Principle of ICAR ATRP; k_a,k_{da},k_p and k_t are the rate coefficients for activation, deactivation, propagation and termination; $k_{a,IX}$, $k_{da,I}$ and $k_{p,I}$ are the rate coefficients for activation, deactivation and propagation related to the conventional initiator; f and k_{dis} correspond to the conventional radical initiator efficiency and the corresponding rate coefficient; i=0 corresponds to ATRP initiator; n(+1) is the oxidation number of the transition metal complex (de)activator; X corresponds to a halogen atom, and L to ligand; normal ATRP is started with activator, monomer and ATRP initiator; ICAR ATRP is started only with deactivator, monomer and ATRP initiator

As shown in Figure 2.1a, in normal ATRP a transition metal complex (M_t^nX/L), which is typically formed from a Cu salt (M_t^nX) and a ligand (L), is employed as mediating agent, while end-group functionality (EGF: X) is incorporated in the polymer chains

via a catalytic cycle starting from an ATRP initiator (R_0X). For a fast ATRP initiation, a good control over chain length can be obtained, since otherwise new dormant chains formed in a later stage have less monomer available to reach the targeted chain length (TCL:$[M]_0/[R_0X]_0$) at complete monomer consumption. Moreover, a successful ATRP can be conducted if a sufficiently high concentration of Cu(I) (≈ 5000-10000 ppm with respect to monomer (molar)) is employed so that every radical species formed has one deactivator molecule available to impede uncontrolled propagation and termination reactions. However, such high Cu(I) concentrations result in too long polymerizations, which are not attractive from an industrial point of view. Additionally, the initial use of air-sensitive Cu(I) species requires stringent experimental procedures. Finally, the process is characterized by an expensive post-polymerization treatment, i.e. time-consuming purification processes are indispensable, since the undesired colored copper species present in the polymer mixture have to be eliminated to ensure a high product quality and to fulfill environmental regulations.

Therefore, in the last years ATRP research has been mainly focused on the development of alternative initiation procedures in which an important decrease of the amount of Cu catalyst necessary to mediate the polymerization (ideally below 50 ppm) can be achieved while preserving the activation/deactivation principle from ATRP and avoiding the difficult handling of Cu(I) species, i.e. requiring initially only Cu(II) species.[12-18] In initiators for continuous activators regeneration (ICAR) ATRP (Figure 2.1b), which is the modified ATRP technique studied in this work, the reduction of the catalyst concentration is possible thanks to the presence of conventional radical initiator fragments (*I*) capable of the (re)generation of activator species (M_t^nX/L) by undergoing a redox reaction with the deactivator species ($M_t^{n+1}X_2/L$) present in the polymerization mixture.

As illustrated in Figure 2.1b, these conventional radical initiator fragments can also participate in propagation (k_{pI}) and activation/deactivation ($k_{aI,daIX}$) reaction steps. However, it has been shown that the latter activation/deactivation reactions have no major influence on the polymerization rate and control over polymer properties.[14, 19, 20] In contrast, it is well known that the values of the activation/deactivation rate

coefficients involving ATRP initiator and macrospecies ($k_{(d)a(0)}$) are crucial for the understanding, optimization and industrial applicability of (ICAR) ATRP. It has been especially indicated that the corresponding activation rate coefficients and ATRP equilibrium coefficients are sensitive to a temperature variation.[21, 22] As will be further illustrated in Chapter 4, the polymerization temperature is indeed important for the fast and controlled synthesis of tailored block copolymers by ICAR ATRP.

Despite the significant relevance of the polymerization temperature for the ATRP catalyst reactivity, most literature reports on activation/deactivation kinetic parameters only relate to the activation of the ATRP initiator (R_0X) in monomer-free environments, i.e. in the presence of solvent only. For example, the temperature influence on the intrinsic activation rate coefficient ($k_{a0,chem}$) has been measured by Pintauer et al.[23] using the stopped-flow UV-VIS technique for various initiator/Cu catalyst combinations in acetonitrile. Additionally, Seeliger and Matyjaszewski[21] reported Arrhenius parameters for a variety of ATRP initiators in the same solvent in the Cu-mediated ATRP with the commercially available ligand N,N,N',N",N"-pentamethyldiethylenetriamine (PMDETA). On the other hand, Tang et al.[24] reported activation/deactivation equilibrium coefficients for these ATRP initiators at 22° and/or 35°C again in acetonitrile. It should be noted that it is very likely that activation/deactivation parameters determined in a polar solvent, such as acetonitrile, cannot be directly used to describe polymerizations especially in less polar media. However, it can be expected that the relative reactivities of ATRP catalysts are solvent independent to a first approximation.

Alternatively, kinetic modeling coupled with experimental validation has proven to be a powerful tool for the determination of activation/deactivation kinetic parameters in a monomer-rich environment.[14, 20, 25, 26] For instance, Matyjaszewski et al.[14] compared the Cu based ATRP of styrene using three important commercially available ligands, namely bipyridine (bpy), PMDETA and tris(2-pyridylmethyl)amine (TPMA) while extrapolating the parameters of Tang et al.[24] at 35°C in acetonitrile and indicated that for low Cu ppm levels (<200 ppm) the polymerization rate is mainly determined by the conventional radical initiator. Furthermore, D'hooge et al.[25] determined Arrhenius

parameters for the secondary species in the ATRP of isobornyl acrylate (iBoA) with CuBr/PMDETA based on regression to an extensive set of experimental data and reported a high livingness. In addition, Fu et al.[26] successfully described the experimental trends of the ATRP of styrene at 110°C considering again CuBr/PMDETA as ATRP catalyst based on activation/deactivation kinetic parameters from related kinetic modeling studies. Similarly, Toloza Porras et al.[20] applied for the same catalyst kinetic modeling to retrieve activation/deactivation parameters for the secondary and tertiary macrospecies at 105°C in the ATRP of *n*-butyl acrylate (*n*BuA) and used these parameters to optimize the related ICAR ATRP system with respect to the targeted chain length (TCL), i.e. the initial molar ratio of monomer to ATRP initiator, and the Cu amount.

In this chapter, kinetic modeling is further used to determine for the first time approximate activation/deactivation Arrhenius parameters for ATRP processes of styrene with CuBr/TPMA as activator. The commercially available TPMA is selected since it has been indicated that this ligand exhibits a high potential for the controlled polymerization of various monomers[17] and forms a relatively active catalyst with CuBr.[14] The parameters are assessed based on a comparison of the simulation results with an extensive set of experimental data covering a systematic variation of the initial concentrations and polymerization temperature. Each experiment is performed batchwise and isothermally.

The ICAR ATRP technique using ethyl 2-bromoisobutyrate (EtBriB) as ATRP initiator and 2,2′-azobis(2-methylpropionitrile) (AIBN) as conventional radical initiator is chosen as ATRP modified technique to facilitate a reliable determination of the key activation/deactivation kinetic parameters. This is possible since contrary to normal ATRP processes, in ICAR ATRP no Cu(I) species have to be added initially, the amount of Cu in the mixture is well below the solubility limits of the activator and deactivator, which are difficult to measure,[26] and a more reasonable polymerization rate is obtained.

In addition, contrary to other modified ATRP techniques, such as activators regenerated by electron transfer (ARGET) ATRP,[12, 14, 27] it can be expected that the simultaneous determination of additional kinetic parameters does not impose a significant error. In ICAR ATRP, the polymerization rate is mainly determined by the conventional radical initiator dissociation, for which intrinsic kinetic parameters have been accurately determined before.[28] On the other hand, for other modified ATRP techniques, no conventional initiation mechanism is applied, implying the use of an external source, such as a reducing agent or an electrode, for which no intrinsic kinetic parameters are currently available.

Furthermore, to minimize the influence of possible side reactions[29-32] and to avoid the interference with diffusional limitations on the activation/deactivation process[33-36] and the conventional radical initiation,[37, 38] this kinetic study is limited to conversions below 0.50. Also, the activation/deactivation parameters for the ATRP initiator are assessed independently based on the measurement of the conversion of these species at different temperatures. Such approach permits to identify whether slow ATRP initiation takes place, a phenomenon known to reduce the level of control over chain length, as explained above.

It is shown that the reported activation/deactivation intrinsic kinetic parameters allow a good description of the experimental data and that, in agreement with literature data, CuBr/TPMA can be classified as a relatively active ATRP catalyst. It is also demonstrated that too low ppm levels of Cu catalyst (~ 10 ppm) result in a loss of control over chain length, particularly in case low TCLs are considered. The proposed strategy for parameter assessment is applicable to CRP in general.

2.2 Experimental Procedure

2.2.1 Materials

Styrene (Sty, monomer (M), ≥99%, Sigma-Aldrich) was passed through a column filled with basic aluminum oxide in order to remove the stabilizer. Copper(II) bromide ($CuBr_2$, 99.999%), tris(2-pyridylmethyl)amine (TPMA, 98%), ethyl 2-bromoisobutyrate (EtBriB, 98%), 2′2 -azobis(2-methylpropionitrile) (AIBN, 98%),

N,N-dimethylformamide (DMF, 99.5%), tetrahydrofuran (THF, ≥99.9%), and dichloromethane (DCM, ≥99.5%) were purchased from Sigma-Aldrich and used without further purification.

2.2.2 Batch ICAR ATRP of styrene

The batch isothermal polymerization of styrene (entry 7 in Table 2.1) was performed with 5% vol% of internal standard (DMF) with respect to monomer for gas chromatography (GC) analysis and to avoid catalyst precipitation. In-situ temperature control was done via a proportional–integral–derivative controller (PID) (see Appendix A).

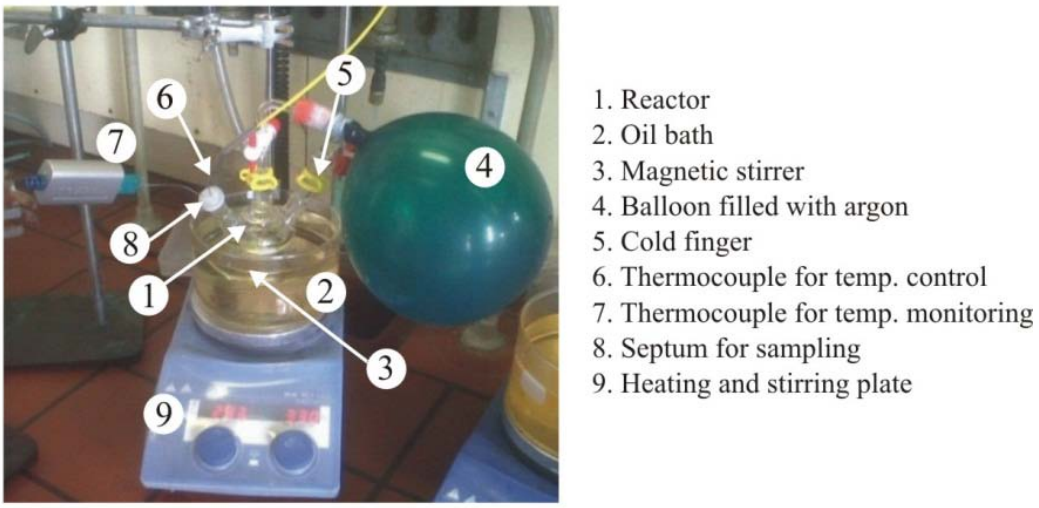

Figure 2.2: Experimental set up used in the ICAR ATRP of styrene with in-situ temperature (temp.) control

The polymerization was performed as follows: $CuBr_2$ (4.63 mg, 0.021 mmol) and TPMA (6.02 mg, 0.021 mmol) were first dissolved in DMF (2.38 mL, 0.031 mol) (catalyst solution) and a part of the total amount of styrene (43 mL, 373 mmol) was mixed with the catalyst solution in a 100-mL three-neck Schlenk flask (reaction flask). A cold-finger was attached to one of the necks as a part of the temperature control. A stopcock was attached to the second neck and the last neck was capped with a rubber septum for sampling (Figure 2.2). Additionally a thermocouple for temperature control was inserted into the reaction flask through this rubber septum. This solution was bubbled three times with argon while applying intermediate vacuum periods. After oxygen removal, the flask was back-filled with argon via the stopcock valve. The

reaction flask was then immersed in an oil bath thermostated at 70^{0}C under mild agitation. As shown in Appendix A, for the studied ATRP system the temperature of the oil bath can be considered as the temperature of the reaction mixture.

Table 2.1: Overview of polymerization conditions covered in the experimental study of the ICAR ATRP of styrene ($[Sty]_0$=8.7 M) with $CuBr_2$/TPMA as deactivator and using ethyl 2-bromoisobutyrate (EtBriB) as ATRP initiator and 2,2′-azobis(2-methylpropionitrile) (AIBN) as conventional radical initiator; isothermal runs

Entry	**Initial molar ratios**					**ppm[a]**	**T(^{0}C)**
	Sty	EtBriB	$CuBr_2$	TPMA	AIBN		
1	50	1	0.0005	0.0005	0.2	10	70
2	50	1	0.00125	0.00125	0.2	25	70
3	50	1	0.0025	0.0025	0.2	50	70
4	100	1	0.001	0.001	0.2	10	70
5	100	1	0.0025	0.0025	0.2	25	70
6	100	1	0.005	0.005	0.2	50	60
7	100	1	0.005	0.005	0.2	50	70
8	100	1	0.005	0.005	0.2	50	80
9	200	1	0.002	0.002	0.2	10	70
10	200	1	0.005	0.005	0.2	25	70
11	200	1	0.01	0.01	0.2	50	70
12	500	1	0.005	0.005	0.2	10	70
13	500	1	0.0125	0.0125	0.2	25	70
14	500	1	0.025	0.025	0.2	50	70
15	100	1	0.005	0.005	0.3	50	80
16	100	1	0.005	0.005	2.0	50	80

[a] ppm of Cu calculated with respect to monomer on a molar basis ($ppm=10^6 \times [CuBr_2]_0/[Sty]_0$)

The remaining small volume of styrene (4.8 mL, 41.6 mmol) was poured into a 10-mL two-neck Schenk flask together with the conventional radical initiator, AIBN (136 mg, 0.829 mmol), and the ATRP initiator, EBriB (0.62 mL, 4.146 mmol). This solution was deaerated by three vacuum-argon cycles and stirred at room temperature. When the temperature in the reaction flask was stable (~40 min later), the polymerization was initiated by injecting the content of the 10-mL flask solution into the reaction flask.

At distinct polymerization times, 1.4-mL samples were withdrawn from the flask with an stainless-steel needle, poured into a 2-mL vial and immediately quenched in liquid nitrogen for a few seconds to prevent further polymerization. At the final

polymerization time, the reaction flask was opened to the air to allow complete oxidation of the Cu(I) species and chilled THF was added to stop the reaction.

As will be demonstrated below, the reproducibility of the experimental data is sufficiently high. An overview of all polymerization conditions is given in Table 2.1. As illustrated further, these conditions cover a broad range of conversions, polydispersity indices (PDIs) and number-average chain lengths (x_n), and are sufficient for a reliable tuning of the intrinsic key activation/deactivation parameters in ATRP.

2.2.3 Analysis

Gas chromatography (GC) and gravimetric analysis (Appendix B) were used for the experimental determination of the monomer and ATRP initiator conversion and size exclusion chromatography (SEC) (Appendix B) analysis was used to measure x_n and PDI as a function of conversion. A trace-GC ultra-Gas Chromatograph equipped with an AS3000 autosampler, flame ionization detector (FID) detector and a CP Wax 52 CB 30m capillary column was employed for the GC analysis. The injector and detector temperature were 275 °C. Helium (flow rate: 30mL/min) was used as carrier gas and a stepwise temperature program was set as follows: 50°C during 3 min, followed by a heating ramp of 10°C/min until a temperature of 110°C was reached. DMF was used as internal standard and DCM as solvent to prepare the samples.

SEC analysis was performed with a PL-GPC*50* plus instrument equipped with a PL-AS RT autosampler, refractive index (RI) detector, and the following columns connected in series: Resipore 50×7.5mm guard column, and two Resipore 300×7.5mm columns. Calibration was performed with polystyrene standard samples (*Agilent Technologies*) ranging from 162 to 3.7 10^5 g mol^{-1} and THF was used as eluent.

2.3 Kinetic model

Table 2.2 summarizes the considered reactions for the ICAR ATRP of styrene using $CuBr_2$/TPMA as deactivator, ethyl 2-bromoisobutyrate (EtBriB) as ATRP initiator and 2,2'-azobisisobutyronitrile (AIBN) as conventional radical initiator. A distinction is made between (ICAR) ATRP specific and ATRP non-specific reactions. Since the

maximal polymerization temperature is 80°C (Table 2.1), styrene thermal self-initiation and chain transfer reactions can be safely neglected.[8, 39, 40] The corresponding continuity equations are integrated similarly as done by Toloza Porras et al.[20] for the ICAR ATRP of *n*BuA.

Table 2.2: Overview of reactions involved in the ICAR ATRP of styrene and corresponding Arrhenius parameters; intrinsic initiator efficiency f^{chem}:0.75;[41] since the simulations are limited to conversions below 0.50, only diffusional limitations on termination have to be accounted for (composite k_t model using RAFT-CLD-T parameters at 90°C[42])

	Elementary Reaction	Equation	Arrhenius parameters[(a)]	k_l^{chem} (70°C) (s^{-1}) or (L mol^{-1} s^{-1})	Reference
Extra for ICAR ATRP	Dissociation	$I_2 \xrightarrow{f^{chem}\,k_{dis}^{chem}} 2I$	A = 1.3 10^{15} E_a = 128.6	4.7 10^{-5}	[43] [43]
	Propagation	$I + M \xrightarrow{k_{p,I}^{chem}} R_1$	A = 4.3 10^{7} E_a = 32.5	4.8 10^{2}	[44] [44]
	Activation	$M_t^n X/L + IX \xrightarrow{k_{a,IX}^{chem}} M_t^{n+1} X_2/L + I$	A = 1.3 10^{7} E_a = 27.8	1.0 10^{3}	[19] This work
	Deactivation	$M_t^{n+1} X_2/L + I \xrightarrow{k_{da,I}^{chem}} M_t^n X/L + IX$	A = 1.0×10^{6} E_a =0	1.0 10^{6}	[14] This work
normal ATRP	Propagation	$R_0 + M \xrightarrow{k_{p0}^{chem}} R_1$	A = 4.3 10^{7} E_a = 32.5	4.8 10^{2}	[44] [44]
		$R_i + M \xrightarrow{k_{p}^{chem}} R_{i+1}$	A = 4.3 10^{7} E_a = 32.5	4.8 10^{2}	[44] [44]
	Activation	$M_t^n X/L + R_0 X \xrightarrow{k_{a0}^{chem}} M_t^{n+1} X_2/L + R_0$	A =4.2 10^{5} E_a =27.8	1.7 10	This work This work
		$M_t^n X/L + R_i X \xrightarrow{k_{a}^{chem}} M_t^{n+1} X_2/L + R_i$	A = 3.1 10^{5} E_a =27.8	1.2 10	This work This work
	Deactivation	$M_t^{n+1} X_2/L + R_0 \xrightarrow{k_{da\,0}^{chem}} M_t^n X/L + R_0$	A = 8.0×10^{7} E_a = 0	8.0 10^{7}	This work This work
		$M_t^{n+1} X_2/L + R_i \xrightarrow{k_{da}^{chem}} M_t^n X/L + R_i X$	A = 8.0×10^{6} E_a = 0	8.0 10^{6}	This work This work
	Termination by recombination	$R_0 + R_0 \xrightarrow{k_{tc,00}^{chem}} R_0 R_0$	RAFT-CLD-T	-	[42]
		$R_0 + R_i \xrightarrow{k_{tc,0i}^{chem}} P_i$	RAFT-CLD-T	-	[42]
		$R_i + R_j \xrightarrow{k_{tc,ij}^{chem}} P_{i+j}$	RAFT-CLD-T	-	[42]

[(a)] pre-exponential factor A in L·$mol^{-1}s^{-1}$ or s^{-1} and activation energy E_a in kJ mol^{-1}

The intrinsic Arrhenius parameters, except for termination, are also listed in Table 2.2. For the reactions common with free radical polymerization (FRP), i.e. conventional radical dissociation and propagation, these parameters are taken from literature,[41, 43] whereas the activation/deactivation parameters are determined in this work and discussed in the Section '2.4. Results and Discussion'. To ensure a reliable determination of the latter parameters a comparison between the simulation and experimental results is limited to conversions below 0.50. As indicated in previous kinetic studies at higher conversions the activation/deactivation process and the conventional radical initiation are influenced by viscosity effects which can disturb the regular activation-growth-deactivation process.[33-36] A similar approach has been successfully followed by D'hooge et al.[25] for the determination of activation/deactivation parameters for secondary macrospecies in the ATRP of iBoA with CuBr/PMDETA as catalyst in order to avoid the formation of tertiary radical species via backbiting.[45]

Based on literature reports, for termination, the chain length and viscosity dependency is accounted for via apparent termination rate coefficients as determined with a composite k_t model.[46, 47] The reported parameters are taken from reversible addition-fragmentation chain transfer chain length dependent termination (RAFT-CLD-T) measurements at 90°C.[42] To a first approximation it can be assumed that these parameters also hold at the lower temperatures studied in this work (60-80 °C; Table 2.1), since styrene termination is characterized by a low activation energy.[48]

2.4 Results and discussion

In this section, a detailed kinetic study of the ICAR ATRP of styrene mediated by $CuBr_2$/TPMA and using EtBriB as ATRP initiator and AIBN as conventional radical initiator is presented up to intermediate conversions to ensure a reliable assessment of activation/deactivation kinetic parameters, as explained above. It is shown that a good reproducibility of the experimental data is obtained and the reported activation/deactivation parameters allow a good description of the influence of the

polymerization conditions (Cu level, TCL, temperature and initial AIBN concentration; Table 2.1) on the ICAR ATRP process.

2.4.1 Reproducibility

In order to attest the reproducibility of the experimental procedure gravimetrical and SEC measurements are repeated five times under reference conditions (entry 7 in Table 2.1) and analyzed at distinct polymerization times. As shown in Figure 2.3 (trial 1-5), a relatively low maximum standard deviation (σ_{max}) value results for the evolution of the conversion, the number-average chain length (x_n) and the polydispersity index (PDI) with time. In Figure 2.3, the mentioned σ_{max} value is the standard deviation at the highest conversion, which can be expected since a significant increase in the viscosity of the reaction mixture at high conversion implies less sampling precision.

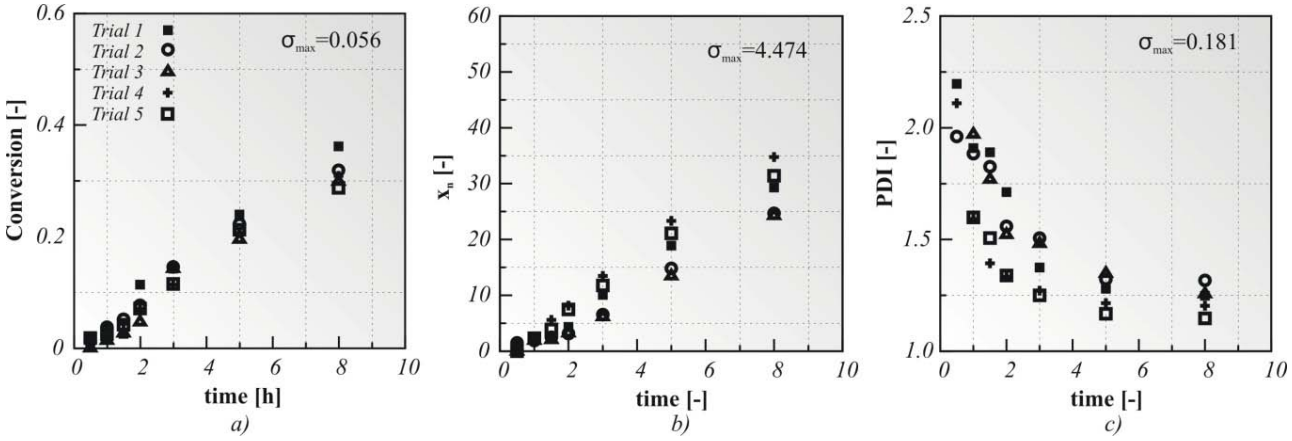

Figure 2.3: Reproducibility measurements for the ICAR ATRP of styrene at 70°C; $[Sty]_0/[EtBriB]_0/[CuBr_2/TPMA]_0/[AIBN]_0$: 100/1/0.005/0.2 (Table 2.1; entry 7); a) conversion profile determined by gravimetric analysis; b) number-average molar mass (x_n) and d) polydispersity index (PDI) determined by SEC using THF as solvent.

However, close inspection of Figure 2.4 reveals that on a conversion basis this increased error is somewhat filtered out, since the different trials lead to similar evolutions of x_n and PDI with conversion. In the remaining figures by convention only the maximum standard deviations are used for the error bars, implying however an overestimation of the error reported for data at low polymerization times/conversions.

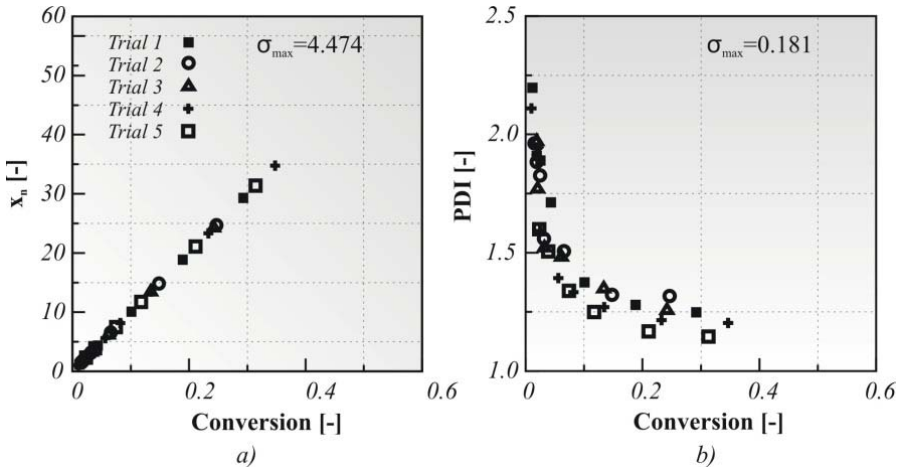

Figure 2.4: Reproducibility measurements for the 'bulk' ICAR ATRP of styrene at 70°C (Table 2.1; entry 7); a) number-average molar mass (x_n) and b) polydispersity index (PDI) as a function of monomer conversion; same conditions as in Figure 2.3.

Next to the reproducibility of the data obtained by gravimetric analysis and SEC, the accuracy of the measured conversion profile is determined. For such purpose, the consistency of the gravimetric analysis for the determination of the monomer conversion, as compared with the data determined by GC analysis, is verified. Figure 2.5 presents the results for two of the five trials in Figure 2.3. Clearly, very similar results are obtained using both methods. In fact, the same σ_{max} is obtained. In the remaining figures, for simplicity, only the gravimetric measured conversions are shown.

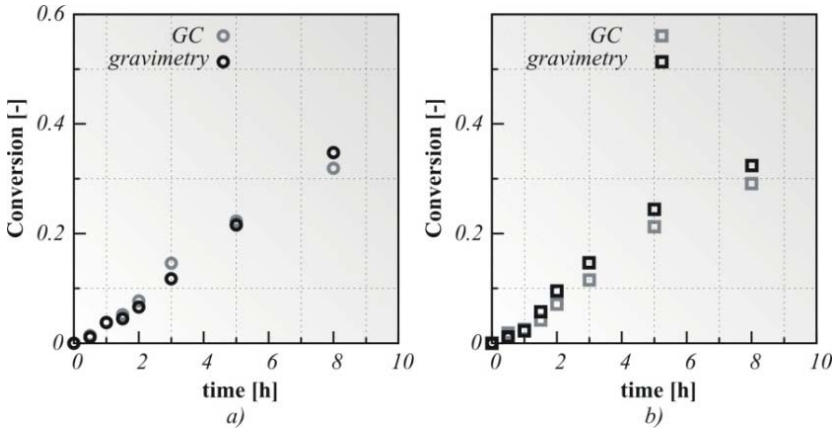

Figure 2.5: Comparison of monomer conversion data obtained by GC and gravimetric analysis for the bulk ICAR ATRP of styrene (Table 2.1; entry 7); a) trial 2 and b) trial 5 in Figure 2.4; in all cases initially 5 vol% of DMF is present; for the gravimetric analysis an error bar of σ_{max}=0.056 is considered.

2.4.2 Intrinsic activation/deactivation parameters

As shown in Table 2.2 for the activation of the ATRP initiator (EtBriB) with CuBr/TPMA a value of 1.7 10 L mol^{-1} s^{-1} is obtained at 70 °C, which is about 2 times higher than the value of Seeliger et al.[21] with CuBr/PMDETA in acetonitrile. This indicates that the expected decrease by going from acetonitrile to a styrene environment is compensated by the higher activity of CuBr/TPMA vs CuBr/PMDETA, in agreement with literature reports. Noteworthy, in both studies an activation energy close to 27 kJ mol^{-1} is obtained.

In addition, it follows from this table that the ATRP initiator activation is circa 1.5 times faster than the one of dormant macrospecies, indicative of a fast ATRP initiation. On the other hand, parameter adjustment with respect to the EtBriB conversion data (see further) revealed that the deactivation of the ATRP initiator radicals is ten times faster than the deactivation of macroradicals, counteracting the favored activation of the ATRP initiator species.

Furthermore, in agreement with earlier kinetic studies,[26] simulations revealed an optimal description of the experimental data in case temperature independent deactivation reactions are considered. In this work, a deactivation rate coefficient of 8.0 10^6 L mol^{-1} s^{-1} is obtained for the macrospecies, which is similar to the value of 2.2 10^6 L mol^{-1} s^{-1} reported by Matyjaszewski et al.[14] in the theoretical part of their kinetic study.

Finally, for the activation/deactivation process with the conventional radical initiator fragments literature data are used while assuming the same activation energies as for the ATRP initiator. However, as indicated above, and reconfirmed in this work these parameters have no significant influence on the main polymerization characteristics and thus the proposed strategy allows a straightforward determination of the ATRP specific activation/deactivation kinetic parameters.

2.4.3 Effect of initial deactivator concentration

For a fixed conventional radical initiator to ATRP initiator molar ratio ($[AIBN]_0/[EtBriB]_0$) of 0.2 and a fixed TCL ($[Sty]_0/[EtBriB]_0$) of 50, the effect of a

change in the initial concentration of deactivator (10, 25 and 50 ppm; entry 1-3 in Table 2.1) on the ICAR ATRP is shown in Figure 2.6. This figure presents the experimental and simulated conversion profiles and the evolution of the experimental and simulated x_n and PDI values with conversion. For each experimental point, error bars as defined above, i.e. using the maximum standard deviation σ_{max}, are indicated. Note that for the x_n and PDI values two error bars are shown, since these data are presented as a function of conversion for which there is also an experimental error.

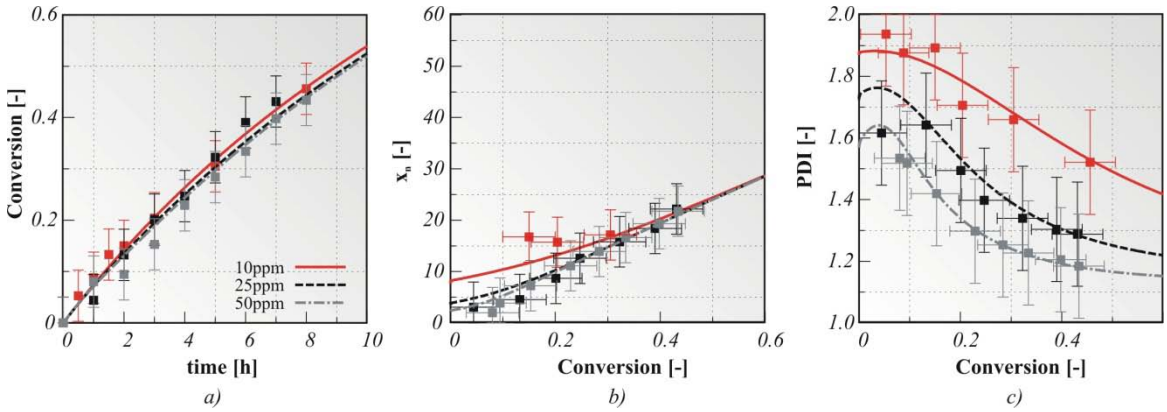

Figure 2.6: a) Conversion as a function of time, b) number- average chain length (x_n) and c) polydispersity index (PDI) as a function of conversion for the ICAR ATRP of styrene mediated by $CuBr_2$/TPMA at 70°C; $[Sty]_0/[EtBriB]_0/[CuBr_2/TPMA]_0/[AIBN]_0$: 50/1/y/0.2 with y: 0.0005 (10ppm; ■), 0.00125 (25ppm; ■) and 0.0025 (50ppm; ■); points correspond to experimental data (Table 2.1; entry 1-3) and lines correspond to the calculated values with the set of parameters given in Table 2.2, for continuity equations see D'hooge et al.[25]

Clearly, the experimental trends are captured well by the kinetic model and in agreement with literature studies[14, 19, 20] only a slightly faster polymerization (Figure 2.6a) is obtained when lower initial catalyst concentrations are employed. This is also confirmed in Figure 2.7a, which shows the corresponding simulated changes of the radical concentration. However, form Figure 2.6b-c it follows that the level of control is significantly reduced. The latter is due to a decrease of the number of available deactivator molecules present in the polymerization mixture to maintain the polymer chains in a dormant state and to generate activator molecules. In particular, a too low amount of activator molecules implies a slower ATRP initiation (Figure 2.7b)

explaining therefore the higher PDI values for lower Cu ppm levels. For such prolonged ATRP initiation, less monomer molecules are available to compensate for the chain length difference induced due to non-instantaneous ATRP initiation, once all R_0X is consumed.

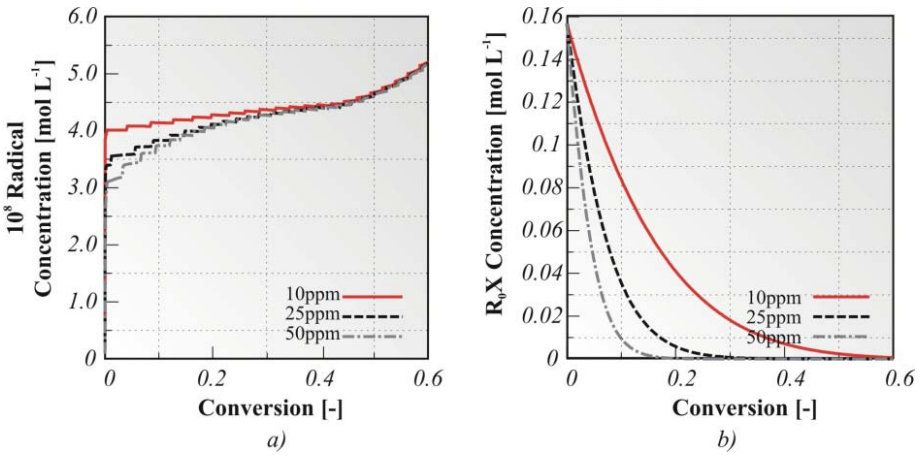

Figure 2.7: Concentrations of a) macroradicals and b) ATRP initiator (R_0X) as a function of monomer conversion calculated with the set of parameters given in Table 2.2, for continuity equations see D'hooge et al.[25]; The conditions are the same as presented in Figure 2.6.

Moreover, the reduced control over chain length for the ICAR ATRP process for low Cu ppm levels can be understood from a comparison of the activation/deactivation rates of the ATRP initiator species, the macrospecies, and the conventional radical initiator derived species. In Figure 2.8, it is shown that for 10 ppm of Cu (Table 2.1; entry 4) the pseudo activation/deactivation equilibrium for the macrospecies (Figure 2.8(a)) is obtained at a higher conversion compared to the case in which 50ppm of Cu are used (Table 2.1; entry 7). In agreement with D'hooge et al.,[19] a controlled ICAR ATRP process can only be obtained in case this pseudo-equilibrium is established sufficiently fast. Note that in both cases the pseudo-equilibrium for the macrospecies starts when the activation/deactivation ATRP initiator rates (Figure 2.8(b)) tend to zero and that, as required for a controlled ICAR ATRP, the activation/deactivation rates related to conventional radical initiator species (Figure 2.8(c)) are well balanced throughout the polymerization.

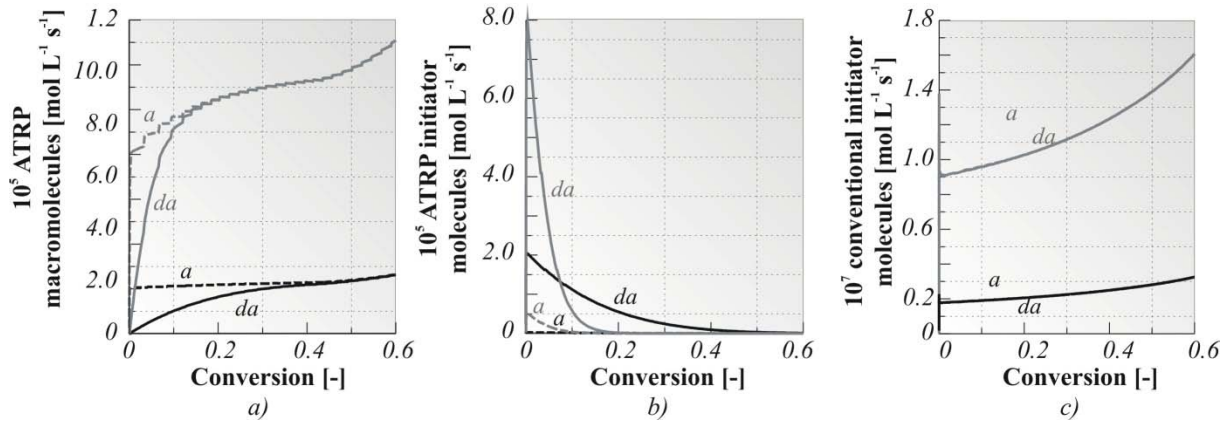

Figure 2.8: Activation (*a*) and deactivation (*da*) rates for the ICAR ATRP of styrene at 70 °C calculated with the set of parameters given in Table 2.2, for continuity equations see D'hooge et al.[25]; a) ATRP macromolecules, b) ATRP initiator molecules and c) conventional initiator molecules; full lines: deactivation; dashed lines: activation; black lines: 10 ppm (Table 2.1; entry 4); grey lines: 50 ppm (Table 2.1; entry 7).

2.4.4 Effect of targeted chain length

The effect of the initial monomer to ATRP initiator ratio, i.e. TCL, is investigated while fixing the conventional radical initiator to ATRP initiator molar ratio ($[AIBN]_0/[EtBriB]_0$) to 0.2. Figure 2.9 illustrates the effect of TCL for the three different initial Cu concentrations employed in this study, i.e. 10, 25 and 50 ppm (with respect to monomer; entry 1-5, 7, 9-14 in Table 2.1). Again a comparison between experimental and simulated data indicates that the proposed intrinsic activation/deactivation parameters are capable of describing well the experimental observations.

In agreement with other CRP processes and in particular as previously reported for normal ATRP,[8, 19, 20] a significant increase in TCL implies a lower polymerization rate with a notable improvement of the control over chain length. This better control can be expected since a higher TCL provokes a faster ATRP initiation (Figure 2.10; 50 ppm), similar to the effect of a reduced ppm level for a fixed TCL, as explained above.

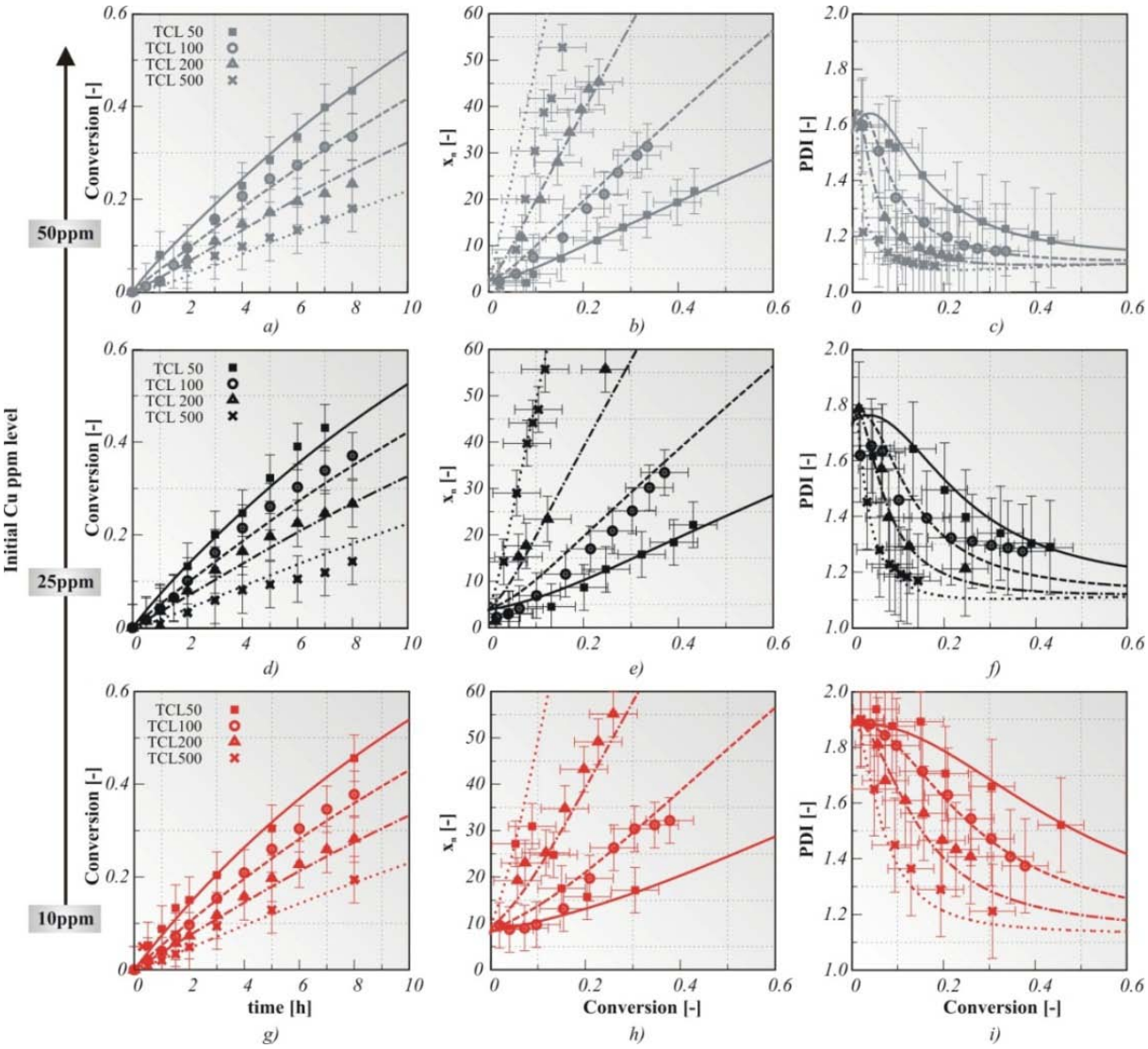

Figure 2.9: Conversion (a, d, g) as a function of time, number-average chain length (x_n) (b, e, h) and polydispersity index (PDI) (c, f, i) as a function of conversion for the ICAR ATRP of styrene mediated by 50 (top row), 25 (middle row) and 10ppm (bottom row) of $CuBr_2$/TPMA at 70°C; $[Sty]_0/[EtBriB]_0/[CuBr_2/TPMA]_0/[AIBN]_0$: w/1/y/0.2 with (w-y: top row): 50-0.0025 (■), 100-0.005 (●), 200-0.01 (▲) and 500-0.025 (×), (w-y: middle row): 50-0.00125 (■), 100-0.0025 (●), 200-0.005 (▲) and 500-0.0125 (×) and (w-y: bottom row): 50-0.0005 (■), 100-0.001 (●), 200-0.002 (▲) and 500-0.005 (×); points correspond to experimental data (Table 2.1; entry 1-5,7, 9-14) and lines correspond to the calculated values with the set of parameters given in Table 2.2, for continuity equations see D'hooge et al.[25]

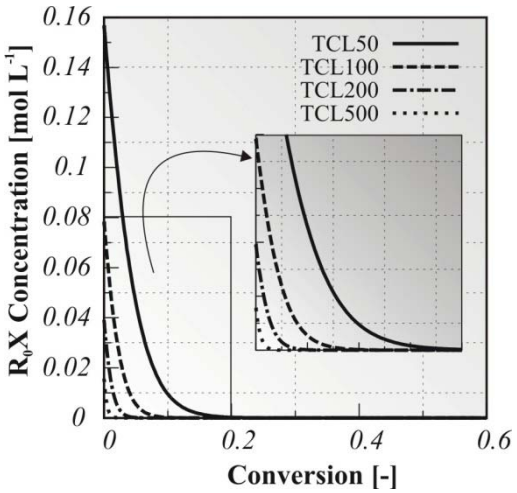

Figure 2.10: ATRP initiator concentration as a function of monomer conversion calculated with the set of parameters given in Table 2.2, for continuity equations see D'hooge et al.[25]; ICAR ATRP of styrene using 50 ppm of $CuBr_2$/TPMA presented in Figure 2.9 (top row) (Table 2.1; entry 3, 7, 11 and 14).

2.4.5 Effect of polymerization temperature

For a fixed TCL of 100, 50 ppm of Cu and an initial molar ratio of conventional radical initiator to ATRP initiator of 0.2 ($[AIBN]_0/[EtBriB]_0$), Figure 2.11a shows that the ATRP initiator related activation/deactivation kinetic parameters in Table 2.2 capture well the experimental tendencies of the conversion of the ATRP initiator. In this figure, for three polymerization temperatures (entry 6-8 in Table 2.1) a comparison between experimental and simulated data is given, which supports the reliability of the followed approach for the model tuning in this work. As can be expected, the fastest ATRP initiation is obtained for the highest polymerization temperature. At 80 °C it takes only half an hour before the ATRP initiator has disappeared, whereas three hours are required at 60 °C. At the latter temperature the non-activated deactivation reaction is relatively more important, explaining thus this effect.

However, for the studied ATRP system the relevance of differentiating between activation/deactivation involving ATRP initiator and macrospecies for the control over chain length is not significant as can be interfered from Figure 2.12. In this figure, the PDI profile of Figure 2.11 (dashed lines, Table 2.1; entry 8) is compared with the one obtained when assuming for the initiator species the same activation/deactivation

intrinsic kinetic parameters as for the macrospecies. Clearly, the simulation results coincide, indicating that for modeling purposes only, it is sufficient to assume equal reactivity for activation/deactivation reaction steps involving ATRP initiator and macrospecies.

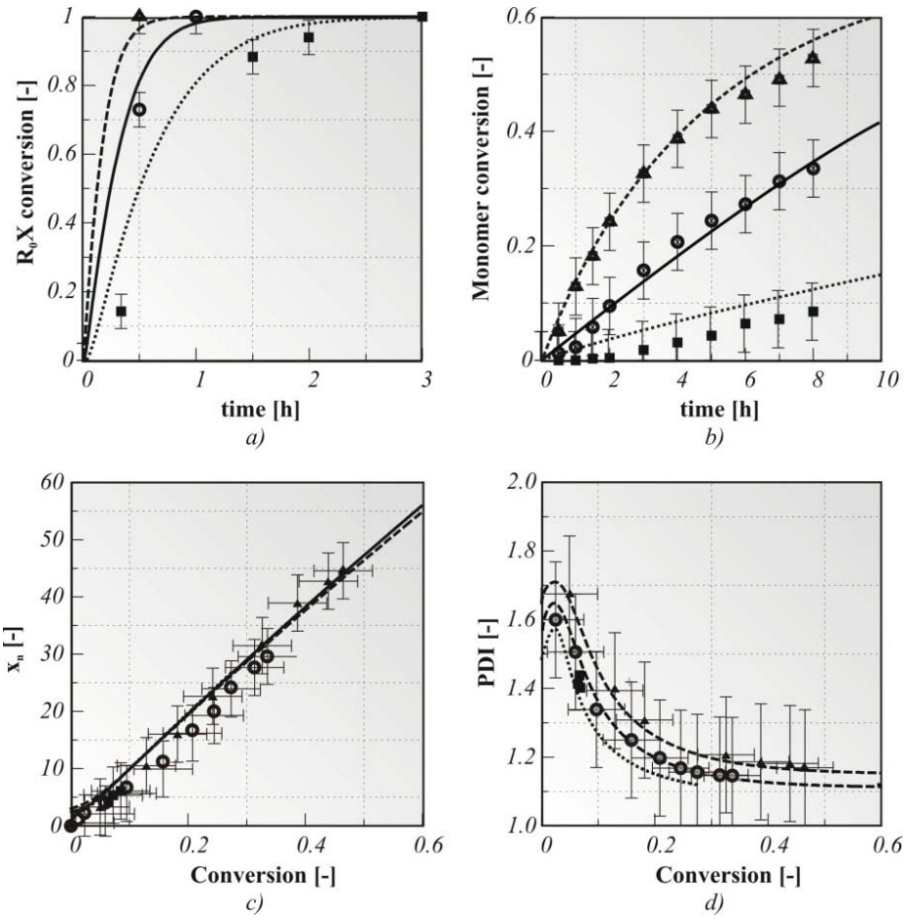

Figure 2.11: a) conversion of R_0X as a function of time, b) monomer conversion profile as a function of time, c) number-average chain length (x_n) and c) polydispersity index (PDI) as a function of conversion ICAR ATRP of styrene by $CuBr_2$/TPMA at 60°C (dotted lines; ■), 70°C (full lines; ●) and 80°C (dashed lines; ▲); $[Sty]_0/[EtBriB]_0/[CuBr_2/TPMA]_0/[AIBN]_0$: 100/1/0.005/0.2; points correspond to experimental data (Table 2.1; entry 6, 7 and 8) and lines correspond to the calculated values with the set of parameters given in Table 2.2, for continuity equations see D'hooge et al.[25]

Figure 2.11(b-d) shows the corresponding profiles for the monomer conversion and control over chain length. Clearly, a significant higher polymerization rate is attained at higher polymerization temperatures. Such acceleration can be expected, since previous kinetic modeling studies revealed that the polymerization rate in ICAR ATRP

is mainly influenced by the conventional radical initiator species, which dissociate faster at higher temperature allowing a faster activator (re)generation. On the other hand, a temperature variation has less impact on the control over chain length, since only slightly higher PDI values are obtained at a higher polymerization temperature.

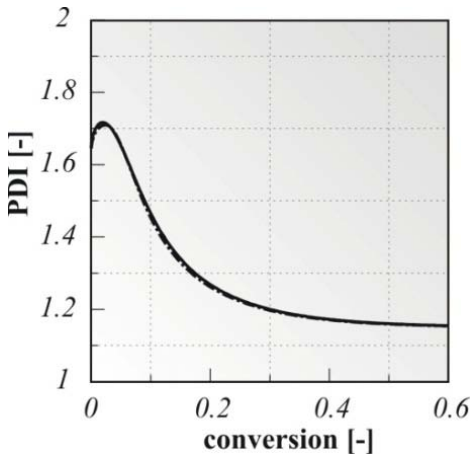

Figure 2.12: Relevance of differentiation of activation/deactivation kinetic parameters between ATRP initiator and macrospecies; Table 2.1, entry 8 (full lines) are compared with those obtained assuming for the initiator species the same activation/deactivation intrinsic kinetic parameters as for the macrospecies (dashed lines); values calculated with the set of parameters given in Table 2.2, for continuity equations see D'hooge et al.[25]

Finally, it should be noted that in particular, the experimental conversion and PDI data in Figure 2.11 are significantly different, allowing the determination of temperature dependent approximate values for the activation/deactivation intrinsic kinetic parameters.

2.4.6 Effect of initial AIBN concentration

Finally, Figure 2.13 shows the effect of the initial AIBN concentration at 80°C with 50ppm of Cu catalyst and selecting a TCL of 100 (entry 8,15 and 16 in Table 2.1). As can be expected a faster ICAR ATRP results for a higher initial conventional radical initiator amount. However, a significant rate acceleration is only obtained for a very high initial AIBN concentration, which is accompanied by a reduced control over chain length as evidenced by the higher PDI values tending toward the typical values obtained in free radical polymerization (FRP). In other words, in order to successfully perform an ICAR ATRP with a low ppm Cu level it is crucial to select an initial

conventional radical initiator concentration which allows a reasonable control over the ATRP process within reasonable polymerization time.

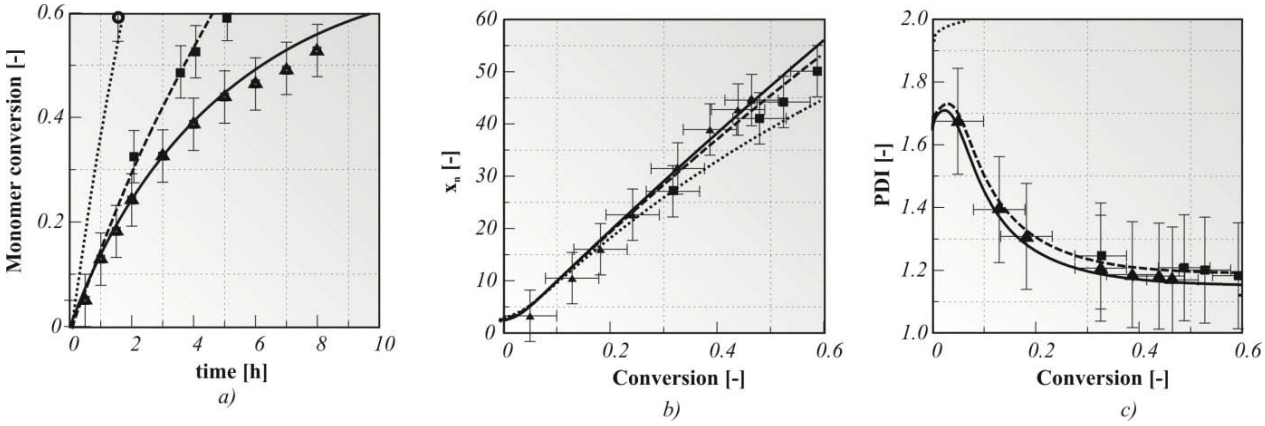

Figure 2.13: a) conversion profile as a function of time, b) number-average chain length (x_n) and c) polydispersity index (PDI) as a function of conversion in the ICAR ATRP of styrene mediated by $CuBr_2$/TPMA at 80°C; $[Sty]_0/[EtBriB]_0/[CuBr_2/TPMA]_0/[AIBN]_0$: 100/1/0.005/y with y: 0.2 (full lines, ▲), 0.3 (dashed lines; ■) and 2 (dotted lines and ● in the conversion profile); for x_n experimental values when y:2 are not shown; for PDI calculated values when y:2 are higher than 2.0; points correspond to experimental data values (Table 2.1; 8, 15 and 16). and lines correspond to the calculated values with the set of parameters given in Table 2.2, for continuity equations see D'hooge et al.[25]

2.5 Conclusions

For the ICAR ATRP of styrene using $CuBr_2$/TPMA as deactivator and EtBriB and AIBN respectively as ATRP and conventional radical initiator, an extensive set of experimental data covering a broad variation of the initial Cu(II) and AIBN concentration, targeted chain length (TCL), and polymerization temperature is reported. Kinetic modeling of the observed experimental trends allows for the first time the assessment of activation/deactivation Arrhenius parameters for EtBriB as well as for the polystyryl-species. In particular ICAR ATRP is proven to be a versatile technique to determine such kinetic parameters, since it allows relatively fast polymerization and avoids the difficult handling of the starting air-sensitive materials and the determination of additional interfering kinetic parameters.

The simulations confirm the high catalytic activity of CuBr/TPMA. Moreover deactivation is shown to be non-activated, whereas the activation reactivity is moderately temperature dependent. Additional measurements of the ATRP initiator conversion allowed to reveal that the deactivation of ATRP initiator radicals is ten times faster than the deactivation of the macroradicals. However, for the simulations of the ICAR ATRP process as such, it suffices to assume the same intrinsic kinetic activation/deactivation parameters for ATRP initiator and macrospecies.

Overall, it can be concluded that depending on the desired characteristics of the polymer and prospective applications, ICAR ATRP can be employed to synthesize well-defined polystyrene, in case appropriate polymerization conditions are selected. However, a meaningful decrease of the Cu concentrations (< 50ppm), as desired for the industrial application of ATRP processes, causes an unavoidable reduction of the level of control over chain length. In addition, too high initial AIBN concentrations should not be considered to avoid a FRP behavior.

References

[1] K. Matyjaszewski; N. V. Tsarevsky, *Nature Chemistry* **2009,** *1*, 276-288.

[2] K. Matyjaszewski; J. H. Xia, *Chemical Reviews* **2001,** *101*, 2921-2990.

[3] N. V. Tsarevsky; K. Matyjaszewski, *Chemical Reviews* **2007,** *107*, 2270-2299.

[4] K. Matyjaszewski; Y. Gnanou; L. Leibler, Macromolecular Engineering. In *Macromolecular Engineering*, Wiley-VCH Verlag GmbH & Co. KGaA: **2007**; pp 1-6.

[5] K. Matyjaszewski; T. P. Davis, *Handbook of Radical Polymerization*. Wiley Interscience Hoboken, **2002**.

[6] C. Barner-Kowollik, *Handbook of RAFT polymerization*. Wiley-VCH Verlag GmbH & Co. KGaA: Weinheim, **2008**.

[7] C. Barner-Kowollik; J. P. Blinco; M. Destarac; K. J. Thurecht; S. Perrier, *Reversible Addition Fragmentation Chain Transfer (RAFT) Polymerization:*

Mechanism, Process and Applications.In *Encyclopedia of Radicals in Chemistry, Biology and Materials*, **2012**.

[8] L. Bentein; D. R. D'Hooge; M. F. Reyniers; G. B. Marin, *Macromolecular Theory and Simulations* **2011,** *20*, 238.

[9] W. A. Braunecker; K. Matyjaszewski, *Progress in Polymer Science* **2008,** *33*, 165.

[10] S. Gaynor; D. Greszta; D. Mardare; M. Teodorescu; K. Matyjaszewski, *J Macromol Sci-Pure Appl Chem* **1994,** *A31*, 1561.

[11] R. P. N. Veregin; P. G. Odell; L. M. Michalak; M. K. Georges, *Abstracts of Papers of the American Chemical Society* **1996,** *212*, 88-POLY.

[12] Y. Kwak; A. J. D. Magenau; K. Matyjaszewski, *Macromolecules* **2011,** *44*, 811-819.

[13] K. Matyjaszewski, *Controlled/Living Radical Polymerization: Progress in ATRP, NMP and RAFT*. ACS: Washington, **2000**.

[14] K. Matyjaszewski; W. Jakubowski; K. Min; W. Tang; J. Y. Huang; W. A. Braunecker; N. V. Tsarevsky, *Proc Natl Acad Sci USA* **2006,** *103*, 15309.

[15] L. Mueller; K. Matyjaszewski, *Macromolecular Reaction Engineering* **2010,** *4*, 180.

[16] T. Pintauer; K. Matyjaszewski, *Chemical Society Reviews* **2008,** *37*, 1087.

[17] Y. Z. Zhang; Y. Wang; C. H. Peng; M. J. Zhong; W. P. Zhu; D. Konkolewicz; K. Matyjaszewski, *Macromolecules* **2012,** *45*, 78-86.

[18] Q. Lou; D. A. Shipp, *Chemphyschem* **2012,** *13*, 3257-3261.

[19] D. R. D'Hooge; D. Konkolewicz; M. F. Reyniers; G. B. Marin; K. Matyjaszewski, *Macromolecular Theory and Simulations* **2012,** *21*, 52.

[20] C. Toloza Porras; D. R. D'Hooge; M. F. Reyniers; G. B. Marin, *Macromolecular Theory and Simulations* **2012**.

[21] F. Seeliger; K. Matyjaszewski, *Macromolecules* **2009,** *42*, 6050.

[22] A. Goto; T. Fukuda, *Macromol Rapid Commun* **1999,** *20*, 633-636.

[23] T. Pintauer; W. Braunecker; E. Collange; R. Poli; K. Matyjaszewski, *Macromolecules* **2004,** *37*, 2679-2682.

[24] W. Tang; Y. Kwak; W. Braunecker; N. V. Tsarevsky; M. L. Coote; K. Matyjaszewski, *Journal of the American Chemical Society* **2008,** *130*, 10702-10713.

[25] D. R. D'Hooge; M. F. Reyniers; F. J. Stadler; B. Dervaux; C. Bailly; F. E. Du Prez; G. B. Marin, *Macromolecules* **2010,** *43*, 8766.

[26] Y. Fu; A. Mirzaei; M. F. Cunningham; R. A. Hutchinson, *Macromolecular Reaction Engineering* **2007,** *1*, 425-439.

[27] W. Jakubowski; K. Min; K. Matyjaszewski, *Macromolecules* **2006,** *39*, 39.

[28] G. S. Moad, D., *The chemistry of free radical polymerization*. Elsevier Science Ltd.: Oxford, **1995**.

[29] R. W. Simms; M. E. Cunningham, *Macromolecular Symposia* **2008,** *261*, 32-35.

[30] J. F. Lutz; K. Matyjaszewski, *Journal of Polymer Science Part a-Polymer Chemistry* **2005,** *43*, 897-910.

[31] K. Matyjaszewski; T. E. Patten; J. H. Xia, *Journal of the American Chemical Society* **1997,** *119*, 674-680.

[32] J. H. Xia; K. Matyjaszewski, *Abstracts of Papers of the American Chemical Society* **1996,** *212*, 164-POLY.

[33] O. Delgadillo-Velazquez; E. Vivaldo-Lima; I. A. Quintero-Ortega; S. P. Zhu, *Aiche Journal* **2002,** *48*, 2597-2608.

[34] A. D. Peklak; A. Butte; G. Storti; M. Morbidelli, *Journal of Polymer Science Part a-Polymer Chemistry* **2006,** *44*, 1071-1085.

[35] A. R. Wang; S. P. Zhu, *Abstracts of Papers of the American Chemical Society* **2002,** *224*, U363-U363.

[36] P. B. Zetterlund, *Macromolecules* **2010,** *43*, 1387-1395.

[37] D. S. Achilias; C. Kiparissides, *Macromolecules* **1992,** *25*, 3739-3750.

[38] J. Wieme; D. R. D'Hooge; M. F. Reyniers; G. B. Marin, *Macromolecular Reaction Engineering* **2009,** *3*, 16-35.

[39] A. Nabifar; N. T. McManus; E. Vivaldo-Lima; L. M. F. Lona; A. Penlidis, *Chemical Engineering Science* **2009,** *64*, 304-312.

[40] J. Gao; A. Penlidis, *Journal of Macromolecular Science, Part C* **1996,** *36*, 199-404.

[41] G. Moad; D. H. Solomon, *The Chemistry of Free Radical poylmerization*. Elsevier Science Ltd: Oxford, **1995**.

[42] G. Johnston-Hall; M. J. Monteiro, *Journal of Polymer Science Part a-Polymer Chemistry* **2008,** *46*, 3155-3173.

[43] J. Brandup; E. H. Immergut; E. A. Grulke; A. B. Abe, D. R., *Polymer Handbook*. 4th Edition ed.; John wiley & Sons: New York, **1999**.

[44] M. Buback; R. G. Gilbert; R. A. Hutchinson; B. Klumperman; F. D. Kuchta; B. G. Manders; K. F. Odriscoll; G. T. Russell; J. Schweer, *Macromolecular Chemistry and Physics* **1995,** *196*, 3267-3280.

[45] N. M. Ahmad; B. Charleux; C. Farcet; C. J. Ferguson; S. G. Gaynor; B. S. Hawkett; F. Heatley; B. Klumperman; D. Konkolewicz; P. A. Lovell; K. Matyjaszewski; R. Venkatesh, *Macromol Rapid Commun* **2009,** *30*, 2002.

[46] G. Johnston-Hall; A. Theis; M. J. Monteiro; T. P. Davis; M. H. Stenzel; C. Barner-Kowollik, *Macromolecular Chemistry and Physics* **2005,** *206*, 2047-2053.

[47] G. B. Smith; G. T. Russell; J. P. A. Heuts, *Macromolecular Theory and Simulations* **2003,** *12*, 299-314.

[48] C. Barner-Kowollik; G. T. Russell, *Prog Polym Sci* **2009,** *34*, 1211.

Chapter 3: Computer aided optimization of conditions for fast and controlled ICAR ATRP of *n*-butyl acrylate

Summary

The potential of Initiators for Continuous Activator Regeneration Atom Transfer Radical Polymerization (ICAR ATRP) for the synthesis of well-defined poly(*n*-butyl acrylate), i.e. with predetermined chain length and branching level, low polydispersity index (PDI) and high end-group functionality (EGF) is analyzed by means of simulations. The kinetic model accounts for reactivity differences in activation/deactivation between secondary and tertiary macrospecies and considers the possible influence of diffusional limitations. Copper (II) bromide is used as transition metal salt and the commercially available N,N,N',N'',N''-pentamethyldiethylenetriamine as ligand. For targeted chain lengths (TCLs) up to 1000, the ICAR ATRP can be performed relatively fast and with ppm levels of ATRP catalyst. For moderate TCLs, slightly higher ppm levels are required if an excellent control over chain length is also desired. In all cases, limited loss of end-group functionality (EGF) results. This work has been published in *Macromolecular Theory and Simulations* 2012, DOI 10.1002/mats.2012200074

3.1 Introduction

Industrial production of polymers is often carried out by free radical polymerization (FRP) since this polymerization technique is applicable to a wide range of monomers, tolerant to impurities and economically beneficial compared to other chain-growth polymerization techniques.[1, 2] In particular, acrylate based polymers contribute significantly to the polymer market as evidenced by their use in a wide variety of applications covering mainly paints, adhesives, textiles and coatings.[3] Typically, polyacrylates are produced via emulsion polymerization but depending on the required production scale and the area of application, solution and bulk FRP are also of practical importance.[3, 4]

For some of the polyacrylates applications, the production process could benefit from a better control over end-group functionality (EGF). For instance, in the coating industry, the controlled incorporation of EGF in the polymer could avoid the use of expensive functional monomers. Moreover, advanced well-defined macromolecular architectures, such as linear gradient copolymers and star-shaped polymers with controlled arm length, cannot by obtained by FRP due to the inherent difficulty to control EGF and chain length. Therefore, in the last decades a variety of so-called controlled radical polymerization (CRP) techniques have been developed at laboratory scale in which a mediating agent (e.g. a nitroxide or a transition metal complex) is added allowing control over the polymer microstructure and thus the synthesis of complex polymer topologies and compositions, involving polyacrylate segments.[5-11]

Since polyacrylates are manufactured almost exclusively by radical polymerization (RP)[3] a thorough understanding of the interplay of the radical reactions involved in its production is of paramount importance. Of special interest are chain transfer to polymer and βC-scission reactions,[12-15] which influence polymer properties, such as the average chain length and branching content. These properties can be directly manipulated in view of the desired application of the final polymer product, e.g. by promoting or inhibiting the occurrence of side reactions.[16-18] Short chain branches (SCBs) originate after propagation of tertiary macroradicals that are generated via intramolecular chain transfer to polymer, i.e. backbiting (left reaction path in Figure 3.1), which consists of self-abstraction of a hydrogen atom from the backbone of a secondary macroradical, mainly involving a cyclic six-membered transition state.[16] In addition, due to the higher stability of the tertiary macroradicals a rate retardation takes place in case backbiting is sufficiently important. On the other hand, long chain branches (LCBs) typically result after propagation of tertiary macroradicals formed by intermolecular chain transfer to polymer (right reaction path in Figure 3.1), in which a secondary macroradical abstracts a hydrogen atom from another polymer chain generating a tertiary macroradical and a dead polymer chain. Alternatively, at elevated temperatures LCBs can be obtained after addition of macroradicals to macromonomers that are formed by βC-scission. However, several kinetic studies have indicated that

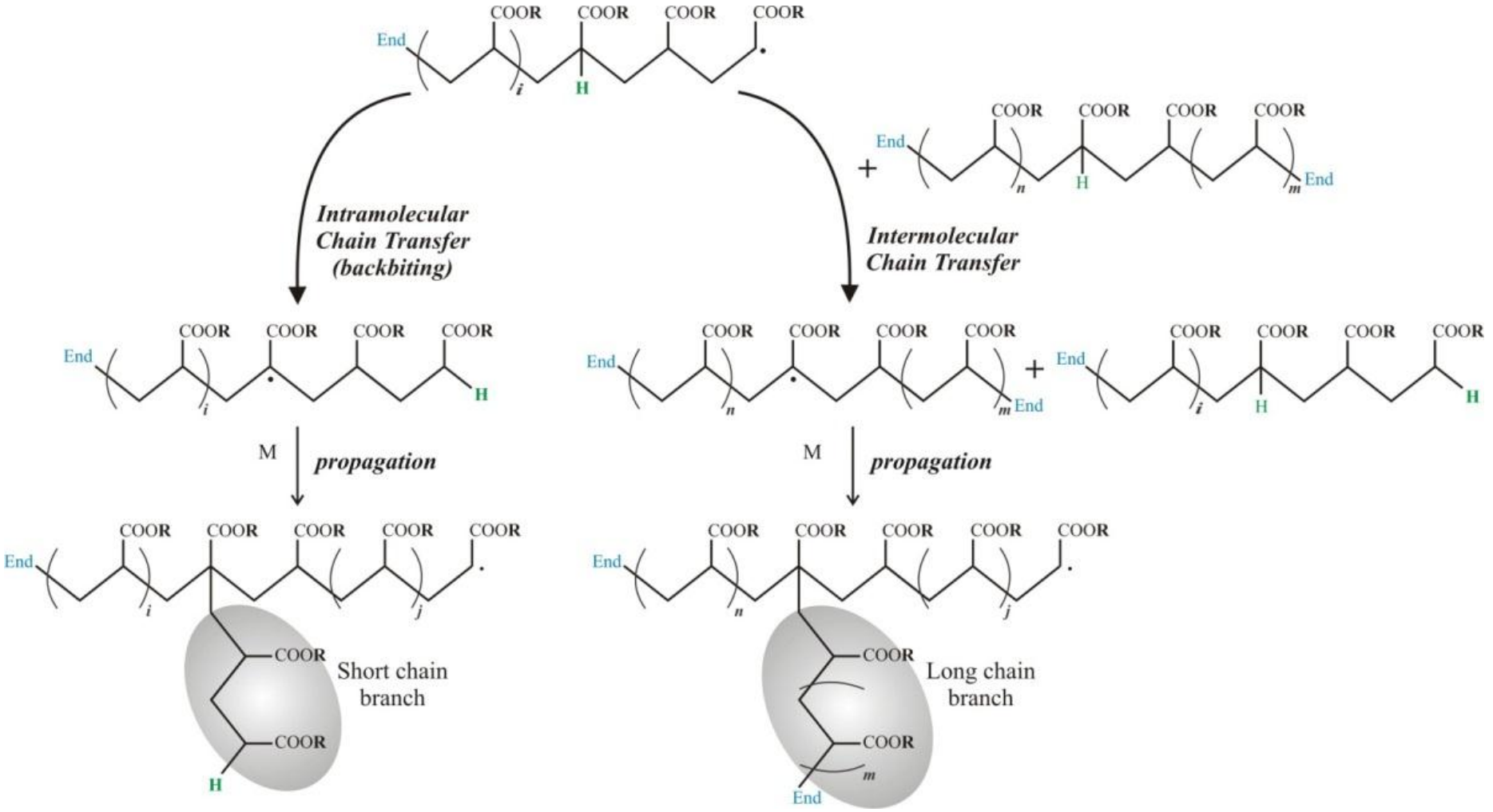

Figure 3.1: Mechanism of chain transfer to polymer reactions in acrylate polymerization. End denotes the ATRP initiator fragment or a hydrogen atom. For *n*BuA polymerization, R corresponds to a *n*-butyl group; M stands for monomer.

the contribution of LCBs to the total amount of branches is very low, especially at low to intermediate conversions.[15, 19-23]

In contrast to RP of ethylene and vinyl acetate in which the occurrence of chain transfer to polymer reactions is a long-standing fact that has been well documented since its discovery more than a half century ago,[24-28] the importance of branching in acrylate RP has only emerged in the early nineties by the detection of quaternary carbons via ^{13}C NMR spectroscopy.[29-31] Interestingly, Ahmad et al.[32] have recently reported that the branching level of poly(*n*-butyl acrylate) can be reduced significantly by performing a CRP instead of a FRP.

One of the most frequently used CRP techniques is (normal) Atom Transfer Radical Polymerization (ATRP),[33, 34] the principle of which is given in Figure 2.1a (Chapter 2). During the polymerization macroradicals (R_i; i: chain length) are temporarily and catalytically deactivated by a transition metal complex (M_t^nX/L) to a dormant form (R_iX), which contains EGF (X). Typically, the ATRP is started with ATRP initiator (R_0X) and activator in absence of deactivator ($M_t^{n+1}X_2/L$). For sufficiently high deactivation rates, termination reactions can be suppressed resulting in a high EGF, i.e. almost no dead polymer molecules are formed. If the ATRP initiation is fast, a polymer characterized by a low polydispersity index (PDI) can be obtained as well.

Crucial for control of the branching level in polyacrylates is the selection of the ATRP catalyst. Based on simulations, Reyes and Asua[35] indicated that ATRP catalysts, which can strongly deactivate macroradicals ,are necessary to obtain a lower branching level than in FRP, in which no mediating agent is present. Later on, Konkolewicz et al.[23, 36] showed that the branching level is also influenced by activation, and is to a large extent determined by the relative importance of the rate of backbiting and tertiary propagation. Only if these two rates are well-balanced from low conversion onwards, ATRP provides branching levels as high as FRP. Moreover, these authors pointed out that the branching level can be increased by increasing the targeted chain length (TCL), i.e. the initial molar ratio of monomer to ATRP initiator.

Even though selection of the appropriate ATRP catalyst enables the synthesis of well-defined polyacrylates and purification methods are available for its removal,[37-41] the amount of catalyst in a normal ATRP process is too high to obtain an economic profitable process.[1, 42] Therefore, in the last years, ATRP modified techniques[5, 43-54] have been developed in which a low catalyst concentration (ppm level with respect to monomer) is employed. Importantly, these techniques can be applied using commercially available ligands, are more environmentally friendly and avoid the oxygen sensitivity of the activator upon storage. Furthermore, they can be carried out within polymerization times similar to industrially applied RP's (~ ≤ 8h). In contrast, normal ATRP processes typically take longer than one day when using low catalyst amounts.

One of the most important techniques to reduce the amount of ATRP catalyst is Initiators for Continuous Activator Regeneration (ICAR) ATRP,[43] in which the polymerization is started in the presence of a conventional radical initiator (I_2), ATRP initiator (R_0X) and deactivator ($M_t^{n+1}X_2/L$). Thermal dissociation of I_2 provides a source of free radicals from which activator molecules (M_t^nX/L), are continuously generated, allowing activation of the ATRP initiator and thus the occurrence of the same reactions as in normal ATRP (Figure 2.1b) (Chapter 2).

Recent simulations[55] have shown that in ICAR ATRP the control over polymerization rate and polymer properties can be directly manipulated by adjusting the polymerization conditions. For instance, it was demonstrated that, depending on the ATRP catalyst reactivity, step-wise addition of conventional radical initiator in the ICAR ATRP of methyl methacrylate and styrene is needed to reach high conversion while still obtaining a good livingness and control over chain length with ppm levels of ATRP catalyst. Moreover, Konkolewicz et al.[56] recently reported for the first time the successful ICAR ATRP of oligo(ethylene oxide) methyl ether acrylate in water using a low (< 100) ppm level of ATRP catalyst further proving the importance of this modified ATRP technique for a broad range of monomers and in particular acrylates. Additionally, the potential of ICAR ATRP for the controlled production of polyacrylates can be inferred from the new polymeric materials prepared via normal

ATRP. For example, Auschra et al.[4] reported the development of new pigment dispersants for the formulation of high solids and waterborne coatings using *n*-butyl acrylate (*n*BuA) and dimethylaminoethyl acrylate (DMAEA) as monomers.

Alternatively, well-defined polyacrylates can be synthesized while using low catalyst amounts through activators regenerated by electron transfer (ARGET) ATRP[47, 57] or electrochemically mediated ATRP (*e*ATRP)[48] in which the activator is regenerated from a reducing agent or by reduction at an electrode. In the presence of metallic copper, a so-called supplementary activator and reducing agent (SARA) ATRP or single electron transfer living radical polymerization (SET-LRP) can be also obtained depending on comproportionation or disproportionation being the dominant side reaction path for the involved catalytic species.[58-60] In particular for methyl acrylate, Chan et al.[61] and Kwak et al.[57] have recently successfully combined ARGET ATRP and the use of a copper wire reducing significantly the residual catalyst amount up to 10 ppm for a TCL of ca. 100.

However, both for ICAR ATRP and these alternative techniques, only a limited number of kinetic studies are available in which the influence of the TCL and catalyst amount on the polymerization rate and control over polymer properties is mapped in detail.[56-58, 62-64] Such information is crucial for a comparison of these techniques to evaluate their potential industrial application, since the ultimate goal of a CRP technique is to produce a wide range of average chain lengths at acceptable polymerization rates while preserving control over PDI and EGF. In this work, such detailed kinetic modeling study is presented for the bulk ICAR ATRP of *n*BuA using the commercially available *N*,*N*,*N'*,*N''*,*N''*- pentamethyl diethylenetriamine (PMDETA) as ligand and copper (II) bromide ($CuBr_2$) as transition metal salt. A similar modeling approach can be followed for other related CRP techniques avoiding time consuming experimental screening procedures for a given catalyst.

The activation/deactivation kinetic parameters are assessed based on the experimental data of Ahmad et al.[32] for the normal bulk ATRP of *n*BuA taking into account the reactivity difference between secondary and tertiary macrospecies. The kinetic model also considers the possible influence of diffusional limitations on termination and

deactivation. For TCLs up to thousand, it is shown that ICAR ATRP can be successfully applied to synthesize well-defined poly(*n*BuA) with ppm levels of ATRP catalyst within reasonable polymerization time and with limited loss of EGF. The simulation results confirm in particular the potential of CRP techniques using low amounts of copper for the controlled incorporation of EGF in polymer chains. Diffusional limitations are shown to be most important on secondary deactivation leading to a rate acceleration at high conversion.

3.2 Kinetic model

The reaction scheme used in the kinetic modeling of the bulk ATRP of *n*BuA and the corresponding intrinsic kinetic parameters are summarized in Table 3.1. Activation, deactivation, backbiting and βC-scission are included next to typical radical polymerization (RP) reactions, i.e. propagation, chain transfer to monomer and termination. A distinction is further made between the reactivity of secondary (s) and tertiary (t) macrospecies. For simplicity, intermolecular chain transfer to polymer is neglected since literature reports indicate that LCBs barely contribute to the total branching content.[15, 19-23] Similarly, termination by disproportionation[65, 66] and addition reactions involving macromonomers are neglected in a first approximation.[67]

The ATRP catalyst and initiator are the same as those used by Ahmad et al.[32] in their experimental study of the bulk normal ATRP of *n*BuA at 105 ^{0}C, i.e. CuBr/PMDETA and methyl 2-bromopropionate (MBrP). For the reactions common with FRP, intrinsic rate coefficients reported in literature are used.[69-72] For activation of the ATRP initiator a value of 3.1 L mol^{-1}s^{-1} is considered based on the experimental study of Seeliger et al.[68] The remaining secondary and tertiary activation and deactivation intrinsic rate coefficients are adjusted according to the experimental data of Ahmad et al.[32] As discussed below, the obtained values are consistent with literature values and confirm the higher stability of tertiary macrospecies.

Table 3.1: Reactions involved in the bulk normal/ICAR ATRP of *n*-butyl acrylate and their intrinsic kinetic parameters ($k_{l,chem}$); i,j=chain length; $R_{i,t}$ and $R_{i,s}$: tertiary and secondary macroradicals; k_l^{app}: apparent rate coefficient for the reaction step *l*; R_0 and I: ATRP initiator and conventional initiator derived radical; T=105 °C; MM: macromonomer.

	Elementary Reaction	Equation	$k_{l,\,chem}$	Reference
Normal ATRP	Activation (a)	$R_0X + M_t^nX/L \xrightarrow{k_{a,0}^{app}} R_0 + M_t^{n+1}X_2/L$	3.1 [L mol^{-1} s^{-1}]	[68]
		$R_i^sX + M_t^nX/L \xrightarrow{k_a^{s,app}} R_i^s + M_t^{n+1}X_2/L$	1.6 [L mol^{-1} s^{-1}]	This work
		$R_i^tX + M_t^nX/L \xrightarrow{k_a^{t,app}} R_i^t + M_t^{n+1}X_2/L$	2.6 10^1 [L mol^{-1} s^{-1}]	This work
	Deactivation (da)	$R_0 + M_t^{n+1}X_2/L \xrightarrow{k_{da,0}^{app}} R_0X + M_t^nX/L$	8.0 10^8 [L mol^{-1} s^{-1}]	This work
		$R_i^s + M_t^{n+1}X_2/L \xrightarrow{k_{da}^{s,app}} R_i^sX + M_t^nX/L$	4.0 10^8 [L mol^{-1} s^{-1}]	This work
		$R_i^t + M_t^{n+1}X_2/L \xrightarrow{k_{da}^{t,app}} R_i^tX + M_t^nX/L$	4.0 10^7 [L mol^{-1} s^{-1}]	This work
	Propagation (p)	$R_0 + M \xrightarrow{k_{p,0}^{app}} R_1$	7.4 10^4 [L mol^{-1} s^{-1}]	[69]
		$R_i^s + M \xrightarrow{k_p^{s,app}} R_{i+1}^s$	7.4 10^4 [L mol^{-1} s^{-1}]	[69]
		$R_i^t + M \xrightarrow{k_p^{t,app}} R_{i+1}^s$	1.5 10^2 [L mol^{-1} s^{-1}]	[70]
	Chain Transfer to Monomer (trM)	$R_0 + M \xrightarrow{k_{trM,0}^{app}} P_0 + R_1$	9.0 [L mol^{-1} s^{-1}]	[71]
		$R_i^s + M \xrightarrow{k_{trM}^{s,app}} P_i + R_1$	9.0 [L mol^{-1} s^{-1}]	[71]
		$R_i^t + M \xrightarrow{k_{trM}^{t,app}} P_i + R_1$	8.5 10^{-2} [L mol^{-1} s^{-1}]	[71]
	Backbiting (bb)	$R_i^s \xrightarrow{k_{bb}^{,app}} R_i^t$	2.0 10^3 [s^{-1}]	[70]
	βC-scission (βC-sc)	$R_i^t \xrightarrow{k_{\beta C-sc}^{app}} R_2^s + MM_{i-2}$ $R_i^t \xrightarrow{k_{\beta C-sc}^{app}} R_{i-3}^s + MM_3$	2.2 [s^{-1}]	[72]
	Termination by recombination (tc)	$R_i^s + R_j^s \xrightarrow{k_{tc}^{ss,app}} P_{i+j}$	2.3 10^8 [L mol^{-1} s^{-1}]	[70]
		$R_i^s + R_j^t \xrightarrow{k_{tc}^{st,app}} P_{i+j}$	4.6 10^7 [L mol^{-1} s^{-1}]	[70]
		$R_i^t + R_j^t \xrightarrow{k_{tc}^{tt,app}} P_{i+j}$	3.0 10^6 [L mol^{-1} s^{-1}]	[70]
Extra for ICAR	Dissociation (dis)	$I_2 \xrightarrow{f,k_{dis}^{app}} 2I$	8×10^{-2} [s^{-1}] with f = 0.75 [-]	[55, 73]
	Activation (a)	$IX + M_t^nX/L \xrightarrow{k_{a,I}^{app}} I + M_t^{n+1}X_2/L$	1.6 10^1 [L mol^{-1} s^{-1}]	Based on[55]
	Deactivation (da)	$I + M_t^{n+1}X_2/L \xrightarrow{k_{da,IX}^{app}} IX + M_t^nX/L$	4.0 10^7 [L mol^{-1} s^{-1}]	Based on[55]
	Propagation (p)	$I + M \xrightarrow{k_{p,I}^{app}} R_1$	7.4 10^5 [L mol^{-1} s^{-1}]	Based on[55]

For ICAR ATRP, dissociation of the conventional radical initiator and activation, deactivation and propagation involving conventional radical initiator fragments are also considered (Table 3.1). *tert*-Butyl peroxy-2-ethylhexanoate (Trigonox21s) is employed as conventional radical initiator, since it is particularly suited for the polymerization of acrylates in the range of 80 to 150 °C.[73, 74] For simplicity, a typical constant initiator efficiency of 0.75 is used and the intrinsic activation and deactivation rate coefficients related to conventional radical initiator fragments are taken equal to those of the secondary macrospecies. The latter approach has been selected since simulations have revealed that a typical tenfold reactivity difference has no significant influence on the results.[55] The conversion profile and the evolution of the polymer properties with time are simulated using the methodology developed by D'hooge et al.,[67, 75] which is based on an extension of the method of moments coupled with an application of the quasi-steady state approximation for the calculation of population weighted apparent rate coefficients using a convergence test.

CRP kinetic studies[75-79] have indicated that diffusional limitations can result in a lowering of the apparent termination reactivity during the polymerization and that deactivation can become diffusion controlled at sufficiently high conversion. Therefore, in this work the possible influence of diffusional limitations on termination and deactivation is considered in agreement with literature reports.[75, 80-84] For more details, the reader is referred to Appendix C.

3.3 Results and Discussion

3.3.1 Normal ATRP of *n*BuA

Figure 3.2 presents a comparison of the model simulations while accounting for possible diffusional limitations (full lines) and the experimental findings for the evolution of conversion with time and the evolution of the number average chain length (x_n^{pol}), the polydispersity index (PDI) and the cumulative branching fraction (on a molar basis) with conversion. As mentioned above, the experimental data are taken from Ahmad et al.[32] and correspond to a polymerization temperature of 105 °C and a targeted chain length (TCL: $[M]_0/[R_0X]_0$) of 289. In the same figure, the simulated EGF and cumulative CC double bond

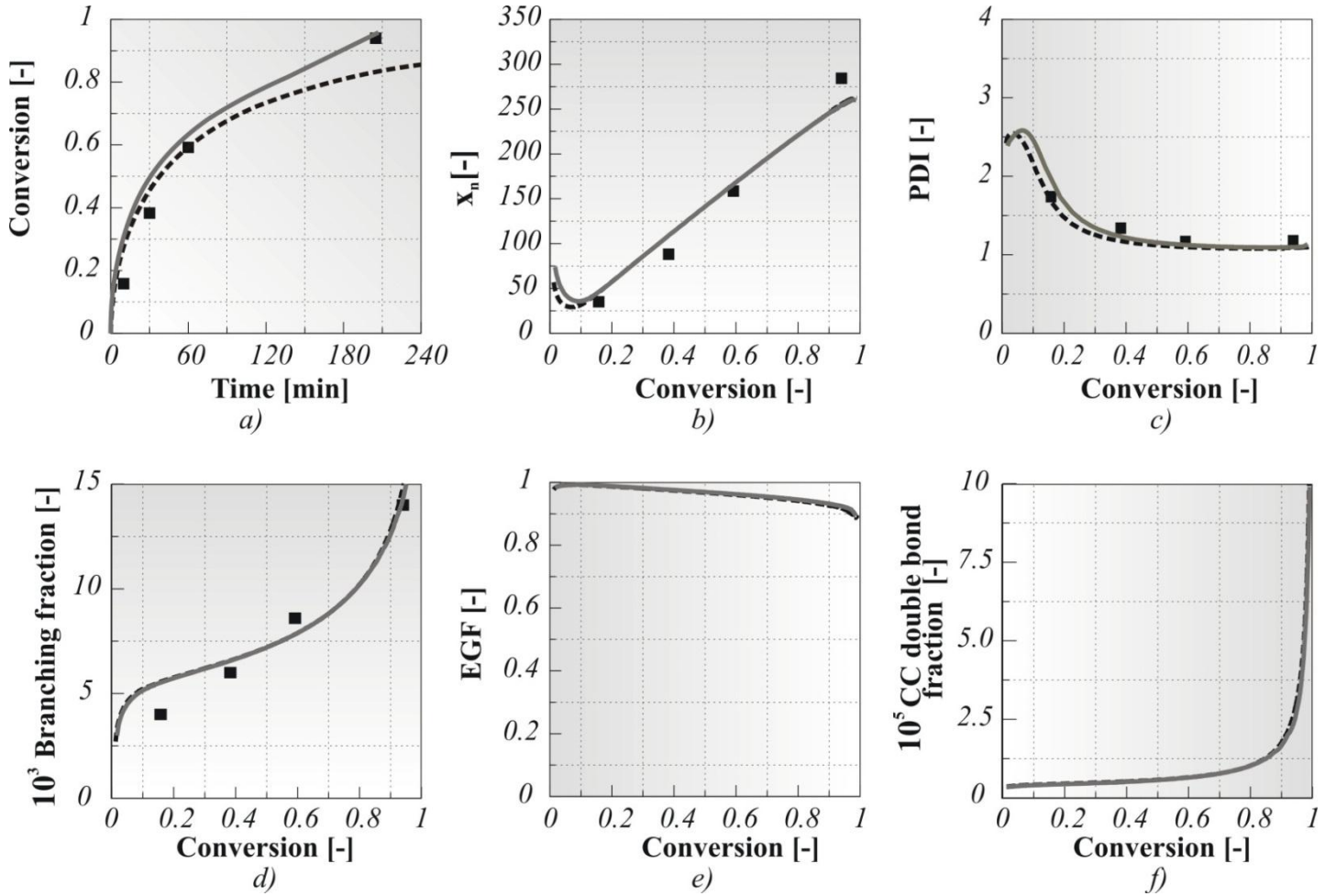

Figure 3.2: Comparison of experimental data and simulations for the bulk normal ATRP of *n*BuA; diffusional limitations considered (full lines) and neglected (dashed lines); a) conversion profile, b) number-average chain length (x_n), c) polydispersity index (PDI), d) branching fraction (cumulative; molar), e) end-group functionality (EGF) and f) CC double bond fraction (cumulative; molar) as a function of conversion; 105 ^{0}C; $[M]_0/[R_0X]_0/[CuBr]_0/[L]_0$:347/1.2/0.6/0.6; experimental data from Ahmad et al.;[32] no experimental data for e) and f); for continuity equations see D'hooge et al.[67]

fraction (on a molar basis) are given as a function of conversion. No experimental data are however available for the latter polymer properties.

Clearly, a good description of the experimental data is obtained. The control over chain length and livingness is good, since PDI values close to 1.2 are simulated and limited loss of EGF takes place during the ATRP. In agreement with simulation results on the ATRP of isobornyl acrylate,[67] the cumulative CC double bond fraction is very low and can therefore be neglected in a first approximation. At high conversion, the cumulative branching fraction amounts to 0.015 corresponding to an average of five branches per polymer chain.

The corresponding kinetic parameters for (de)activation of secondary and tertiary macrospecies are listed in Table 3.1. An equilibrium coefficient K_{eq}^{s} of 4 10^{-9} results for the secondary macrospecies, whereas the equilibrium coefficient for tertiary macrospecies (K_{eq}^{t} = 6.4 10^{-7}) is about two orders of magnitude higher. In accordance with Seeliger et al.,[68] a value of 1.6 L mol^{-1} s^{-1} is obtained for the secondary activation rate coefficient, which is approximately twenty times lower than the tertiary activation rate coefficient. For deactivation, the rate coefficient for tertiary macroradicals is about ten times lower than for secondary macroradicals reflecting the higher stability of these species in agreement with the theoretical kinetic study of Konkolewicz et al.[23]

Figure 3.2 also reveals that the increase of the viscosity upon polymerization leads to a rate acceleration at high conversion while the control over polymer properties is barely affected. This rate acceleration can be explained based on the difference in reaction probabilities for secondary and tertiary macroradicals in case diffusional limitations are accounted for or neglected (Figure 3.3). The reaction probability of a species for a reaction l (P_l) is defined as the ratio of the rate of the reaction R_l to the summation of all reaction rates for the considered species:

$$P_l = \frac{R_l}{\sum_k R_k} \tag{3.1}$$

For secondary macroradicals a distinction is made among the reaction probability for deactivation, propagation and backbiting while for tertiary macroradicals deactivation, propagation and βC-scission are considered. As demonstrated in Appendix C, the reaction probabilities for termination are very low at high conversion and can thus be neglected to explain the rate acceleration mentioned above.

In agreement with Figure 3.2, diffusional limitations influence the reaction probabilities mainly at high conversion. In particular, the probability of secondary macroradicals to deactivate (Figure 3.3a) plummets, since the mobility of the deactivator is significantly reduced from a conversion of ca. 0.60. As a consequence, propagation of secondary macroradicals is strongly favored (Figure 3.3b), leading to an increase of the conversion and the probability of backbiting (Figure 3.3c). In contrast, a much less pronounced effect of diffusional limitations on the reaction probabilities for tertiary species is observed (Figure 3.3d-f). Only a slightly lower and higher reaction probability, respectively, is obtained for tertiary deactivation and propagation accompanied by a minimal increase of the βC-scission probability that takes place at high conversion. In other words, the increase in backbiting does not induce a rate retardation due to the ca. hundred times lower propagation of tertiary macrospecies. Hence, it can be concluded that the conversion profile at high conversion is determined by diffusional limitations on secondary deactivation, which promote the observed rate acceleration.

For an amount of copper (I) bromide (CuBr) of 250 ppm (with respect to monomer), the effect of TCL on the conversion profile and control over polymer properties is shown in Figure 3.4 for TCLs varying between 50 and 1000, the latter being a typical maximum TCL in experimental CRP studies.[57, 85-87] For the considered range of TCLs, a good livingness and control over chain length is obtained as evidenced by the high EGF and low PDI values at high conversion. In agreement with Konkolewicz et al.,[23] a higher cumulative branching fraction is obtained for higher TCLs. Note that for sufficiently low TCLs the polymerization proceeds relatively fast.

However, when the initial amount of CuBr is lowered further as required for industrial application,[43] the considered normal ATRP process slows down considerably

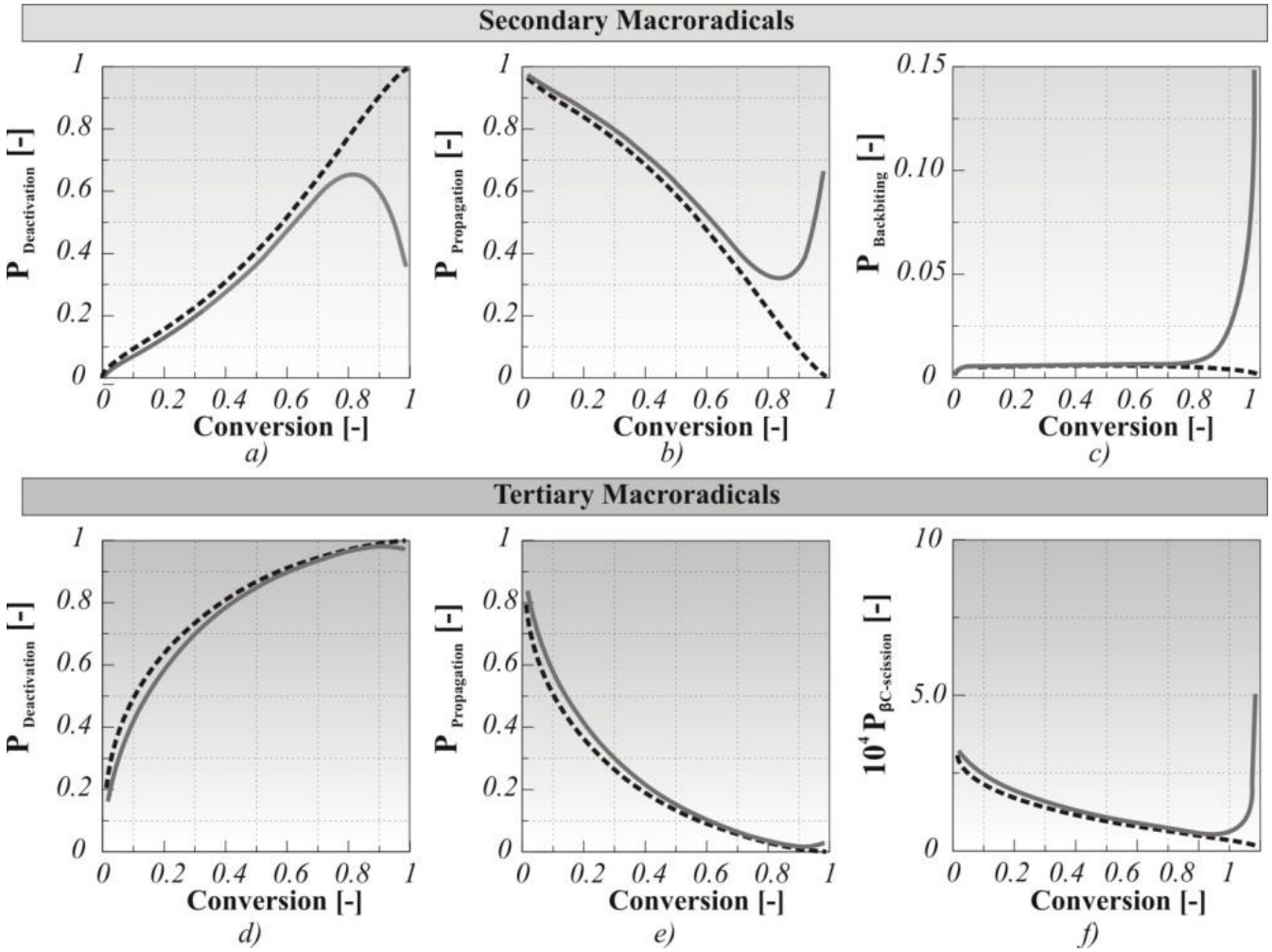

Figure 3.3: Effect of diffusional limitations on the reaction probabilities for secondary (*a-c*) and tertiary (*d-f*) macroradicals for the bulk normal ATRP of nBuA; a) deactivation, b) propagation and c) backbiting of secondary macrospecies; d) deactivation, e) propagation and f) βC-scission of tertiary macrospecies; diffusional limitations considered (full lines) and neglected (dashed lines); 105 °C; $[M]_0/[R_0X]_0/[CuBr]_0/[L]_0$=347/1.2/0.6/0.6; for continuity equations see D'hooge et al.[67]

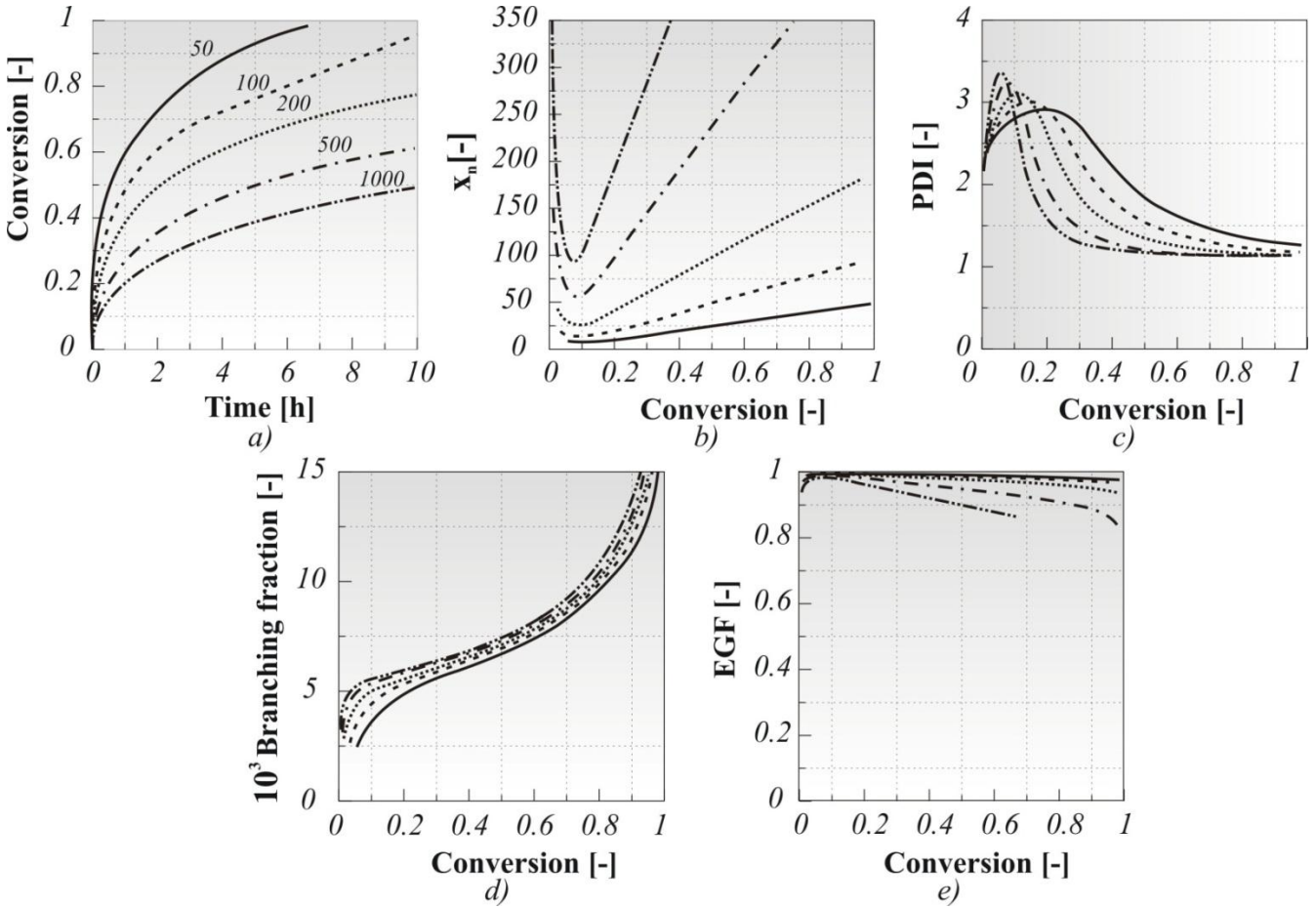

Figure 3.4: Effect of TCL for the bulk normal ATRP of *n*BuA on a) the conversion profile, evolution of b) number-average chain length (x_n), c) polydispersity index (PDI), d) branching fraction (cumulative; molar) and e) end-group functionality (EGF) with conversion; 105 ^{0}C with 250 ppm of ATRP catalyst; $[M]_0/[R_0X]_0/[CuBr]_0/[L]_0$:50/1/0.0125/0.0125, 100/1/0.025/0.025, 200/1/0.05/0.05, 500/1/0.125/0.125 and 1000/1/0.25/0.25; for continuity equations see D'hooge et al.[67]

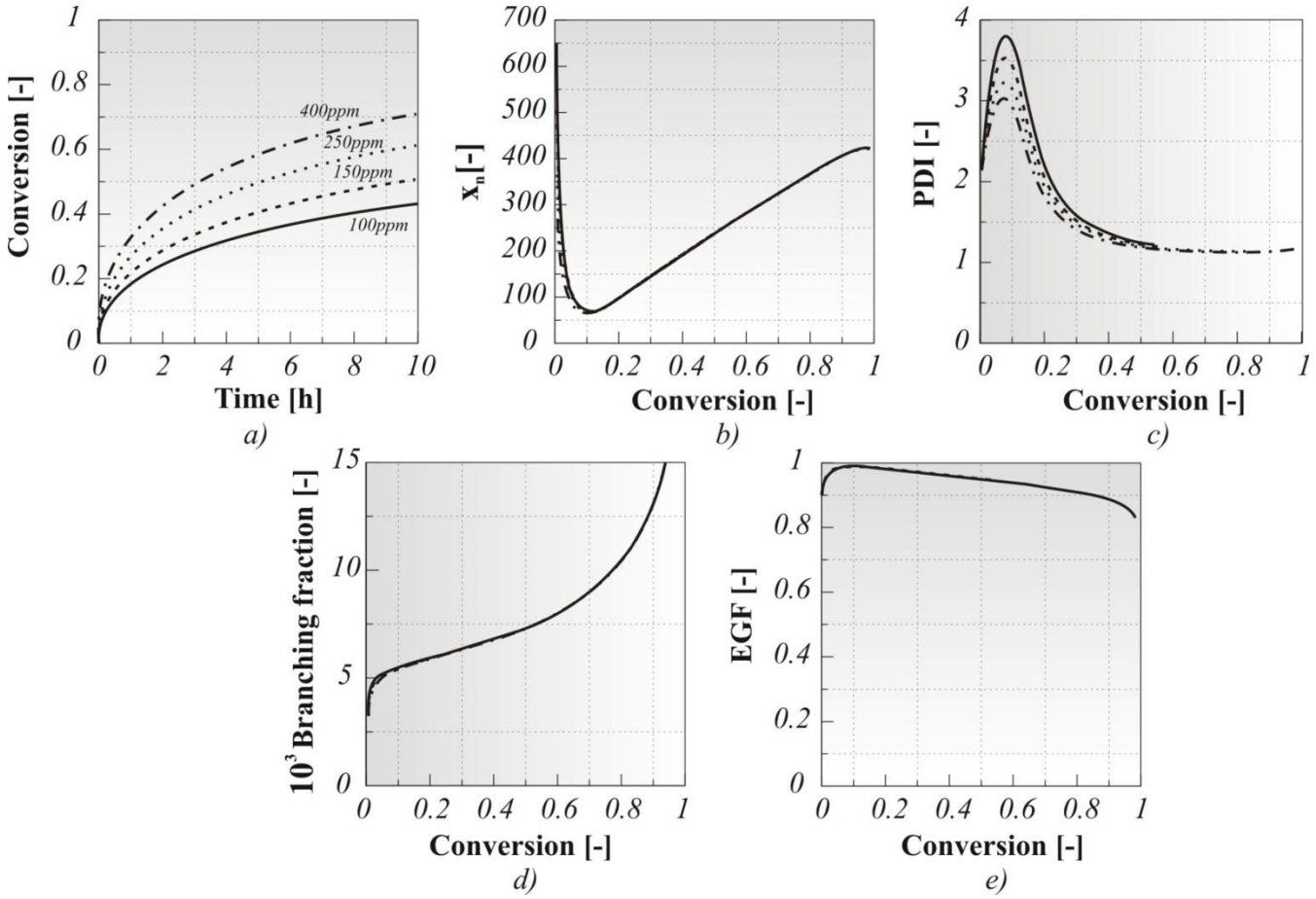

Figure 3.5: Effect of initial amount of CuBr (ppm with respect to monomer) for the bulk normal ATRP of *n*BuA on a) the rate of polymerization, evolution of the b) number-average chain length (x_n), c) polydispersity index (PDI), d) branching fraction (cumulative; molar) and e) end-group functionality (EGF) with conversion;105 ^{0}C; $[M]_0/[R_0X]_0/[CuBr]_0/[L]_0$:500/1/*y*/*y* with *y*=0.05 (100ppm), 0.075 (150ppm), 0.125 (250ppm), 0.2 (400ppm); for continuity equations see D'hooge et al.[67]

resulting in polymerization times that are too long from an industrial point of view, as illustrated in Figure 3.5 for a TCL of 500. For example, for an initial amount of CuBr of 100 ppm it takes about two days to reach a conversion of 0.80 and a good control over polymer properties. As will be illustrated in the next section, ICAR ATRP can resolve the former issue while preserving control over polymer properties. For the particular case mentioned above, it is shown that with ICAR ATRP only half a day is required.

3.3.2 ICAR ATRP of *n*BuA

Figure 3.6 and 3.7 present the simulated trends of polymerization time, average chain length (x_n), PDI, EGF, and cumulative branching fraction related to the initial ppm level of Cu(II) and TCL at a fixed conversion of 0.80. The initial amount of Cu(II) is varied between 5 and 250 ppm, the latter being a typical value for a normal ATRP (Figure 3.4 and 3.5). For TCL, again an upper limit of 1000 is considered.[57, 85-87] For all simulations presented in Figure 3.6 and 3.7, the initial molar ratio of conventional radical initiator to ATRP initiator is fixed at 0.02.

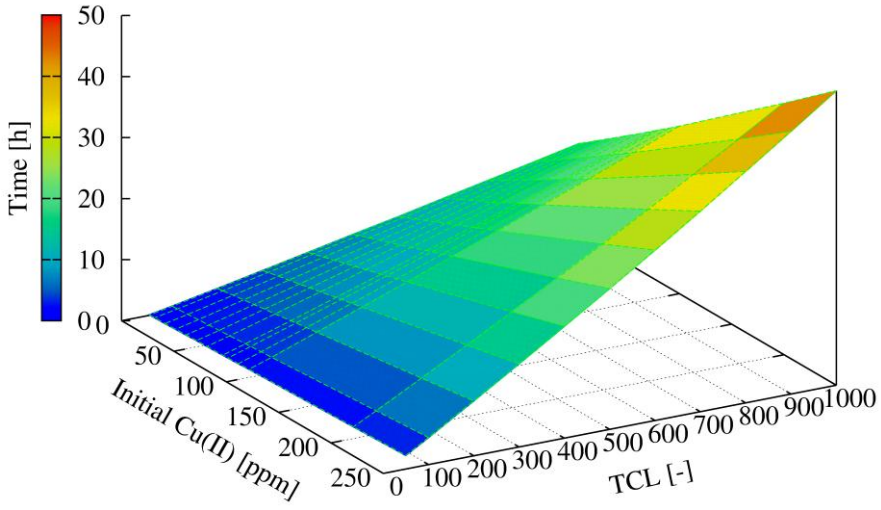

Figure 3.6: Polymerization time required to reach a conversion of 0.8 as a function of initial amount of Cu(II) (ppm with respect to monomer) and TCL in the bulk ICAR ATRP of *n*BuA at 105 ^{0}C; $[I_2]_0/[R_0X]_0$:0.02/1; for continuity equations see D'hooge et al.[67]

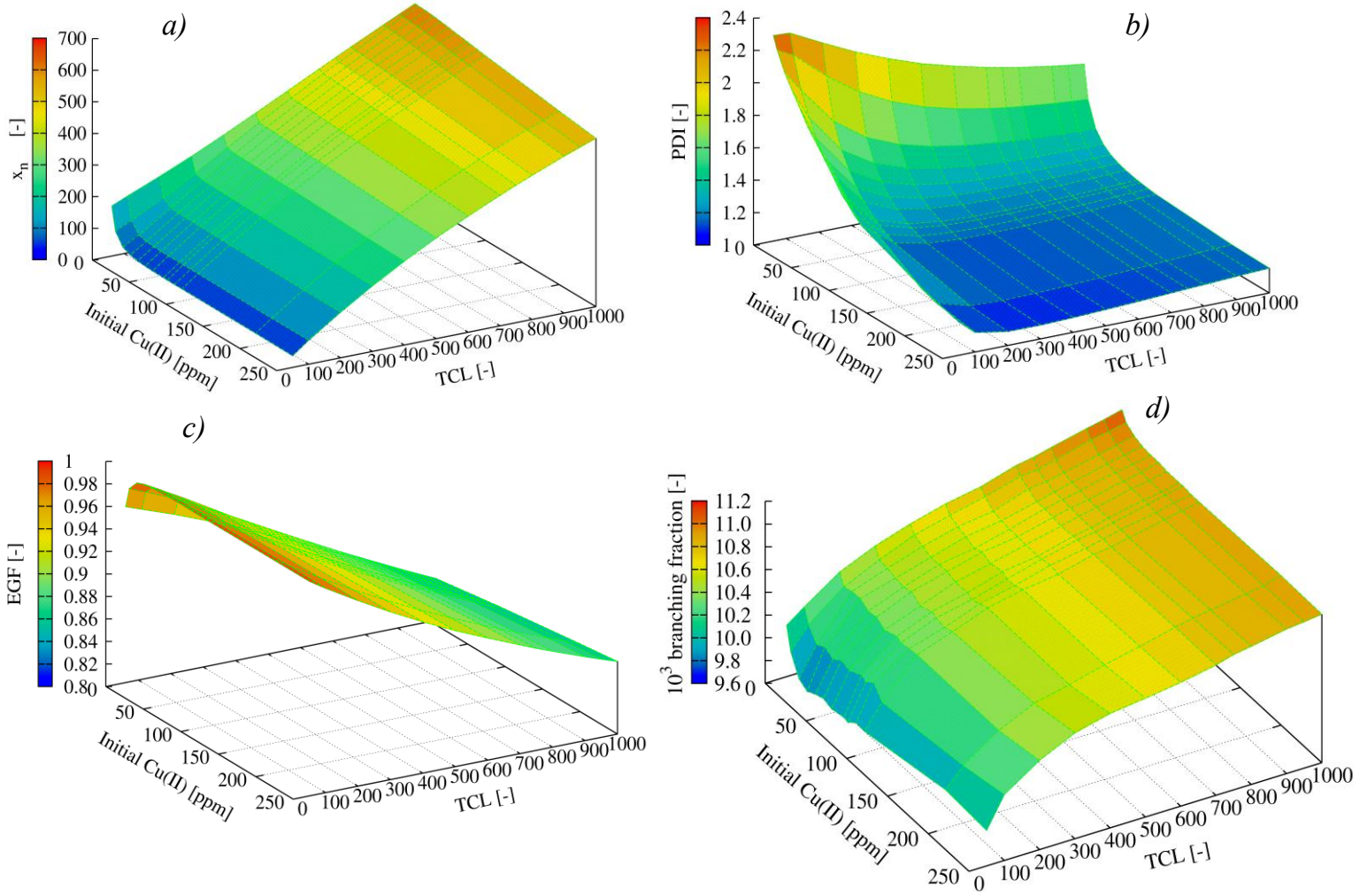

Figure 3.7: Polymer properties for the bulk ICAR ATRP of *n*BuA as function of the initial amount of Cu(II) (ppm with respect to monomer) and TCL; a) number-average chain length (x_n), b) polydispersity index (PDI), c) end-group functionality (EGF) and d) branching fraction (cumulative; molar); 105 ^{0}C; $[I_2]_0/[R_0X]_0$:0.02/1; conversion: 0.8; for continuity equations see D'hooge et al.[67]

It appears from Figure 3.6 that longer polymerization times are required to reach a conversion of 0.80 for higher initial ppm levels of Cu(II) and TCLs. For example, using 40 ppm of Cu(II) one hour is required for a TCL of 50, whereas approximately twenty hours are required for a TCL of 1000. Similarly, for a TCL of 300, four hours are necessary when using 5 ppm of Cu(II), which increases to half a day for 250 ppm. In particular, with 100 ppm Cu(II) and for a TCL of 500 only half a day is needed, which confirms the potential of ICAR ATRP in terms of short polymerization times. As explained above (Figure 3.5a) for the same TCL and ppm level of catalyst, normal ATRP requires approximately two days.

The inverse relationship between EGF and TCL, described previously by Goto and Fukuda,[88] is shown in Figure 3.7c. Close inspection reveals that even at relatively high TCLs good livingness is still obtained. For example, for a TCL of 700 and an initial Cu(II) amount of 50 ppm, the simulated EGF is ca. 0.90. Furthermore, a similar EGF results with 5 ppm demonstrating the limited influence of the initial Cu(II) concentration on the livingness of ICAR ATRP. In agreement with the recent simulations of Zhong and Matyjaszewski,[89] ICAR ATRP thus allows to use a low initial amount of Cu(II) while preserving EGF (Figure 3.7c) and maintaining fast polymerization rate.

As for the normal ATRP of *n*BuA, the cumulative branching fraction in the ICAR ATRP process (Figure 3.7d) changes only as a function of TCL and is rather independent of the initial amount of Cu(II). By varying TCL e.g. from 50 to 700 the branching fraction can be increased by about 10%, independent of the initial amount of Cu(II). Comparison of Figure 3.4d and 3.7d reveals that for each TCL a similar branching fraction is simulated for normal and ICAR ATRP.

Based on Figure 3.6, the initial amount of Cu(II) required to reach a conversion of 0.8 in eight and twelve hours can be calculated, as shown in Figure 3.8(a-b). In the same figures two regions are highlighted indicating longer ($t > 8$ h or $t > 12$ h) and shorter ($t < 8$h or $t < 12$ h) polymerization times. Clearly, if a polymerization time of twelve hours or less is demanded, the full range of TCLs can be covered using initial amounts of Cu(II) well below 250 ppm with a broader range of ppm levels available for low

TCLs. If the polymerization time demanded is shorter, for instance eight hours, a narrower range of ppm levels is available for high TCLs. Interestingly, for all TCLs, fast ICAR ATRPs can be performed using very low ppm levels, i.e. lower than 5 ppm.

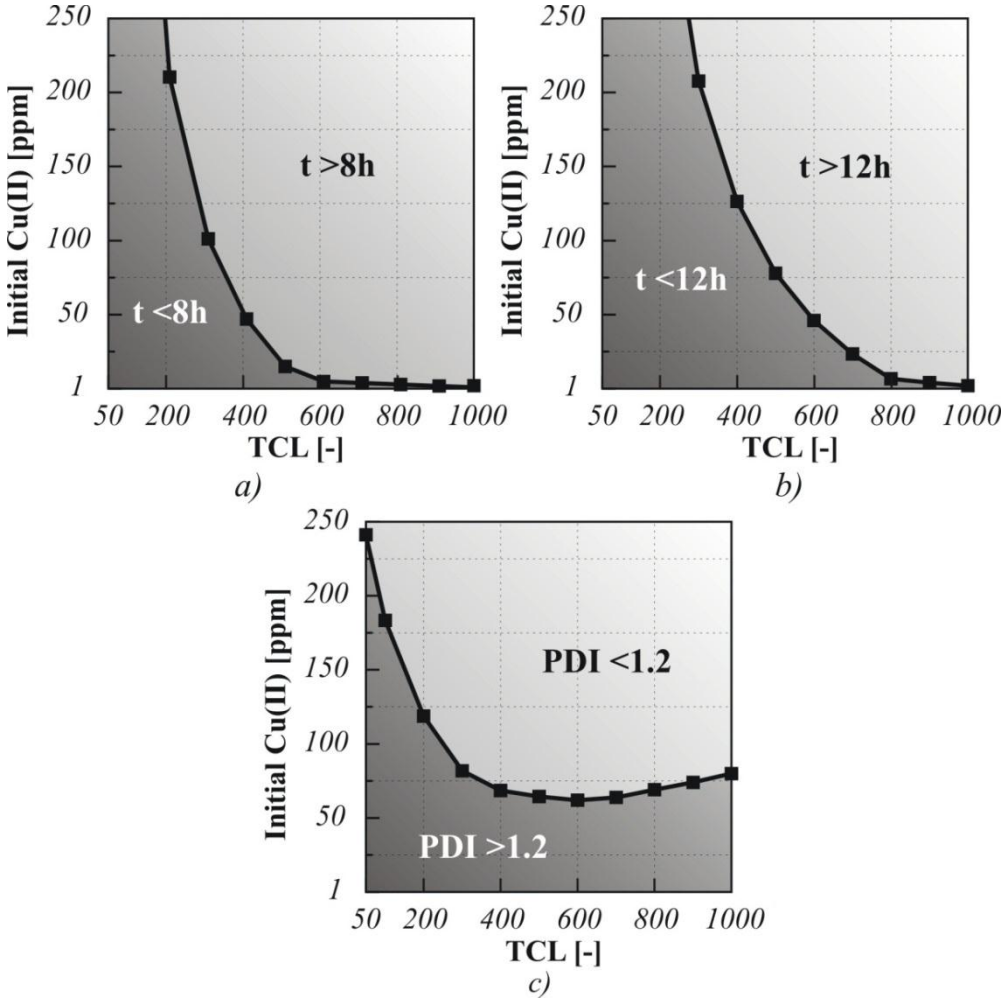

Figure 3.8: Full lines: initial amount of Cu(II) (ppm with respect to monomer) for the bulk ICAR ATRP of *n*BuA to obtain a conversion of 0.8 in a) 8 hours, b) 12 hours, c) a PDI value equal to 1.2 at a conversion of 0.8 as a function of TCL; 105 °C; $[I_2]_0/[R_0X]_0$:0.02/1; for continuity equations see D'hooge et al.[67]

As reported by D'hooge et al.,[55] who studied the ICAR ATRP of methyl methacrylate and styrene, too high initial levels of Cu(II) lead to too high initial deactivation rates and, hence, retard the polymerization. Figure 3.9(a-b) shows that for the ICAR ATRP of *n*BuA the same conclusion can be drawn. In this figure, the initial deactivation rate of secondary macroradicals is shown as a function of conversion using 5, 50 and 250

ppm of Cu(II) for a TCL of 50 and 500. For the latter TCL, the retardation is more pronounced as a result of the decrease in initial concentration of both the ATRP and conventional initiator, since their ratio remains equal to 0.02, as mentioned above.

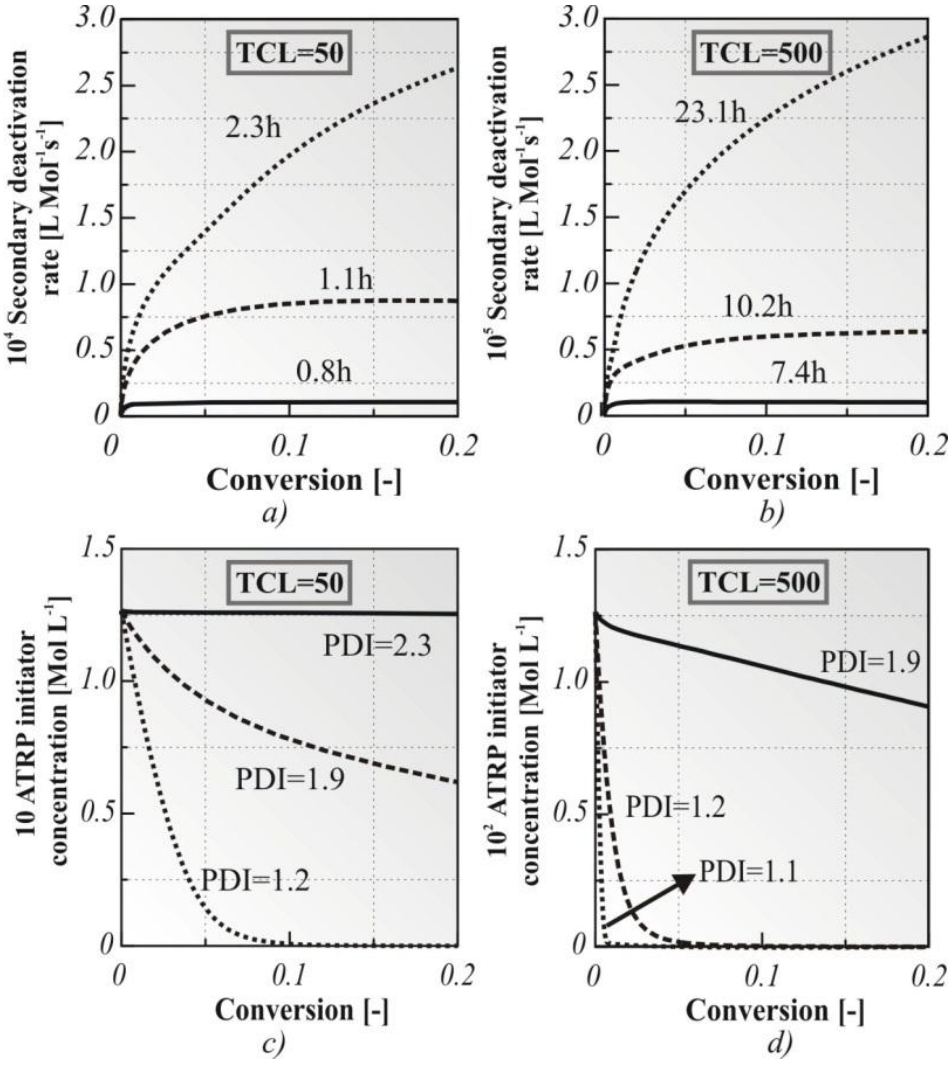

Figure 3.9: Effect of initial amount of Cu(II) (ppm with respect to monomer) on secondary deactivation rate (a-b) and ATRP initiator concentration (c-d) as a function conversion in the bulk ICAR ATRP of *n*BuA; full line: 5 ppm; dashed line 50 ppm; dotted line: 250 ppm; in a) and b) time is given for a conversion of 0.8; in c) and d) PDI is given at a conversion of 0.8; 105 ^{0}C; $[I_2]_0/[R_0X]_0$:0.02/1; for continuity equations see D'hooge et al.[67]

However, as depicted in Figure 3.7(a-b) a sufficiently high initial ppm level of Cu(II) is demanded for a good control over chain length, particularly for relatively low TCLs. For TCLs between 50 and 200, PDI values much higher than 1.5 result for initial

amounts of Cu(II) lower than 75 ppm and a good control over chain length (PDI~1.2) is only obtained when this initial amount is higher than ca. 100 ppm. Too low initial amounts of ATRP catalyst result in a too slow activator (re)generation as evidenced by the too slow disappearance of the ATRP initiator on a conversion basis shown in Figure 3.9(c-d). For a good control over chain length, the ATRP initiation has to be completed at a relatively low conversion so that enough monomer is available to compensate for the chain length difference caused by the non-instantaneous ATRP initiation. Since for higher TCLs the ATRP initiation is finished at lower conversions (Figure 3.9d), less Cu(II) can thus be employed to obtain a PDI of 1.2 at conversion of 0.8 (Figure 3.8c).

Although, for TCLs higher than 600 a slight increase of the ppm level of Cu(II) is observed. As suggested by D'hooge et al.,[55] well-defined ICAR ATRP based polymers can only be prepared if the initial concentration of conventional radical initiator is sufficiently low with respect to the initial concentration of ATRP initiator. Therefore, it can be expected that for higher TCLs, the ppm level of Cu(II) shown in Figure 3.8c can be further decreased by lowering the initial ratio of conventional radical initiator to ATRP initiator from 0.02 to e.g. 0.01. Indeed, Figure 3.10a demonstrates that in case this initial ratio is reduced to 0.01 from a TCL of 700 onwards, the necessary amount of Cu(II) to reach a PDI of 1.2 (conversion of 0.8) decreases further as a function of TCL. However, as shown in Fig 3.10b this approach is accompanied by a significant increase in the required polymerization time.

Summarizing, the above simulations clearly indicate that ICAR ATRP can be used to prepare well-defined poly(*n*BuA) using low initial amounts of Cu(II). In particular, due to high EGF values it is expected that poly(*n*BuA) based block copolymers can be synthesized provided that appropriate conditions are selected for the addition of a second block. Moreover, the level of control over the polymer properties can be adjusted by selecting the appropriate initial ppm Cu(II) level for a given TCL and required polymerization time. This is illustrated in Figure 3.11, in which the polymerization time required to reach a conversion of 0.80 is plotted as a function of the initial amount of Cu(II) (1 to 250 ppm) and TCL (50 to 1000). In the same figure,

six lines are indicated to delineate regions of conditions according to constraining values for EGF and PDI, i.e. those conditions which lead to a PDI of 1.1, 1.2 and 1.3 on the one hand and to a EGF of 0.85, 0.9 and 0.95 on the other hand.

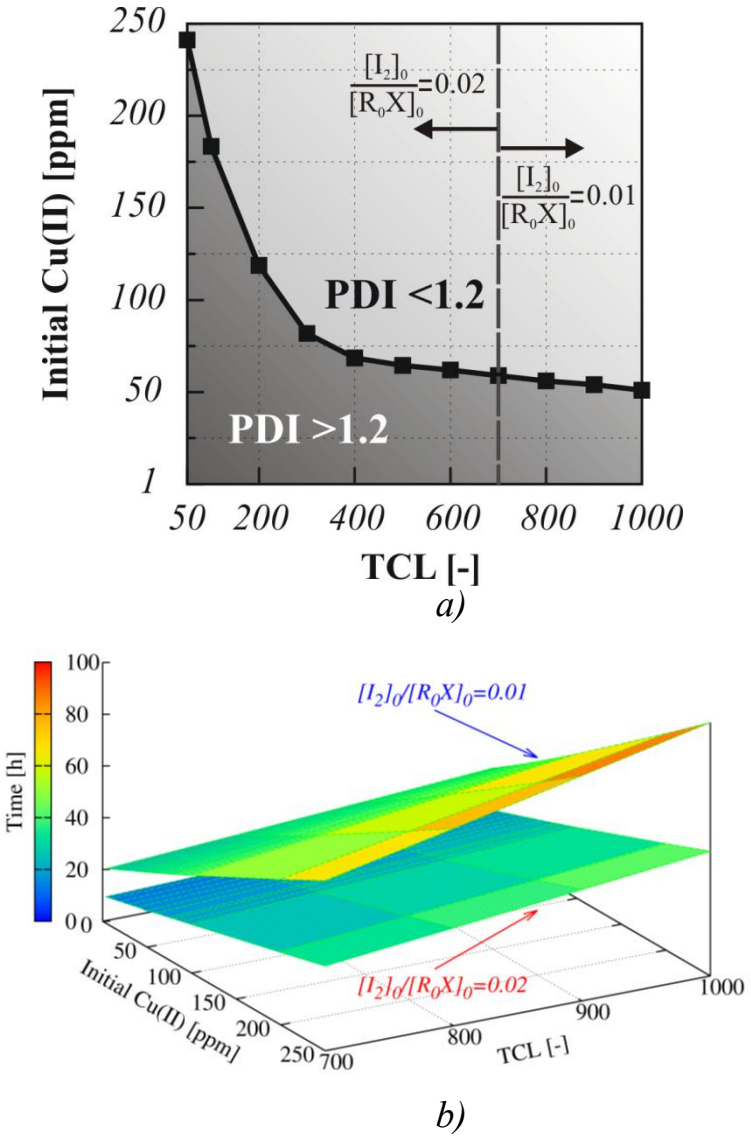

Figure 3.10: a) Full line: initial amount of Cu(II) (ppm with respect to monomer) in the bulk ICAR ATRP of *n*BuA to obtain a PDI value equal to 1.2 at a conversion of 0.8; 105 ^{0}C; $[I_2]_0/[R_0X]_0$:0.02/1 for TCL < 700; $[I_2]_0/[R_0X]_0$:0.01/1 for TCL ≥ 700. b) Polymerization time needed to reach a conversion of 0.8 for TCLs ≥ 700; conditions as in a); for continuity equations see D'hooge et al.[67]

Overall, Figure 3.11 confirms the effectiveness and robustness of ICAR ATRP of acrylates and in particular of *n*BuA. For TCLs lower than 500, well-defined poly(*n*BuA) (1.1 < PDI < 1.2 and EGF > 0.9) can be obtained within relatively short polymerization times (~12h) employing initial amounts of Cu(II) between 60 and 250

ppm. For higher TCLs, still relatively fast polymerizations can be conducted with very low (< 10) Cu(II) ppm levels at the expense of a reduction of the control over chain length (PDI > 1.3) and livingness (0.85 < EGF < 0.9). In case for these TCLs the control over chain length is important (PDI ~1.1), initial amounts of Cu(II) above 65 ppm are required leading to longer polymerization times (> 12h).

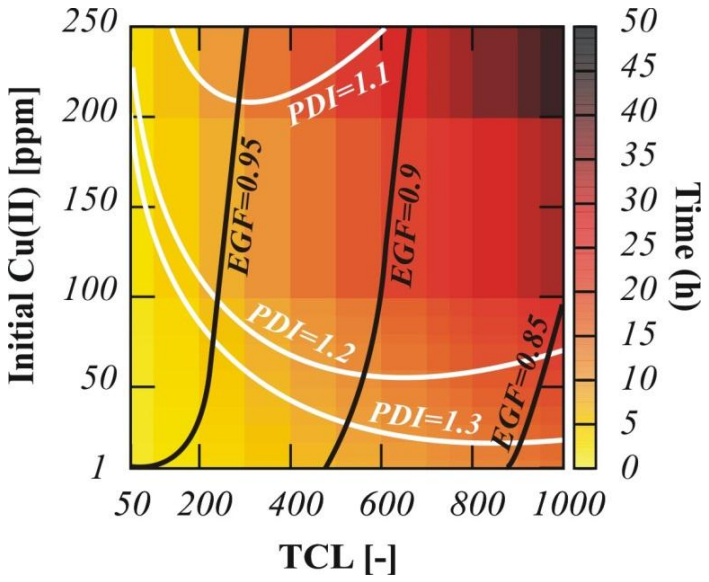

Figure 3.11: Diagram for the bulk ICAR ATRP of *n*BuA illustrating control over chain length, livingness and the required polymerization time for a conversion of 0.80 as a function of the initial amount of Cu(II) (ppm with respect to monomer) and TCL; 105 ^{0}C; $[I_2]_0/[R_0X]_0$:0.02/1; full lines indicate the limits: PDI (white) equal to 1.1, 1.2 and 1.3, EGF (black) equal to 0.85, 0.9 and 0.95; for continuity equations see D'hooge et al.[67]

3.4 Conclusions

A computational kinetic study is performed for ICAR ATRP to support the synthesis of well-defined poly(*n*BuA), i.e. with predetermined chain length and cumulative branching level, low PDI and high EGF. Kinetic parameters related to activation and deactivation are assessed based on literature experimental data for the corresponding normal ATRP system. The obtained parameter values are in line with the expected higher stability of tertiary macroradicals compared to secondary species. As for normal ATRP, in ICAR ATRP higher branching level are obtained for higher TCLs. Diffusional limitations are mainly important on secondary deactivation leading to a rate acceleration at high conversion.

The advantages of the ICAR ATRP technique are illustrated and guidelines are provided for the selection of relevant polymerization conditions, such as initial catalyst concentration and polymerization time for a given TCL. Up to TCLs of thousand, ICAR ATRP of *n*BuA can be performed while reaching a high conversion relatively fast and attaining reasonable control over polymer properties at low (< 50) ppm level of ATRP catalyst. Only for moderate TCLs, slightly higher ppm levels of ATRP catalyst are needed, when low PDI values are desired. In all cases, the livingness of the ICAR ATRP is sufficiently high.

References

[1] P. Nesvadba, *Radical Polymerization in Industry*.In *Encyclopedia of Radicals in Chemistry, Biology and Materials*, Jonh Wiley & Sons, Ltd, 2012.

[2] G. Odian, *Principles of polymerization*. Wiley-Interscience: USA, 1981.

[3] E. Penzel, *Polyacrylates*.In *Ullmann's Encyclopedia of Industrial Chemistry*, 2000; p 515.

[4] C. Auschra; E. Eckstein; A. Muhlebach; M. O. Zink; F. Rime, *Prog Org Coat* 2002, *45*, 83.

[5] W. A. Braunecker; K. Matyjaszewski, *Prog Polym Sci* 2008, *33*, 165.

[6] K. Matyjaszewski, *Controlled/Living Radical Polymerization: Progress in ATRP, NMP and RAFT*. ACS: Washington, 2000.

[7] C. Barner-Kowollik, *Handbook of RAFT polymerization*. Wiley-VCH Verlag GmbH & Co. KGaA: Weinheim, 2008.

[8] S. Gaynor; D. Greszta; D. Mardare; M. Teodorescu; K. Matyjaszewski, *J Macromol Sci-Pure Appl Chem* 1994, *A31*, 1561.

[9] C. Barner-Kowollik; J. P. Blinco; M. Destarac; K. J. Thurecht; S. Perrier, *Reversible Addition Fragmentation Chain Transfer (RAFT) Polymerization:*

Mechanism, Process and Applications.In *Encyclopedia of Radicals in Chemistry, Biology and Materials*, 2012.

[10] G. Moad; E. Rizzardo; S. H. Thang, *Polymer* 2008, *49*, 1079-1131.

[11] J. Nicolas; Y. Guillaneuf; C. Lefay; D. Bertin; D. Gigmes; B. Charleux, *Prog Polym Sci* 2012.

[12] T. Junkers; C. Barner-Kowollik, *J Pol Sci, Part A: Polym Chem* 2008, *46*, 7585.

[13] J. Chiefari; J. Jeffery; R. T. A. Mayadunne; G. Moad; E. Rizzardo; S. H. Thang, *Macromolecules* 1999, *32*, 7700.

[14] T. Junkers; C. Barner-Kowollik, *Macromol Theory Sim* 2009, *18*, 421.

[15] J. Barth; M. Buback; P. Hesse; T. Sergeeva, *Macrom Rapid Commun* 2009, *30*, 1969.

[16] X. Yu; L. J. Broadbelt, *Macromol Theory Sim* 2012, *21*, 461.

[17] M. C. Grady; W. J. Simonsick; R. A. Hutchinson, *Macromol Symp* 2002, *182*, 149.

[18] A. N. F. Peck; R. A. Hutchinson, *Macromolecules* 2004, *37*, 5944.

[19] C. Plessis; G. Arzamendi; J. R. Leiza; H. A. S. Schoonbrood; D. Charmot; J. M. Asua, *Ind Eng Chem Res* 2001, *40*, 3883.

[20] C. Plessis; G. Arzamendi; J. R. Leiza; H. A. S. Schoonbrood; D. Charmot; J. M. Asua, *Macromolecules* 2000, *33*, 4.

[21] C. Farcet; J. Belleney; B. Charleux; R. Pirri, *Macromolecules* 2002, *35*, 4912.

[22] B. Yamada; M. Azukizawa; H. Yamazoe; D. J. T. Hill; P. J. Pomery, *Polymer* 2000, *41*, 5611.

[23] D. Konkolewicz; S. Sosnowski; D. R. D'Hooge; R. Szymanski; M. F. Reyniers; G. B. Marin; K. Matyjaszewski, *Macromolecules* 2011, *44*, 8361.

[24] M. S. Matheson; E. E. Auer; E. B. Bevilacqua; E. J. Hart, *J Am Chem Soc* 1949, *71*, 2610.

[25] M. J. Roedel, *J Am Chem Soc* 1953, *75*, 6110.

[26] P. M. Ehrlich, G., *Adv Polym Sci* 1970, *7*, 386.

[27] R. A. Hutchinson; J. R. Richards; M. T. Aronson, *Macromolecules* 1994, *27*, 4530.

[28] P. J. Flory, *J Am Chem Soc* 1937, *59*, 241.

[29] N. M. Ahmad; F. Heatley; P. A. Lovell, *Macromolecules* 1998, *31*, 2822.

[30] P. A. Lovell; T. H. Shah; F. Heatley, *Polym Commun* 1991, *32*, 98.

[31] E. F. McCord; W. H. Shaw; R. A. Hutchinson, *Macromolecules* 1997, *30*, 246.

[32] N. M. Ahmad; B. Charleux; C. Farcet; C. J. Ferguson; S. G. Gaynor; B. S. Hawkett; F. Heatley; B. Klumperman; D. Konkolewicz; P. A. Lovell; K. Matyjaszewski; R. Venkatesh, *Macrom Rapid Commun* 2009, *30*, 2002.

[33] M. Kato; M. Kamigaito; M. Sawamoto; T. Higashimura, *Macromolecules* 1995, *28*, 1721.

[34] J. S. Wang; K. Matyjaszewski, *J Am Chem Soc* 1995, *117*, 5614.

[35] Y. Reyes; J. M. Asua, *Macrom Rapid Commun* 2011, *32*, 63.

[36] D. Konkolewicz; D. R. D'hooge; S. Sosnowski; R. Szymanski; M. F. Reyniers; G. B. Marin; K. Matyjaszewski, In *Progress in Controlled Radical Polymerization: Mechanisms and Techniques*, Matyjaszewski, K.; Sumerlin, B. S.; Tsarevsky, N. V., Eds. American Chemical Society, Washington D.C., 2012; Vol. 1100, p 145.

[37] K. Matyjaszewski; T. Pintauer; S. Gaynor, *Macromolecules* 2000, *33*, 1476.

[38] Y. Q. Shen; H. D. Tang; S. J. Ding, *Prog Polym Sci* 2004, *29*, 1053.

[39] N. V. Tsarevsky; K. Matyjaszewski, *Chem Rev* 2007, *107*, 2270-2299.

[40] M. E. Honigfort; W. J. Brittain, *Macromolecules* 2003, *36*, 3111-3114.

[41] I. Y. Ma; E. J. Lobb; N. C. Billingham; S. P. Armes; A. L. Lewis; A. W. Lloyd; J. Salvage, *Macromolecules* 2002, *35*, 9306-9314.

[42] D. F. Grishin; I. D. Grishin, *Russ J Appl Chem* 2011, *84*, 2021.

[43] K. Matyjaszewski; W. Jakubowski; K. Min; W. Tang; J. Y. Huang; W. A. Braunecker; N. V. Tsarevsky, *Proc Natl Acad Sci USA* 2006, *103*, 15309.

[44] T. Pintauer; K. Matyjaszewski, *Chem Soc Rev* 2008, *37*, 1087.

[45] L. Mueller; K. Matyjaszewski, *Macromol React Eng* 2010, *4*, 180.

[46] Y. P. Borguet; N. V. Tsarevsky, *Polym Chem* 2012, *3*, 2487.

[47] W. Jakubowski; K. Min; K. Matyjaszewski, *Macromolecules* 2006, *39*, 39.

[48] A. J. D. Magenau; N. C. Strandwitz; A. Gennaro; K. Matyjaszewski, *Science* 2011, *332*, 81.

[49] K. A. Payne; M. F. Cunningham; R. A. Hutchinson, In *Progress in Controlled Radical Polymerization: Mechanisms and Techniques*, Matyjaszewski, K.; Sumerlin, B. S.; Tsarevsky, N. V., Eds. American Chemical Society: 2012; Vol. 1100, p 183.

[50] R. Nicolay; Y. Kwak; K. Matyjaszewski, *Angew Chem Int Edit* 2010, *49*, 541.

[51] W. Jakubowski; K. Matyjaszewski, *Angew Chem Int Edit* 2006, *45*, 4482.

[52] K. Matyjaszewski, *Macromolecules* 2012, *45*, 4015.

[53] S. E. Averick; A. J. D. Magenau; A. Simakova; B. F. Woodman; A. Seong; R. A. Mehl; K. Matyjaszewski, *Polym Chem* 2011, *2*, 1476.

[54] W. Li; K. Matyjaszewski, *Polym Chem* 2012, *3*, 1813.

[55] D. R. D'Hooge; D. Konkolewicz; M. F. Reyniers; G. B. Marin; K. Matyjaszewski, *Macromol Theory Sim* 2012, *21*, 52.

[56] D. Konkolewicz, A. J. D.; Averick, S. E.; Simakova, A.; He, H.; Matyjaszewski, K., *Macromolecules* 2012, *45*, 4461.

[57] Y. Kwak; A. J. D. Magenau; K. Matyjaszewski, *Macromolecules* 2011, *44*, 811-819.

[58] N. H. Nguyen; M. E. Levere; V. Percec, *J Pol Sci, Part A: Polym Chem* 2012, *50*, 860-873.

[59] Y. Z. Zhang; Y. Wang; C. H. Peng; M. J. Zhong; W. P. Zhu; D. Konkolewicz; K. Matyjaszewski, *Macromolecules* 2012, *45*, 78-86.

[60] N. H. Nguyen; V. Percec, *J Pol Sci, Part A: Polym Chem* 2011, *49*, 4756-4765.

[61] N. Chan; M. F. Cunningham; R. A. Hutchinson, *Polym Chem* 2012, *3*, 1322-1333.

[62] G. X. Wang; M. Lu; M. Zhong; H. Wu, *Polymer* 2012, *53*, 1093.

[63] A. Nese; Y. Li; S. S. Sheiko; K. Matyjaszewski, *ACS Macro Letters* 2012, *1*, 991.

[64] K. Schroder; R. T. Mathers; J. Buback; D. Konkolewicz; A. J. D. Magenau; K. Matyjaszewski, *ACS Macro Letters* 2012, *1*, 1037.

[65] G. Arzamendi; C. Plessis; J. R. Leiza; J. M. Asua, *Macromol Theory Sim* 2003, *12*, 315.

[66] D. H. Li; M. C. Grady; R. A. Hutchinson, *Ind Eng Chem Res* 2005, *44*, 2506.

[67] D. R. D'Hooge; M. F. Reyniers; F. J. Stadler; B. Dervaux; C. Bailly; F. E. Du Prez; G. B. Marin, *Macromolecules* 2010, *43*, 8766.

[68] F. Seeliger; K. Matyjaszewski, *Macromolecules* 2009, *42*, 6050.

[69] J. M. Asua; S. Beuermann; M. Buback; P. Castignolles; B. Charleux; R. G. Gilbert; R. A. Hutchinson; J. R. Leiza; A. N. Nikitin; J. P. Vairon; A. M. van Herk, *Macromol Chem Phys* 2004, *205*, 2151.

[70] A. N. Nikitin; R. A. Hutchinson; M. Buback; P. Hesse, *Macromolecules* 2007, *40*, 8631.

[71] S. Maeder; R. G. Gilbert, *Macromolecules* 1998, *31*, 4410.

[72] W. Wang; R. A. Hutchinson, *AIChE Journal* 2011, *57*, 227.

[73] A. Nobel Product Data Sheet of Trigonox 21S. http://www.akzonobel.com/polymer (June, 2012)

[74] O. L. Mageli; C. S. Sheppard, Organic Peroxides and Peroxy Compounds - General Description. In *Organic Peroxides*, Swern, D., Ed. John Wiley & Sons, Ltd: USA, 1970; Vol. 1, pp 1-104.

[75] D. R. D'Hooge; M. F. Reyniers; G. B. Marin, *Macromol React Eng* 2009, *3*, 185.

[76] L. Bentein; D. R. D'Hooge; M. F. Reyniers; G. B. Marin, *Macromol Theory Sim* 2011, *20*, 238.

[77] L. Bentein; D. R. D'Hooge; M. F. Reyniers; G. B. Marin, *Polymer* 2012, *53*, 681.

[78] P. B. Zetterlund, *Macromolecules* 2010, *43*, 1387.

[79] A. R. Wang; S. P. Zhu, *Macromolecules* 2002, *35*, 9926.

[80] J. B. L. de Kock; A. M. Van Herk; A. L. German, *J Macromol Sci Pol R* 2001, *C41*, 199.

[81] R. G. Gilbert, *Pure Appl Chem* 1992, *64*, 1563.

[82] J. Wieme; D. R. D'Hooge; M. F. Reyniers; G. B. Marin, *Macromol React Eng* 2009, *3*, 16.

[83] E. Vivaldo-lima; A. E. Hamielec; P. E. Wood, *Polym Reac Eng* 1994, *2*, 17.

[84] J. Wieme; T. De Roo; G. B. Marin; G. J. Heynderickx, *Ind Eng Chem Res* 2007, *46*, 1179.

[85] J. F. Lutz; P. Lacroix-Desmazes; B. Boutevin, *Macrom Rapid Commun* 2001, *22*, 189.

[86] J. Y. Huang; T. Pintauer; K. Matyjaszewski, *J Pol Sci, Part A: Polym Chem* 2004, *42*, 3285.

[87] K. Matyjaszewski; T. P. Davis, *Handbook of Radical Polymerization*. Wiley-Interscience: Hoboken, 2002.

[88] A. Goto; T. Fukuda, *Prog Polym Sci* 2004, *29*, 329.

[89] M. J. Zhong; K. Matyjaszewski, *Macromolecules* 2011, *44*, 2668.

Chapter 4: A theoretical exploration of the potential of ICAR ATRP for one- and two-pot synthesis of well-defined diblock copolymers

Summary

Kinetic Monte Carlo simulations are performed to investigate the capability of bulk ICAR ATRP for the synthesis of well-defined poly(isobornyl acrylate-*b*-styrene) block(-like) copolymers using one-pot semi-batch and two-pot batch procedures. The block copolymer quality is quantified via a block deviation (<BD>) value. For <BD> values lower than 0.30, the quality is defined as good and for well-chosen polymerization conditions the formation of homopolymer chains upon addition of the second monomer can be suppressed. A better block quality is obtained when isobornyl acrylate is polymerized first and a sufficiently low polymerization temperature is selected for the synthesis of each block. For lower Cu levels a one-pot semi-batch procedure allows a much faster ATRP and better control over the polymer properties than a two-pot batch procedure. This work has been submitted to *Macromolecular Reaction Engineering.*

4.1 Introduction

Since the early nineties an important breakthrough in the field of polymer science has been made with the development of controlled radical polymerization (CRP) techniques.[1-6] Contrary to conventional free radical polymerization (FRP), these techniques allow the production of new well-defined polymeric materials with controlled composition and topology, and predetermined average chain length.

The main feature of CRP is the controlled growth of polymer chains due to the presence of a mediating agent able to intermittently deactivate radicals (R_i; i:chain length; Figure 4.1) to a dormant or 'capped' state (R_iX) while incorporating end-group functionality (X;EGF), which allows further modification of the macromolecular

structure. For a well-chosen mediating agent, this deactivation process is dominant so that radicals have only milliseconds available to add to monomer before they return to the dormant state. In that case, the radical concentration remains low, minimizing thereby unavoidable termination reactions that lead to the unwanted formation of dead polymer molecules and loss of EGF. Furthermore, for a fast CRP initiation, a polymer with a narrow chain length distribution (CLD) can be obtained.[2, 4]

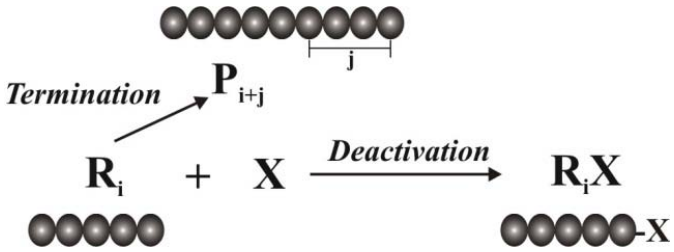

Figure 4.1: Deactivation mechanism in CRP; termination leading to loss of EGF (no X) also shown.

In the past decade, CRP research has been mainly directed toward the synthesis of different copolymer compositions, such as gradient, block and graft copolymers.[2] In general, copolymerization enables to obtain an optimal balance of different properties in a single polymer chain by combining favorable characteristics from two or more comonomers and is therefore commonly applied to produce a wide assortment of polymeric materials for commercial applications.[7] In particular, styrenes,[8, 9] acrylates[10, 11] and methacrylates[12, 13] have been succesfully copolymerized with CRP techniques, such as nitroxide mediated radical polymerization (NMP),[14] reversible addition fragmentation chain transfer (RAFT) polymerization[15] and atom transfer radical polymerization (ATRP),[16] the CRP technique considered in this work.

Using ATRP, tailored amphiphilic block copolymers of polystyrene and poly(acrylic acid) have been prepared and successfully used as stabilizers in emulsion polymerization.[9] Di- and triblock copolymers involving *tert*-butyl acrylate (*t*BuA), methyl acrylate (MA) and styrene (Sty) as comonomers have been synthesized as polymer precursors for the preparation of amphiphilic and hydrophilic nanostructured materials.[11] Additionally, the ATRP-mediated synthesis of catenated poly(Sty-*b*-

MMA) block copolymers (MMA: methyl methacrylate), i.e. with interlocked cyclic topologies, has been reported by Bunha et al.[13] On the other hand, isobornyl acrylate (iBoA) and *n*-butyl acrylate (*n*-BuA) have been successfully copolymerized with various acrylate comonomers via ATRP in order to obtain modified thermomechanical properties compared to the pure homopolymers.[17] Interestingly, the ATRP made poly(iBoA) is characterized by a low polydispersity index (PDI < 1.3) and a high glass transition temperature ($T_{g,p}$ = 94 ^{0}C)[18] and can thus be used as a substitute for ATRP based poly(MMA) ($T_{g,p}$ = 125 ^{0}C), which typically displays ill-defined properties (PDI ≥ 1.3).[19, 20]

As illustrated in Figure 1.3 (third row), in (normal) ATRP processes a mostly Cu-based transition metal complex (M_t^nX/L; activator) is used as mediating agent and an alkyl halide (R_0X) as ATRP initiator to generate initiator radicals (R_0) and deactivator molecules ($M_t^{n+1}X_2/L$). The latter provide EGF to the growing macroradicals (R_i) resulting in the formation of dormant polymeric species (R_iX). For a given monomer, a good control over chain length and livingness is obtained if a catalyst characterized by a sufficiently low ATRP equilibrium coefficient (k_a/k_{da}) is employed.[21]

Although (normal) ATRP allows unique polymer properties, the production of large volumes of ATRP based materials is being thwarted by the excessive concentrations of Cu-based catalysts that are usually necessary to achieve a fast and controlled polymerization.[22] Several issues, such as toxicity of the ATRP catalyst, handling of the air-sensitivy activator species and expensive purification operations, constitute the main current obstacles hindering the development of ATRP at industrial scale.[3] Consequently, in the last years various modifications have been introduced to overcome these issues, such as the improvement of the ATRP catalyst,[23-25] the optimization of the ATRP catalyst removal,[26-28] and the development of modified ATRP techniques using low catalyst amounts.[29-32]

The most frequently applied modified ATRP techniques for the promotion of the ATRP process toward industrial application are initiators for continuous activator regeneration (ICAR) ATRP,[29] activators regenerated by electron transfer (ARGET) ATRP,[29, 30] electrochemically mediated ATRP (*e*ATRP)[31] and supplementary

activator and reducing agent (SARA) ATRP.[32] In ICAR and ARGET ATRP, the activator is (re)generated from the oxygen-stable deactivator by, respectively, a conventional radical initiator (I_2) and a reducing agent (*Red*) while in *e*ATRP an electrode is employed. On the other hand, in SARA ATRP additionally Cu^0 are utilized as source for the formation of the ATRP activator while reducing the deactivator. However, it should be noted that the SARA ATRP technique can shift to a single electron transfer-living radical polymerization (SET-LRP)[32-34] when the added Cu^0 species favorably incline towards disproportionation instead of comproportionation and the activation with Cu^0 is very important.[32]

In the case of ICAR and ARGET ATRP, a large number of studies published in the last few years[24, 29, 30, 35-46] demonstrate the growing interest and potential of modified ATRP techniques to (co)polymerize a wide range of monomers. Particularly, well-defined block copolymers involving styrene, *n*BuA and MMA have been prepared using low catalyst concentrations (< 50 ppm (with respect to monomer)).[35, 36] Similarly, *e*ATRP has been recently applied for the controlled synthesis of poly(MA) using Cu-catalyst concentrations as low as 50 ppm[31] and Li et al.[47] have successfully applied this technique to grow homopolymer brushes on gold surfaces using both 3-sulfopropyl methacylate potassium salt and 2-hydroxyethyl methacrylate as monomers. On the other hand, for SARA ATRP the amount of Cu in solution is still too high[30, 32] and more advanced macromolecular copolymer structures have not been extensively investigated, suggesting a higher industrial potential for ARGET, ICAR and *e*ATRP. However, it can be expected that the current more elaborated polymerization procedure for *e*ATRP somewhat counteracts its industrial implementation.

As indicated in recent studies,[30, 46] the reducing species in ICAR and ARGET ATRP have to be present in a sufficiently high amount to ensure a reasonable polymerization rate, which corresponds to the selection of sufficiently high potential for the *e*ATRP process. Too high initial amounts of the reducing agents or too high potentials should however be avoided since they promote excessive termination reactions and, hence, result in a pronounced loss of control over polymer properties.

It should be stressed that the success of ICAR ATRP for the synthesis of tailored AB diblock copolymers depends on the possibility to suppress the formation of non-diblock copolymer chains once the second monomer is present. Unwanted B homopolymer molecules (B…B) can be formed, since in ICAR ATRP propagating conventional radical initiator fragments are present (Figure 1.6a), in contrast to ARGET ATRP (Figure 1.6b) in which no extra initiator radicals are generated. In addition, the termination of diblock macroradicals leads to undesired triblock copolymer chains (A…AB…BA…A). It can nevertheless be expected that the selection of appropriate polymerization conditions allows to limit these side effects. Currently, no information on the selection of such optimal conditions is although available.

Up to now, ICAR ATRP diblock copolymerization research has been mainly focused on two-pot batch procedures (Figure 4.2 (left)). In these procedures, the first block (A...A) is polymerized, isolated and used as a macro-initiator for the polymerization of the second block (B...B). The final polymer product is obtained after a second isolation step, contrary to one-pot semi-batch procedures (Figure 4.2 (right)), in which the second monomer (B) is added when a high conversion is reached for the first block and in which a diblock-like copolymer is envisaged. Both procedures are however confronted with the same challenge, i.e. the reduction of the formation of non-diblock copolymer chains, as explained above.

Note that the one-pot semi-batch procedure is in principle industrially more attractive, since the intermediate purification steps in two-pot procedures contribute to a higher operation cost and thus can lead to a negative economical overall balance. However, the latter is only true in case the obtained diblock-like copolymer from a one-pot semi-batch procedure displays similar or even improved properties than the “pure” diblock copolymer obtained from a two-pot batch procedure. Such comparison can however be only made in case the explicit copolymer composition, which is difficult to access experimentally, is known.

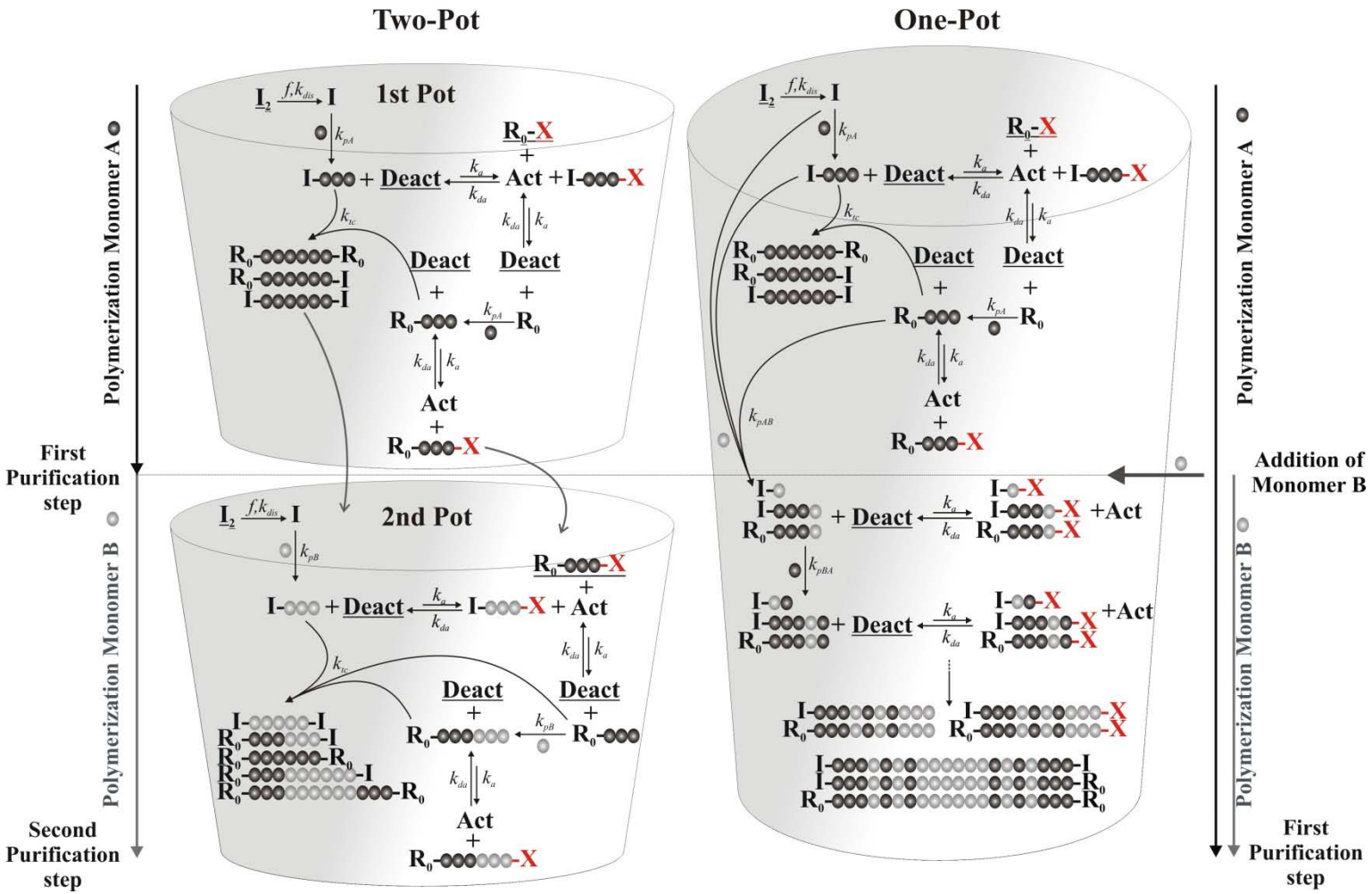

Figure 4.2: Illustration of two-pot batch (left) and one-pot semi-batch (right) copolymerization procedures applied to ICAR ATRP; I_2 and R_0X are the conventional radical and ATRP initiator; Act: activator and Deact: deactivator; the species which are initially present in the polymerization are underlined; the dead polymer chains from the first pot are transferred to the second pot; for visualization, only one-propagation step is shown.

In this work, detailed kinetic Monte Carlo (kMC) simulations are therefore used to investigate the potential of ICAR ATRP for the synthesis of well-defined poly(iBoA-*b*-Sty) diblock(-like) copolymers. Both, one-pot semi-batch and two-pot batch procedures are considered while selecting initial polymerization conditions, which result in the suppression of the formation of homopolymer chains and triblock copolymer chains. Analogously to the gradient deviation (<GD>) value proposed by Van Steenberge et al.[48] to quantify the (linear) gradient quality of copolymers, a block deviation value (<BD>) ranging between 0 and 1 is introduced which allows to evaluate the block copolymer quality.

It is shown that the block copolymer quality is good for <BD> values lower than 0.30 and that the one-pot semi-batch procedure is better suited in case a fast polymerization is desired and a low Cu amount is used. In addition, it is demonstrated that the success of the ICAR ATRP depends on the selected polymerization temperature, the initial conventional radical initiator concentration(s), the overall Cu level, and the order in which the monomers are polymerized.

4.2 Kinetic Model

In this work, the kinetic Monte Carlo (kMC) technique[49] is applied to study the ICAR ATRP of iBoA and styrene in bulk for the synthesis of their diblock(-like) copolymers. As deactivator $CuBr_2$/PMDETA (PMDETA: N,N,N',N'',N''-pentamethyl-diethylenetriamine) is selected and lauryl peroxide (LPO) and methyl 2-bromo propionate (MBrP) are used, respectively, as conventional radical initiator I_2 and ATRP initiator R_0X (Figure 1.6a). All simulations are limited to a molar conversion of 0.80, since this conversion is frequently the final conversion in experimental CRP kinetic studies and, for illustration purposes, only symmetric diblocks are envisaged, i.e. ideally the length of both blocks is the same in each polymer chain. To ensure a direct comparison of the one-pot semi-batch and two-pot batch approach, in both synthesis steps of the two-pot batch approach the simulations are stopped at a molar conversion of 0.80. Also, at every moment the length of a polymer chain corresponds to the overall chain length, i.e. the sum of the length of the first and second block.

4.2.1 Reactions and model parameters

In Table 4.1 an overview is given of the considered reactions. Note that only for the one-pot semi-batch approach, these reactions occur simultaneously. Additionally, for both approaches backbiting reactions are neglected for the acrylate macroradicals. This assumption can be made, since it is known that isobornyl acrylate macroradicals, due to their higher rigidity, are less prone to backbiting[50] and controlled ATRP's of acrylates lead to a much lower amount of branching compared to FRP.[51, 52] Moreover, recent work of Klumperman et al.[53] showed that in CRP copolymerizations involving acrylates the branching amount is further reduced, since other comonomers are typically not susceptible to backbiting. On the other hand, for styrene, the influence of thermal self-initiation and chain transfer reactions can be safely neglected at the considered temperatures in this work.[54-57]

For simplicity, a typical conventional radical initiator efficiency of 0.75 is considered[58] and an intrinsic terminal model[59] is applied, i.e. the intrinsic reactivity of each macromolecular reaction step is limited to the last monomer unit. For propagation of the radical species and dissociation of the conventional radical initiator, the Arrhenius parameters (see Table 4.1) are taken from FRP literature data,[60-62] whereas for activation and deactivation these parameters (see also Table 4.1) are based on ATRP literature data.[46] For the ATRP of iBoA with CuBr/PMDETA as ATRP catalyst, activation/deactivation Arrhenius parameters are directly available,[50] while for the ATRP of styrene, the ATRP initiation and the activation/deactivation process involving *I* 'capped' species, these values are assessed based on literature data of related ATRP systems.

For the activation of the ATRP initiator (MBrP) and of dormant macrospecies 'capped' with a styrene unit, the Arrhenius parameters reported by Seeliger et al.[63] are used as such to a first approximation. For deactivation of styrene radicals, the value of 1.1 10^7 mol L^{-1} s^{-1} in Table 4.1 is taken from the experimental study of Fu et al.[64] for the ATRP of styrene with CuBr/PMDETA as ATRP catalyst at 110 ^{0}C assuming a negligible temperature dependence, which is consistent with the very low activation

Table 4.1: Overview of reactions (except termination by recombination) and their Arrhenius parameters used in the kinetic Monte Carlo model for the batch ICAR ATRP of iBoA and styrene in bulk toward well-defined poly(iBoA-*b*-Sty) diblock copolymers; for termination: apparent chain length dependent rate coefficients: for "AB cross-termination" the geometric mean is used of the corresponding homo-polymerizations; for "AA homo-termination": encounter pair model from D`hooge et al.[50] is used; for "BB homo-termination": composite k_t model with RAFT-CLD-T parameters;[72] for the conventional radical initiator a chemical efficiency (f^{chem}) of 0.75 is used;[58] the reactivity ratios (r_A, r_B) of a representative alkyl acrylate and a styrene monomer are considered.[59]

	Reaction	Equation	Arrhenius Parameters[(a)]
Normal ATRP	Activation of R_0X and $R_{B,i}X$	$R_0X + M_t^n X / L \xrightarrow{k_{a,0}^{chem}} R_0 + M_t^{n+1} X_2 / L$ $R_{B,i}X + M_t^n X / L \xrightarrow{k_{a,B}^{chem}} R_{B,i} + M_t^{n+1} X_2 / L$	A = 3.7 10^4 [(b)] E_a = 33.2 [(b)]
	Activation of $R_{A,i}X$	$R_{A,i}X + M_t^n X / L \xrightarrow{k_{a,A}^{chem}} R_{A,i} + M_t^{n+1} X_2 / L$	A = 1.5 10^4 [(c)] E_a = 32.6 [(c)]
	Deactivation of R_0X and $R_{B,i}$	$R_0 + M_t^{n+1} X_2 / L \xrightarrow{k_{da,0}^{chem}} R_0X + M_t^n / L$ $R_{B,i} + M_t^{n+1} X_2 / L \xrightarrow{k_{da,B}^{chem}} R_{B,i}X + M_t^n X / L$	A = 1.1 10^7 [(d)] E_a = 0 [(e)]
	Deactivation of $R_{A,i}$	$R_{A,i} + M_t^{n+1} X_2 / L \xrightarrow{k_{da,A}^{chem}} R_{A,i}X + M_t^n X / L$	A = 1.5 10^8 [(c)] E_a = 0.1 [(c)]
	Propagation of R_0 with A and $R_{A,i}$ with A	$R_{0A} + A \xrightarrow{k_{p,A}^{chem}} R_{1,A}$ $R_{i,A} + A \xrightarrow{k_{p,A}^{chem}} R_{i+1,A}$	A = 1.1 10^7 [(f)] E_a = 17.0 [(f)]
	Propagation of R_0 with B and $R_{B,i}$ with B	$R_0 + B \xrightarrow{k_{p,B}^{chem}} R_{1,B}$ $R_{i,B} + B \xrightarrow{k_{p,B}^{chem}} R_{i+1,B}$	A = 4.3 10^7 [(g)] E_a = 32.5 [(g)]
	Propagation of $R_{A,i}$ with B	$R_{i,A} + B \xrightarrow{k_{p,AB}^{chem}} R_{i+1,B}$	$k_{p,A}$ / r_A with r_A = 0.2 [(h)]
	Propagation of $R_{B,i}$ with A	$R_{i,B} + A \xrightarrow{k_{p,BA}^{chem}} R_{i+1,A}$	$k_{p,B}$ / r_B with r_B = 0.8 [(h)]
Extra for ICAR ATRP	Dissociation (dis)	$I_2 \xrightarrow{f^{chme} k_{dis}^{chem}} 2I$	A = 2.2 10^{16} [(i)] E_a = 137.7 [(i)]
	Activation of IX	$IX + M_t^n X / L \xrightarrow{k_{a,I}^{chem}} I + M_t^{n+1} X_2 / L$	A = 8.2 10^8 [(j)] E_a = 33.2 [(b)]
	Deactivation of I	$I + M_t^{n+1} X_2 / L \xrightarrow{k_{da,I}^{chem}} IX + M_t^n X / L$	A = 1.0 10^6 [(k)] E_a = 0 [(l)]
	Propagation with A and B	$I + A \text{ or } B \xrightarrow{k_{p,A}^{chem} \text{ or } k_{p,B}^{chem}} R_{1,A} \text{ or } R_{1,B}$	A = 1.1 10^7 [(f)], 4.3 10^7 [(g)] E_a = 17.0 [(f)], E_a = 32.5 [(g)]

[(a)] A: L mol^{-1} s^{-1} or s^{-1} and E_a: kJ mol^{-1}; [(b)] Seeliger et al.;[63] [(c)] D'hooge et al.;[50] [(d)] Fu et al.;[64] [(e)] based on [(c)]; [(f)] prop. with A: Dervaux et al.;[60] [(g)] prop. with B: Buback et al.;[61] [(h)] based on the values reported by Asua;[59] [(i)] Akzo Nobel;[62] [(j)] based on D'hooge et al.[46] at 80^{0}C with E_a from [(b)]; [(k)] based on D'hooge et al.;[46] [(l)] based on [(c)]

energy for the deactivation of isobornyl acrylate macroradicals.[50] Again for simplicity, the same value is used for the deactivation of ATRP initiator radicals.

For the activation and deactivation process involving conventional radical initiator fragments, the theoretical values reported in the modeling study of D'hooge et al.[46] at 80 ^{0}C are used while assuming the same activation energy as for MBrP. This approach is valid to a first approximation taking into account that simulations reported by Toloza Porras et al.[65] have indicated that the polymerization characteristics are almost unaffected upon a significant variation of these kinetic parameters.

Furthermore, diffusional limitations on the activation/deactivation process and conventional radical initiation are neglected taking into account that they typically become only important at very high conversions,[56, 66-69] which are not considered in this work. For termination, however, apparent rate coefficients have to be used to capture the influence of diffusional limitations when the viscosity and/or chain length increases.

In this work, the apparent termination reactivity is described based on the number average chain length only. For the "cross-termination" of iBoA and styrene radicals, the geometric mean of the corresponding "homo-terminations" is considered similar to the work of Van Steenberge et al.[48] For "iBoA homo-termination", the apparent termination rate coefficients are taken from D'hooge et al.,[50] in which an encounter pair approach[70, 71] was followed with diffusion coefficients fitted to experimental dynamic viscosity data. On the other hand, for "styrene homo-termination", a composite k_t model is used with the corresponding RAFT-chain length dependent-termination (RAFT-CLD-T) parameters taken from Johnston-Hall and Monteiro.[72] For completeness it is mentioned here that for iBoA, no such RAFT-CLD-T parameters are available.

4.2.2 Calculation of polymer properties and introduction of <BD> value as new copolymer property

For a detailed description of the kinetic model, the reader is referred to Van Steenberge et al.[48, 73] Besides the conversion profile and the evolution of average

polymer properties, such as the number average chain length (x_n), the polydispersity index (PDI) and the end-group functionality (EGF) with conversion, the kMC model allows the explicit representation of the copolymer composition along the polymerization, i.e. for a representative number of polymer chains the monomer sequence can be tracked. Based on a benchmarking of the simulations starting from a sufficiently high number of monomer molecules (~10^7), 10000 to 20000 polymer chains have to be typically tracked to obtain reliable results in ICAR ATRP. For visualization (e.g. Figure 4.7), it suffices however to select 1000 polymer chains out of a representative kMC sample.

Based on the calculation of the explicit copolymer composition of a representative kMC sample, it was recently shown[48] that the linear gradient quality of copolymers can be quantified by the introduction of a linear gradient deviation (<GD>) value. The <GD> ranges between 0 (perfect linear gradient copolymer) and 1 (homopolymer). In this work, for the first time, a similar so-called block deviation (<BD>) value is introduced as a new copolymer property, which allows to assess the block copolymer quality and thus offers a direct comparison of one- and two-pot procedures for the synthesis of well-defined block(-like) copolymers. The calculation of the <BD> value is applicable both for symmetric and asymmetric diblock copolymers and the diblock quality is defined as a universal polymer property, i.e. an asymmetric perfect diblock copolymer consisting of 25% A and 75% B is evaluated the same (i.e. the same <BD>) as the corresponding one consisting of 75% A and 25% B (see Appendix D).

Figure 4.3 illustrates the basic principle of the method for a ‘left to right’ evaluation of the AB block copolymer quality of a single polymer chain *z* with length i = 100 aiming at an equal chain length for each block, i.e. considering a symmetric diblock chain as reference chain. Ideally, the cumulative amount of A (S_A) should increase linearly until a value of 50 (i/2) is obtained at the position corresponding to the middle of the chain (y=50), whereas for higher positions no further iFigure 4.4ncrease may take place (full line in Figure 4.3a; $S_{A,ideal,AB}$). Similarly, Figure 4.3(b) shows the corresponding evolution of $S_{B,ideal,AB}$, the ideal cumulative amount of B as function of (chain) position y. In reality, a copolymer chain can however deviate from the perfect case, taking into

account that this chain can be asymmetric and/or can originate from a 'one-pot' synthesis approach, in which it can be expected that no pure block characteristics are obtained (dashed lines in Figure 4.3; S_A and S_B).

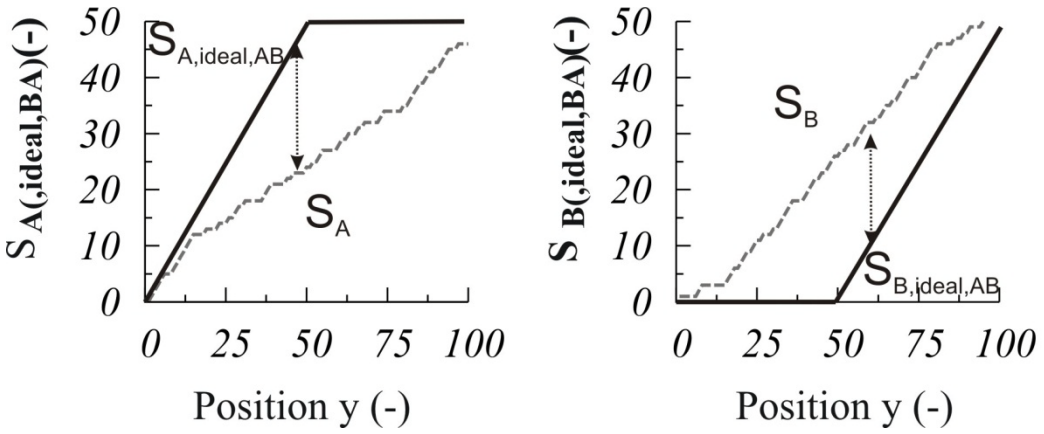

Figure 4.3: 'A to B' block deviation evaluation ('left to right') applied to a single polymer chain with a chain length *i* of 100; here a symmetric block copolymer is assumed as the reference case, i.e. both blocks should possess the same length of 50.

For a larger deviation between both profiles in Figure 4.3a and 4.3b, it clearly follows that the copolymer composition reflects less a symmetric AB diblock copolymer. Mathematically this deviation can be captured by the introduction of a $BD_{AB}(z)$ value for the considered chain *z* (see Appendix D):

$$BD_{AB}(z) = \sum_{y=1}^{i} \frac{1}{2} \frac{\left|S_{A,ideal,AB} - S_A\right| + \left|S_{B,ideal,AB} - S_B\right|}{i^2} \qquad (1)$$

in which the ideal profiles are given by the following piecewice functions:

$$\begin{aligned} S_{A,ideal,AB} &= y \quad (1 \le y \le i/2) \\ S_{A,ideal,AB} &= i/2 \quad (i/2 \le y \le i) \\ S_{B,ideal,AB} &= 0 \quad (1 \le y \le i/2) \\ S_{B,ideal,AB} &= y - i/2 \quad (i/2 < y \le i) \end{aligned} \qquad (2)$$

As explained in Appendix D and similar to the calculation of the <GD> value reported by Van Steenberge et al.,[48] three other evaluations can be defined of which the minimum BD(z) reflects the unique defined block quality of the considered polymer

chain *z* and from which an average block deviation value (<BD*>) can be calculated for all polymer chains:

$$< BD^* >= \sum_{z=1}^{z_{max}} \frac{BD(z)}{z_{max}} \quad (3)$$

In equation (3), z_{max} is the number of polymer chains of the representative polymer sample. A rescaled value, ranging between 0 and 1, can be obtained by dividing <BD*> by the value for a homopolymer with the same average chain length x_n and a PDI of 1, i.e. $<BD^*_{hp}>$:

$$< BD >= \frac{< BD^* >}{< BD^*_{hp} >} \quad (4)$$

In particular, for a x_n of 80 the following rescaling has to be performed:

$$< BD >= \frac{< BD^* >}{0.128} \quad (5)$$

However, as explained in Appendix D, for average chain lengths higher than 100 a constant value of 0.125 can be used as scaling factor.

As will be shown below a value of 0.30 can be used for <BD> to distinguish good from bad diblock(-like) copolymers and an appreciable amount of dead polymer or homopolymer chains can already lead to a significant increase of the <BD> value, explaining this relatively high value as criterion.

Finally, it is mentioned here that for asymmetric blocks the above formulas can be directly applied in case the ideal cumulative profiles given in Equation (2) are appropriately adjusted (see Appendix D).

4.3 Results and Discussion

In this section, the potential of ICAR ATRP for the synthesis of well-defined symmetric poly(iBoA-*b*-Sty) diblock(-like) copolymers is explored considering both one- and two-pot procedures. Copper(II) bromide ($CuBr_2$) is used as transition metal salt, *N*,*N*,*N*′,*N*′,*N*″-pentamethyl-diethylenetriamine (PMDETA) as ligand, methyl 2-

bromo propionate (MBrP) as ATRP initiator and lauryl peroxide (LPO) as conventional radical initiator. In both procedures, the final molar conversion per pot is taken equal to 0.80 at which an average chain length, x_n of 80 is targeted. Both the effect of the overall Cu amount and polymerization temperature on the ICAR ATRP is evaluated focusing on the overall polymerization time, the control over chain length and livingness, and the block copolymer quality via the calculation of a <BD> value.

4.3.1 Symmetric diblock copolymers made from iBoA and S in a two-pot batch procedure

Figure 4.4 (full lines) presents the conversion profile per pot and the corresponding copolymer properties for the synthesis of a symmetric poly(iBoA-*b*-Sty) diblock prepared at a reference temperature of 80^0C with a two-pot batch procedure, starting with iBoA as monomer. In the first pot, $[iBoA]_0/[MBrP]_0/[CuBr_2/PMDETA]_0/[LPO]_0$ is equal to 50/1/0.01/0.02, which are the same ratios as for $[Sty]_0/[\ \sum_{i=0} R_i X\ ]_0/[CuBr_2/PMDETA]_0/[LPO]_0$ in the second pot. Note that $[\ \sum_{i=0} R_i X\ ]_0$ is determined by the (simulated) dormant poly(iBoA) macrospecies amount produced after an iBoA conversion of 0.8 and that it is assumed that a perfect poly(iBoA) isolation is performed and, hence, that all dormant and dead poly(iBoA) chains from the first pot are transferred to the second pot after the purification step (Figure 4.2).

It can be seen in Figure 4.4 (full lines) that a very good control over the average polymer properties is obtained, as evidenced by the PDI values below 1.25 (Figure 4.4(c), full lines) and the EGF values close to 0.98 (Figure 4.4(d), full lines) at high styrene conversion. Moreover, the excellent livingness of the first block also facilitates its chain length extension with styrene and the PDI values for low styrene conversions are lower than the corresponding values at low iBoA conversions. The latter can be explained from the consideration of the CLD of the ATRP macro-initiator for the calculation of the PDI, as highlighted in the kinetic modeling section. However, at high iBoA conversions high PDI values are obtained, since very low deactivator concentrations are reached at these conversions, as shown in Figure 4.5(d). Furthermore, the iBoA block is polymerized with a higher rate (Figure 4.4(a), full

lines), which can be related to the higher intrinsic propagation reactivity of the acrylate radicals, despite their higher affinity toward deactivation compared to styrene radicals (see Table 4.1).

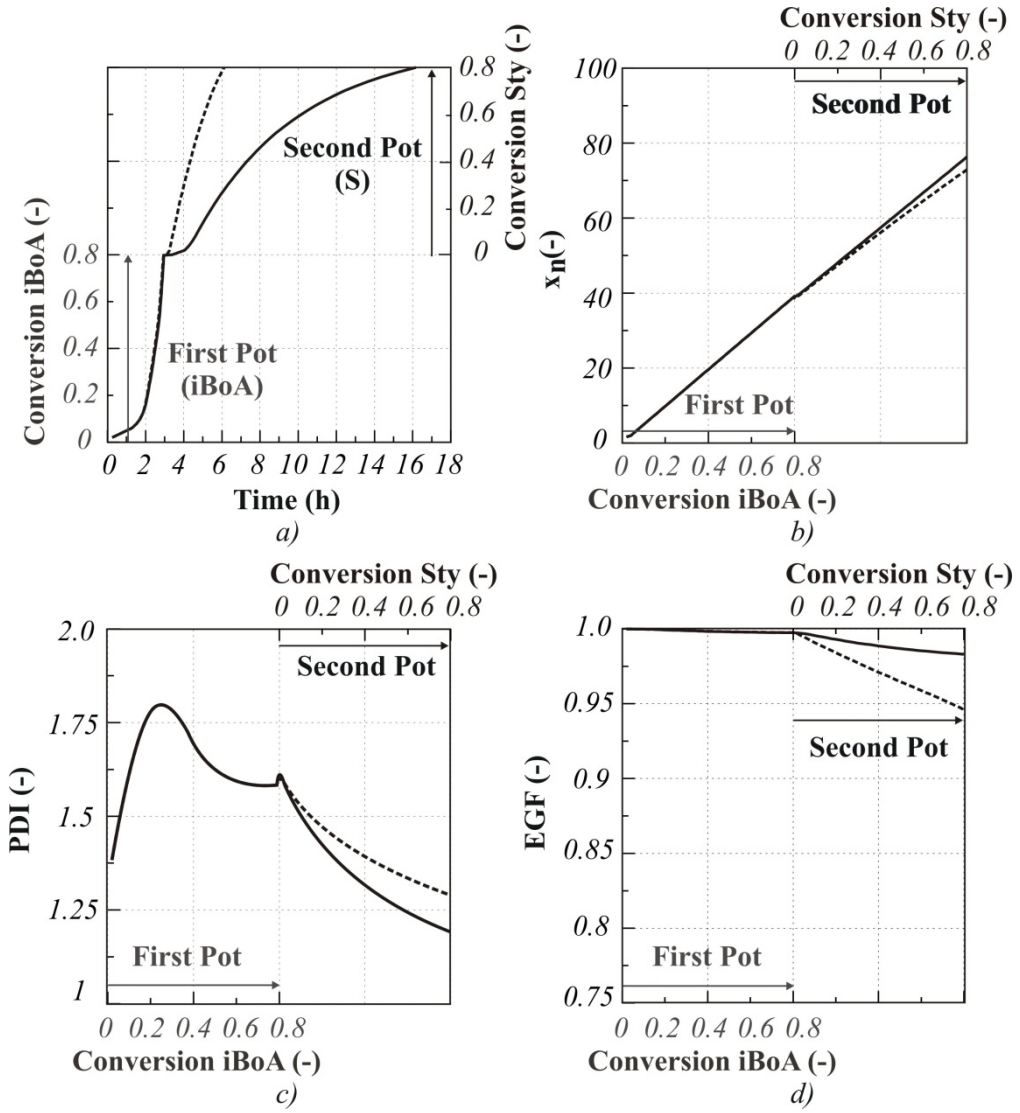

Figure 4.4: Two-pot batch ICAR ATRP of iBoA and styrene: a) conversion of the iBoA and Sty block as a function of time; b) number-average chain length (x_n) c) polydispersity index (PDI) and d) end-group functionality (EGF) as a function of the conversion of the iBoA/Sty block; first block: $[iBoA]_0/[R_0X]_0/[CuBr_2/PMDETA]_0/[LPO]_0$ = 50/1/0.01/0.1; second block: $[Sty]_0/[\ \sum_{i=0} R_iX\ ]_0/[CuBr_2]_0/[PMDETA]_0/[LPO]_0$ = 50/1/0.01/0.02 (full lines) and $[Sty]_0/[\ \sum_{i=0} R_iX\ ]_0/[CuBr_2]_0/[PMDETA]_0/[LPO]_0$ = 50/1/0.01/0.1 (dashed lines) ; reference temperature of 80^0C.

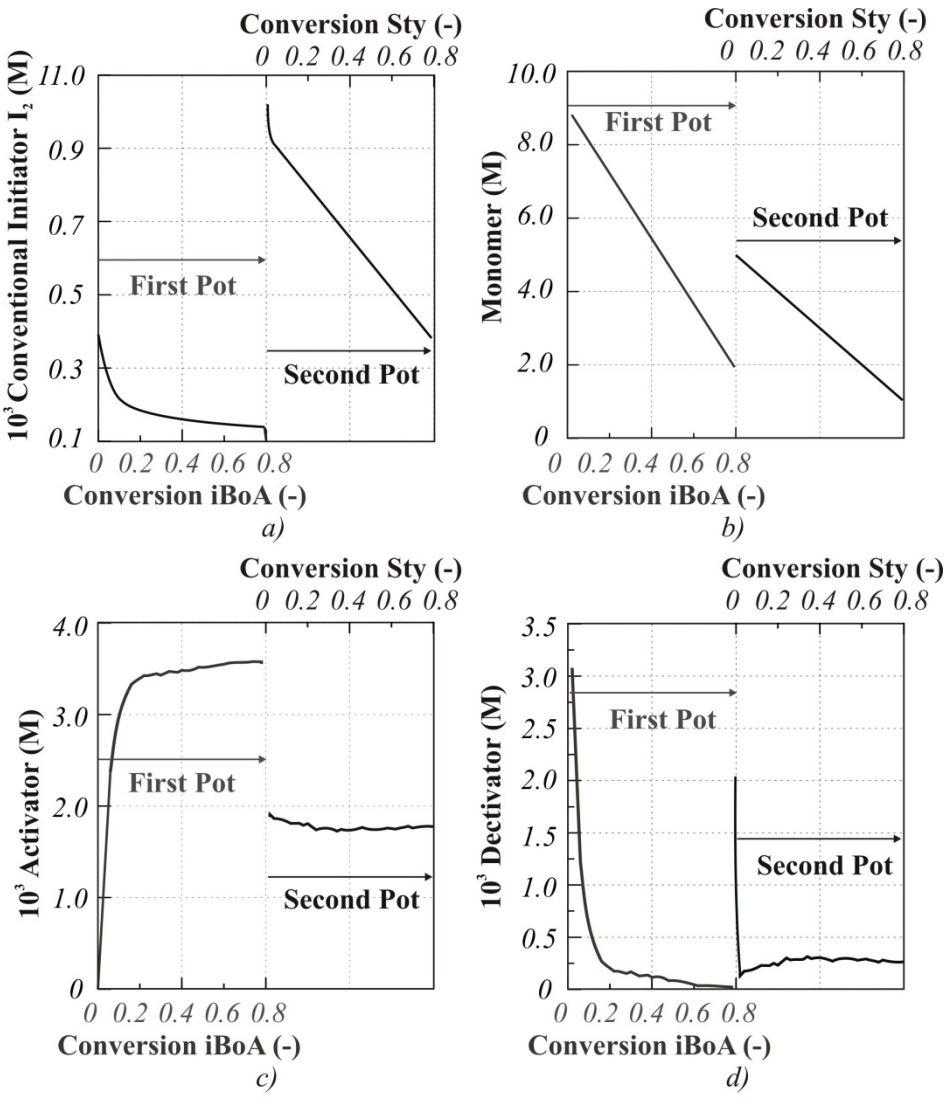

Figure 4.5: Concentration of a) conventional radical initiator (I_2), b) monomer, c) activator (CuBr/PMDETA) and d) deactivator ($CuBr_2$/PMDETA) as a function of conversion in the first pot (iBoA) and second pot (Sty); initial conditions equal to those mentioned in Figure 4.4 (dashed lines; $[\sum_{i=0} R_i X\ ]_0/[\mathrm{LPO}]_0=1/0.1$).

However, the overall polymerization time (~16 hours) is quite long, suggesting the use of a higher initial amount of LPO for the second pot in order to overcome this issue. Indeed, by using 5 times more LPO ($[\sum_{i=0} R_i X\ ]_0/[\mathrm{LPO}]_0=1/0.1$) only 6 hours are required, however reducing the level of control over the average polymer properties (Figure 4.4, dashed lines). Close inspection of Figure 4.4(c-d) reveals that for this increased initial LPO amount somewhat lower EGF and higher PDI values are obtained in the second pot. Similarly, a less controlled ICAR ATRP process results in case the order of the monomers is reversed (see Appendix E).

It should be stressed that the initial concentrations of the monomer and the deactivator in the second pot are ca. 1.5 times lower than the initial ones in the first pot (see Figure 4.5(b)-(d); $[\sum_{i=0} R_i X]_0/[\mathrm{LPO}]_0=1/0.1$ in the second pot), since the polymer obtained after the first pot possesses a much higher volume than the MBrP initiator. For LPO (Figure 4.5a), however, this volume effect is counteracted since a ca. five times higher amount with respect to the dormant species is added in the second pot. It can be further seen in Figure 4.6 that initially in both pots the deactivator concentration decreases significantly since the initial high conventional radical and deactivator concentration results in a high activator generation (Figure 4.5(c)). At high conversions, however, a more or less constant deactivator concentration is obtained reflecting a pseudo-equilibrium between activation and deactivation and confirming the good control over the average polymer properties. The latter is in agreement with the theoretical work of D'hooge et al.[46] on ICAR ATRP for homopolymers, in which it was shown that a controlled ICAR ATRP process necessitates well-balanced activation and deactivation rates and in particular the establishment of a pseudo-equilibrium for the macrospecies from low conversions onwards.

The relatively good control over average polymer properties is also confirmed in Figure 4.6(a)-(b), which presents an end-group analysis of all polymer chains taking into account both the α- and ω-end. For the dormant polymer molecules, this implies a differentiation on the one hand between polymer chains having *X* and R_0 as end-groups and *X* and *I* on the other hand. For the dead polymer molecules, the end-group combinations $R_0 \ldots R_0$, $R_0 \ldots I$, and $I \ldots I$ have to be considered. Note that such α- and ω-end-group information is very difficult to access experimentally, since even an accurate determination of the livingness (end-group X) is currently not straightforward[74] and both ends have to be tracked per polymer chain. It can be seen in Figure 4.6(a) that almost all dormant polymer molecules have been initiated with R_0 as required for a controlled ICAR ATRP and most termination products (Figure 4.6(b)) are formed based on dormant R_0-ending species, i.e. there is only a small contribution of termination between macroradicals ending on R_0 and *I*, accompanied by a negligible

contribution, at least in the second pot, of termination involving macroradicals containing two *I* end-groups.

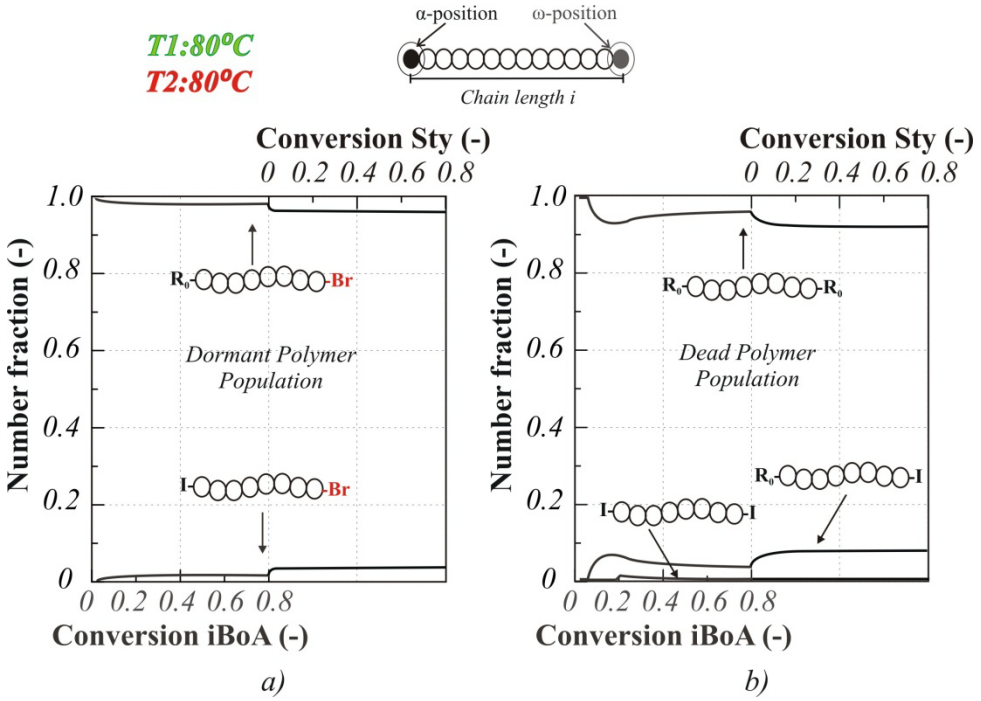

Figure 4.6: Number fraction of a) dormant and b) dead polymer molecules with specific α- and ω end-groups in the two-pot bacth bulk ICAR ATRP of iBoA and styrene as a function of the conversion in each block; end-group resulting from conventional radical initiator fragments indicated by *I*, those from the ATRP initiator by R_0; X is Br (EGF); initial conditions equal to those mentioned in Figure 4.4 (dashed lines; $[\sum_{i=0} R_i X\ ]_0/[\mathrm{LPO}]_0$=1/0.1 in second pot); EGF profile: Figure 4.4(d); for illustration, only 5 of the possible α,ω-polymer structures are shown.

The explicit copolymer composition of the poly(iBoA-*b*-Sty) diblock copolymer, as simulated with the two-pot approach with a conversion of 0.8 for each pot and a reference temperature of 80^{0}C, is shown in Figure 4.7(a). In this figure, the dormant and dead polymer molecules are shown respectively at the bottom and top of the figure and separated by a full blue line. In agreement with Figure 4.4, it follows that most polymer molecules (> 90%) in Figure 4.7(a) are dormant and a good control over chain length is obtained. Close inspection reveals that only a small part of the dormant polymer molecules (< 10 %) are pure styrene (red) homopolymer molecules, i.e. careful selection of the polymerization conditions allows to resolve the inherent

disadvantage of the ICAR ATRP technique for the synthesis of block copolymers (Figure 4.2).

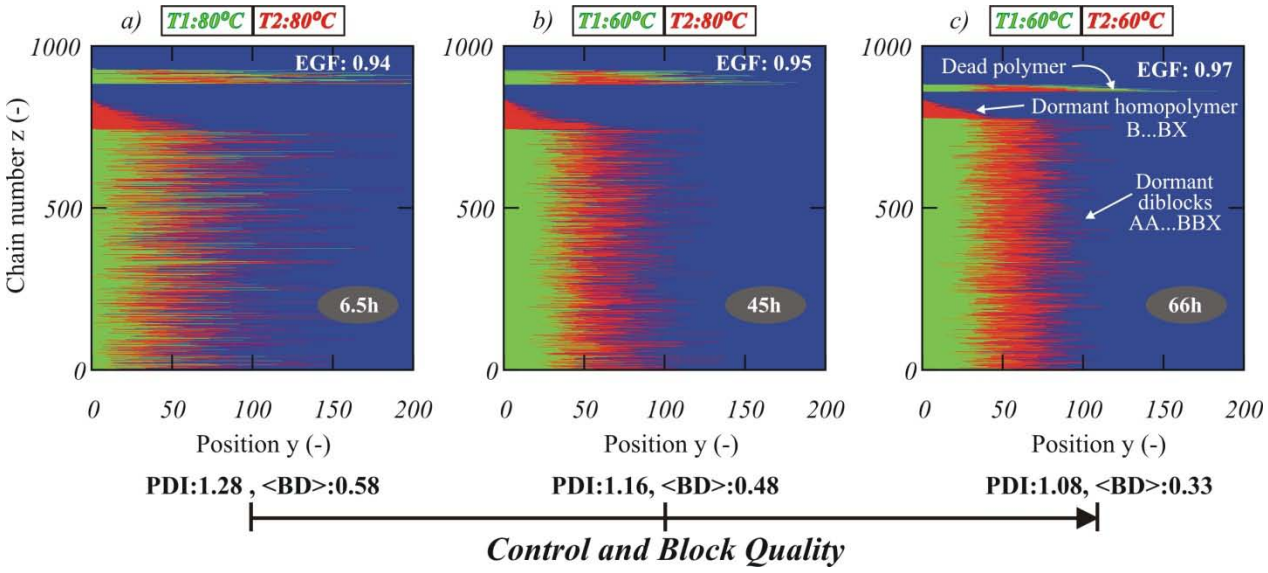

Figure 4.7: Copolymer composition of the poly(iBoA-*b*-Sty) diblock copolymer prepared by ICAR ATRP using a two-pot procedure; a) both blocks synthesized at a temperature of 60 ^{0}C; b) iBoA block synthesized at 60 ^{0}C and styrene block at 80 ^{0}C; c) both blocks synthesized at a temperature of 80 ^{0}C; initial conditions equal to those mentioned in Figure 4.4 (dashed lines; $[\sum_{i=0} R_i X\ ]_0/[\mathrm{LPO}]_0$=1/0.1 in the second pot)

Furthermore, it can be seen in Figure 4.7(a) that the dead polymer molecules possess on average a higher chain length than the dormant polymer molecules and are mainly formed during the second synthesis step, as evidenced by the presence of long ABA dead triblock copolymer chains (Figure 4.2; left). In contrast, the small fraction of short dead homopolymers chains is negligible in this visualization. In addition, it can be seen that a rather high <BD> value of 0.58 is simulated, which can be attributed on the one hand to the asymmetric amounts of both monomers in the dormant polymer chains with as extreme case the unwanted styrene dormant homopolymer chains, and on the other hand to the bad diblock quality of the dead triblock polymer chains.

Figure 4.7(a)-(c) illustrate the effect of the polymerization temperature on the <BD> value for a conversion of 0.80 in each pot. Two extra polymerization temperature profiles are considered besides the reference isothermal temperature profile (80°C; Figure 4.7(a)). In the first case (Figure 4.7(c)), the iBoA and styrene block are

obtained at 60 and 80 ^{0}C, respectively, while in the second case (Figure 4.7(b)), both blocks are synthesized at 60 ^{0}C. Note that the lowest block deviation, i.e. very strong symmetric diblock character (Figure 4.7(c)), corresponds to a <BD> value of ca. 0.30 and this value can therefore be considered to distinguish good from bad symmetric diblock copolymers, as stated before. This optimal block copolymer quality is obtained if, for both pots, a polymerization temperature of 60 ^{0}C is used at the expense of a very significant increase in the overall polymerization time. The latter can be explained by the steep decrease of the radical concentration with decreasing temperature, since both $K_{eq,iBoA}$ and $K_{eq,S}$ are then strongly reduced (Table 4.1).

Hence, it can be concluded that the studied two-pot ICAR ATRP processes, in which the Cu level is 200 ppm in each pot, are industrially less attractive in case a good block copolymer quality is desired. As explained in Appendix E, for lower Cu levels a similar conclusion can be drawn since a too high loss of control over the average polymer properties results. In the next section, it is however shown that a one-pot procedure can partially overcome the former issues in case the polymerization conditions are carefully selected.

4.3.2 Diblock-like copolymers made from iBoA and styrene in a one-pot semi-batch procedure

Figure 4.8 (full lines) presents the molar overall conversion profile and the control over chain length and livingness as a function of the overall conversion for the one-pot batch synthesis of diblock-like poly(iBoA-*b*-Sty) using the ICAR ATRP technique and starting with iBoA as the first block. The term molar *overall* conversion is used in this chapter to stress that this conversion is normalized with the molar amount of monomer that would be present if both monomers (iBoA and styrene) would be simultaneously added at the start of the ATRP process. The polymerization is performed under similar reference conditions as those selected for the two-pot procedure, i.e. $[iBoA]_0/[MBrP]_0/[CuBr_2/PMDETA]_0/[LPO]_0$= 50/1/0.04/0.02, with the addition of a molar amount of styrene equal to the initial molar amount of iBoA at an overall conversion of 0.4 and with the polymerization temperature kept constant at 80 ^{0}C along the whole polymerization. Note in particular that the overall Cu level is again

400 ppm and that the same initial molar ratio of conventional radical initiator to ATRP initiator species is used as in each stage of the two-pot procedure, i.e. $[LPO]_0/[R_0X]_0$=0.02. Also, for the sake of comparison, the polymerization is stopped at an overall conversion of 0.8.

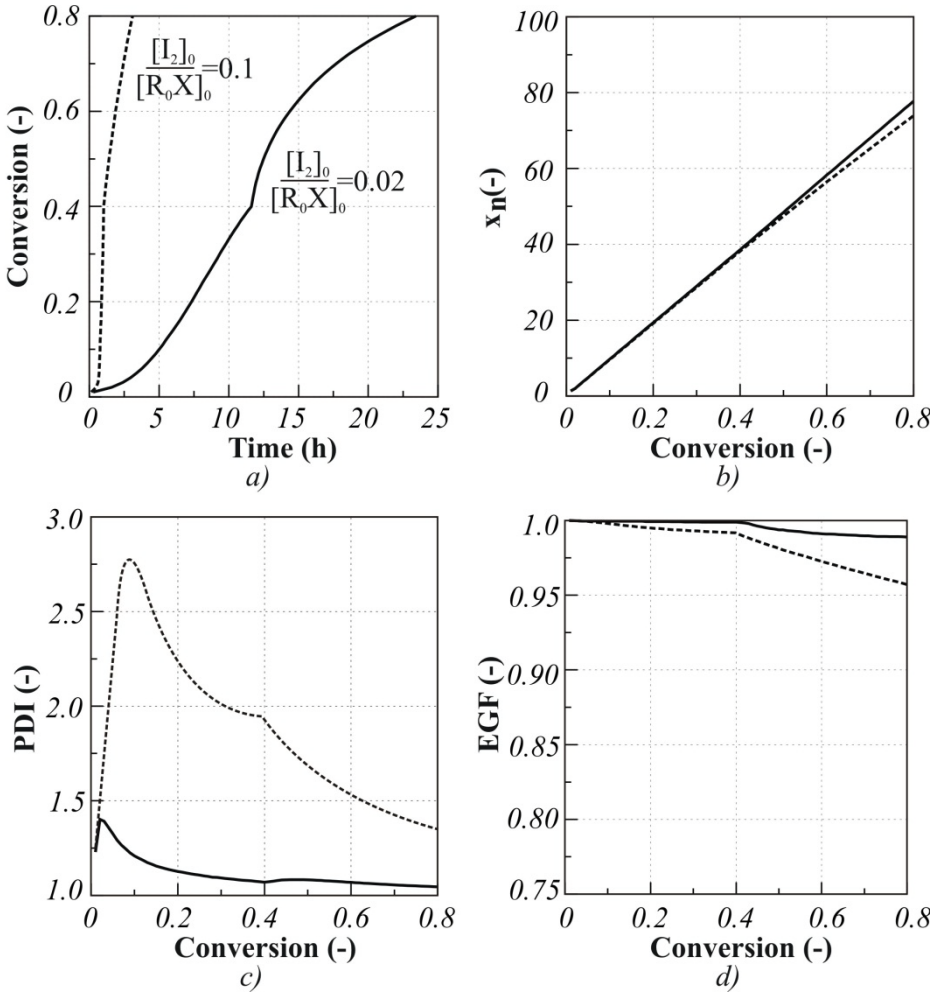

Figure 4.8: One-pot bulk ICAR ATRP of iBoA and styrene; a) overall conversion as a function of time; b) number-average chain length (x_n) c) polydispersity index (PDI) and d) end-group functionality (EGF) as a function of the overall conversion; full lines: $[iBoA]_0/[MBrP]_0/[CuBr_2/PMDETA]_0/[LPO]_0$= 50/1/0.04/0.02 while adding at an overall conversion of 0.40 an amount of styrene which is equal to the initial amount of iBoA; dashed lines: same except $[MBrP]_0/[LPO]_0$= 1/0.1; conversions and amounts on a molar basis.

Although a controlled ICAR ATRP is obtained (Figure 4.8 (full lines)), as under the two-pot batch conditions (Figure 4.4, full lines), a too long overall polymerization time results, as a consequence of the low $[MBrP]_0/[LPO]_0$ of 0.02. However, by increasing

this initial ratio by a factor 5 (dashed lines in Figure 4.8), as was also proven for the second pot in the two-pot approach, a relatively good control over the polymer properties can still be obtained with a much higher polymerization rate. More precisely, a conversion of 0.8 can be reached in a few hours instead of a day while obtaining a x_n close to 80, a PDI of 1.35 and a EGF of 0.95. Moreover, Figure 4.9 shows that most dormant polymer molecules have an ATRP initiator end and most dead polymer molecules originate from termination of the corresponding macroradicals.

It should be emphasized that the one-pot semi-batch procedure results in a diblock-like copolymer due to the presence of both iBoA and styrene at overall conversions higher than 0.4 and hence a reduction of the block quality is to be expected. As can be seen in Figure 4.10 (top left; $[MBrP]_0/[LPO]_0$= 1/0.1; 80^0C), indeed a gradient-like second block is obtained, which is reflected by the relatively high <BD> of 0.58. However, in the one-pot approach less ill-defined triblock copolymer and homopolymer chains are formed compared to the two-pot approach (Figure 4.10 (top left) vs Figure 4.7(a)) leading to similar <BD> values in both approaches. These results thus suggest at this stage an unexpected equivalency of both approaches to synthesize diblock copolymers.

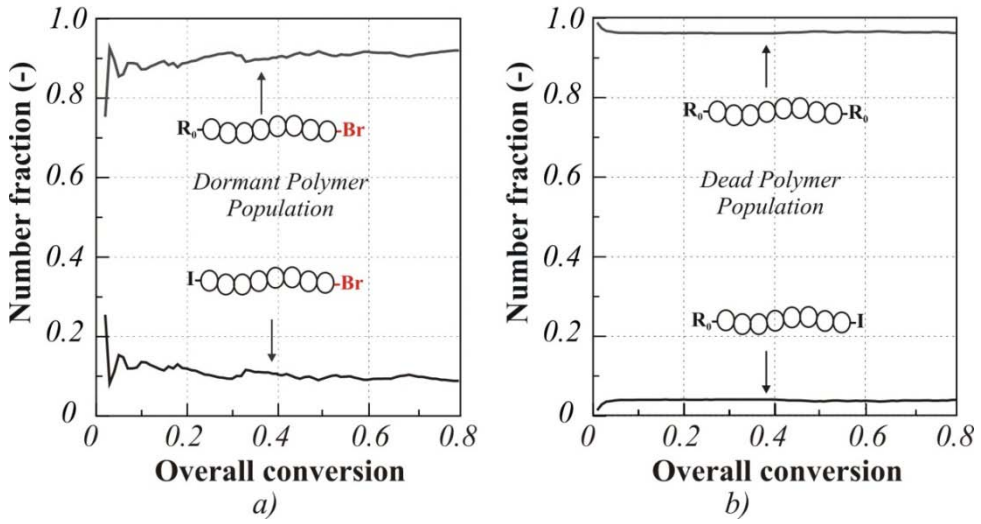

Figure 4.9: Number fraction of dormant and dead polymer molecules with specific α- and ω end-groups in the one-pot semi-batch bulk ICAR ATRP of iBoA and styrene as a function of the overall conversion; end-group resulting from conventional radical initiator fragments indicated by *I*, those from the ATRP initiator by R_0; X is Br (EGF); initial conditions equal to those mentioned in Figure 4.8 (dashed lines); for illustration, only 4 of the possible α,ω-polymer structures are shown.

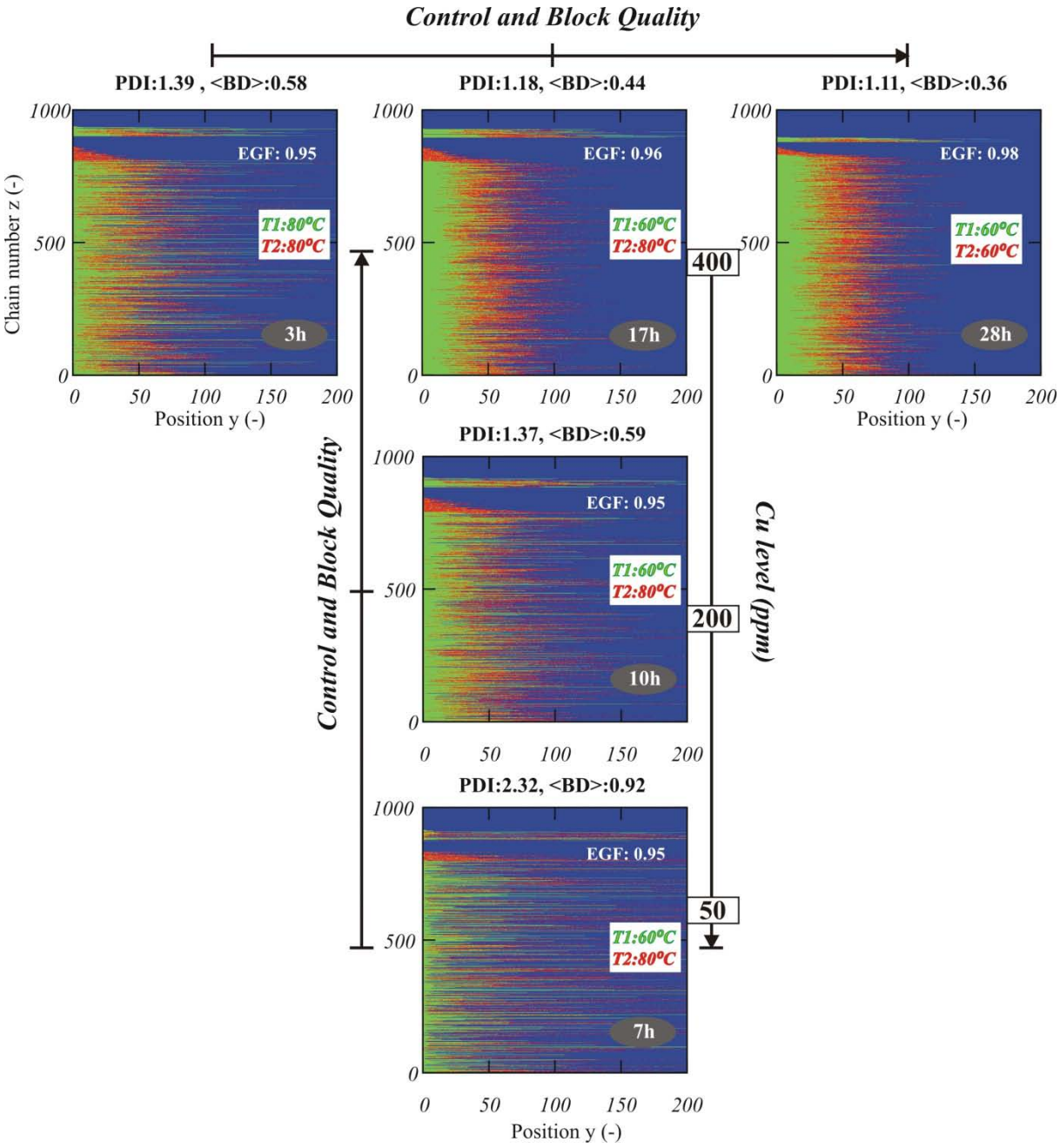

Figure 4.10: Copolymer composition for the one-pot semi-batch ICAR ATRP of iBoA and S at an overall conversion of 0.8; top row: difference in temperature with T_1 and T_2 respectively the temperature before and after an overall conversion of 0.4 and $[iBoA]_0/[MBrP]_0/[CuBr_2/PMDETA]_0/[LPO]_0$= 50/1/0.04/0.1 while adding at an overall conversion of 0.40 an amount of styrene which is equal to the initial amount of iBoA; middle column: effect of Cu ppm level for the stepwise temperature profile: $[iBoA]_0/[MBrP]_0/[CuBr_2/PMDETA]_0/[LPO]_0$= 50/1/v/0.1 with v=0.04 (400ppm), 0.02 (200ppm) and 0.005 (50ppm); addition of same amount of styrene, i.e. the initial iBoA amount, at an overall conversion of 0.4.

Additionally, in Figure 4.10 (top row; $[MBrP]_0/[LPO]_0$= 1/0.1) the effect of a variation of the polymerization temperature on the copolymer composition in the one-

pot semi-batch approach is shown. Clearly, a lower polymerization temperature improves the block copolymer quality. Analogously, as explained for the two-pot batch procedure, the best block copolymer quality is obtained at a polymerization temperature of 60 °C (Figure 4.10 top right) at the expense of a significant increase of the polymerization time. However contrary to the two-pot batch approach, an acceptable <BD> value and a reasonable overall polymerization time are obtained using a step-wise temperature profile with a temperature of 60 °C for overall conversions below 0.4, and a temperature of 80 °C at higher conversions (Figure 4.10 top middle).

Importantly, a comparison of Figure 4.10 (top row) and the corresponding copolymer compositions for the two-pot approach (Figure 4.7) allows to confirm the similarity of the <BD> values with both approaches. Although the two-pot batch procedure allows to reach slightly lower <BD> values and PDIs, it should be emphasized that this approach implies a tremendous increase in the overall polymerization time. Consequently, from an industrial point of view, the one-pot semi-batch procedures are more profitable than the two-pot batch procedures.

Finally, for the same temperature profile, the middle column in Figure 4.10 ($[MBrP]_0/[LPO]_0$= 1/0.1) indicates that a significant decrease of the Cu ppm level results in faster polymerization rates, in accordance with previous ICAR ATRP theoretical studies.[46, 65] However, this rate promotion is accompanied by an important increase of the <BD> value and a substantial decrease of the control over chain length, whereas the livingness is only slightly affected. Hence, it follows that also for the one-pot semi-batch approach a limiting value exist for the Cu ppm level to ensure a sufficiently good block copolymer quality.

4.4 Conclusions

Kinetic Monte Carlo simulations indicate that well-defined poly(iBoA-*b*-Sty) diblock(-like) copolymers with an average chain length of ca. 80 at an overall conversion of 0.80 can be synthesized by bulk ICAR ATRP using both one-pot semi-batch and two-

pot batch approaches with $CuBr_2$/PMDETA as deactivator, LPO as conventional radical initiator and MBrP as ATRP initiator.

In order to quantify the block copolymer quality, a block deviation value (<BD>), which ranges between 0 and 1, is introduced based on the calculation of the explicit copolymer composition. This value reflects the average deviation of a representative polymer sample with respect to perfect diblock references copolymer chains. For <BD> values lower than 0.3, the block copolymer quality is defined as good.

If the polymerization conditions are carefully selected, the formation of (dormant) homopolymer and dead triblock copolymer chains upon addition of the second monomer can be effectively suppressed based on end-group analysis of both the dead and dormant polymer chains and the calculation of the explicit copolymer composition. In both the one- and two-pot approach, the iBoA block should be polymerized first and as soon as styrene is added a sufficiently high LPO amount is necessary to ensure an industrially attractive polymerization rate. Moreover, for an optimal control over average polymer properties and a good block copolymer quality in particular, a sufficiently low polymerization temperature should be selected.

However, too low polymerization temperatures should be avoided since they lead to extremely slow ICAR ATRPs especially if a two-pot batch procedure is followed while considering the same overall Cu ppm level as in the one-pot semi-batch procedure. A higher polymerization temperature for the second pot/block could resolve this time issue, accelerating the polymerization of the second block with moderate loss of control over chain length and livingness. In addition, a one-pot procedure is also more suitable toward industrial application due to its less intensive polymer isolation and capability to produce well-defined diblock(-like) copolymers down to lower Cu ppm levels under otherwise similar polymerization conditions.

References

[1] W. H. Ray; J. B. P. Soares; R. A. Hutchinson, *Macromolecular Symposia* **2004,** *206*, 1-13.

[2] M. Krzysztof, Controlled Radical Polymerization: State-of-the-Art in 2011. In *Progress in Controlled Radical Polymerization: Mechanisms and Techniques*, American Chemical Society: **2012**; Vol. 1100, pp 1-13.

[3] M. Destarac, *Macromolecular Reaction Engineering* **2010,** *4*, 165-179.

[4] W. A. Braunecker; K. Matyjaszewski, *Progress in Polymer Science* **2007,** *32*, 93-146.

[5] K. Matyjaszewski; T. P. Davis, *Handbook of Radical Polymerization*. Wiley-Interscience: Hoboken, **2002**.

[6] A. H. E. Mueller; K. Matyjaszewski, *Controlled and Living Polymerizations: From Mechanisms to Applications*. Wiley-VCH: Weinheim, **2009**.

[7] A. E. Hamielec; H. Tobita, Polymerization Processes, 1. Fundamentals. In *Ullmann's Encyclopedia of Industrial Chemistry*, Wiley-VCH Verlag GmbH & Co. KGaA: **2000**.

[8] J. Maul; B. G. Frushour; J. R. Kontoff; H. Eichenauer; K.-H. Ott; C. Schade, Polystyrene and Styrene Copolymers. In *Ullmann's Encyclopedia of Industrial Chemistry*, Wiley-VCH Verlag GmbH & Co. KGaA: **2000**.

[9] C. Burguiere; S. Pascual; C. Bui; J. P. Vairon; B. Charleux; K. A. Davis; K. Matyjaszewski; I. Betremieux, *Macromolecules* **2001,** *34*, 4439-4450.

[10] E. Penzel, Polyacrylates. In *Ullmann's Encyclopedia of Industrial Chemistry*, Wiley-VCH Verlag GmbH & Co. KGaA: **2000**.

[11] Q. G. Ma; K. L. Wooley, *Journal of Polymer Science Part a-Polymer Chemistry* **2000,** *38*, 4805-4820.

[12] M. Stickler; T. Rhein, Polymethacrylates. In *Ullmann's Encyclopedia of Industrial Chemistry*, Wiley-VCH Verlag GmbH & Co. KGaA: **2000**.

[13] A. K. Bunha; J. Mangadlao; M. J. Felipe; K. Pangilinan; R. Advincula, *Macromolecular Rapid Communications* **2012,** *33*, 1214-1219.

[14] D. Bertin; D. Gigmes; S. R. A. Marque; P. Tordo, *Chem Soc Rev* **2011,** *40*, 2189-2198.

[15] G. Moad; S. H. Thang, *Australian Journal of Chemistry* **2009,** *62*, 1379-1381.

[16] K. Matyjaszewski; N. V. Tsarevsky, *Nat Chem* **2009,** *1*, 276-288.

[17] W. Jakubowski; A. Juhari; A. Best; K. Koynov; T. Pakula; K. Matyjaszewski, *Polymer* **2008,** *49*, 1567-1578.

[18] B. Dervaux; W. Van Camp; L. Van Renterghem; F. E. Du Prez, *Journal of Polymer Science Part a-Polymer Chemistry* **2008,** *46*, 1649-1661.

[19] M. Machado; S. Faucher; S. P. Zhu, *Journal of Polymer Science Part a-Polymer Chemistry* **2010,** *48*, 2294-2301.

[20] H. Y. Gu; S. Faucher; S. P. Zhu, *Polymer* **2011,** *52*, 2025-2031.

[21] K. Matyjaszewski; J. H. Xia, *Chemical Reviews* **2001,** *101*, 2921-2990.

[22] D. F. Grishin; I. D. Grishin, *Russ J Appl Chem* **2011,** *84*, 2021.

[23] W. Tang; Y. Kwak; N. V. Tsarevsky; K. Matyjaszewski, *Abstracts of Papers of the American Chemical Society* **2007,** *233*.

[24] N. V. Tsarevsky; K. Matyjaszewski, *Chem Rev* **2007,** *107*, 2270-2299.

[25] H. D. Tang; N. Arulsamy; M. Radosz; Y. Q. Shen; N. V. Tsarevsky; W. A. Braunecker; W. Tang; K. Matyjaszewski, *Journal of the American Chemical Society* **2006,** *128*, 16277-16285.

[26] Y. Q. Shen; H. D. Tang; S. J. Ding, *Prog Polym Sci* **2004,** *29*, 1053.

[27] K. Matyjaszewski; T. Pintauer; S. Gaynor, *Macromolecules* **2000,** *33*, 1476.

[28] M. E. Honigfort; S. Liou; J. Rademacher; D. Malaba; T. Bosanac; C. S. Wilcox; W. J. Brittain, Copper removal in atom transfer radical polymerization. In *Advances in Controlled/Living Radical Polymerization*, Matyjaszewski, K., Ed. **2003**; Vol. 854, pp 250-266.

[29] K. Matyjaszewski; W. Jakubowski; K. Min; W. Tang; J. Y. Huang; W. A. Braunecker; N. V. Tsarevsky, *Proc Natl Acad Sci USA* **2006,** *103*, 15309.

[30] Y. Kwak; A. J. D. Magenau; K. Matyjaszewski, *Macromolecules* **2011,** *44*, 811-819.

[31] A. J. D. Magenau; N. C. Strandwitz; A. Gennaro; K. Matyjaszewski, *Science* **2011,** *332*, 81.

[32] Y. Z. Zhang; Y. Wang; C. H. Peng; M. J. Zhong; W. P. Zhu; D. Konkolewicz; K. Matyjaszewski, *Macromolecules* **2012,** *45*, 78-86.

[33] N. H. Nguyen; M. E. Levere; V. Percec, *J Pol Sci, Part A: Polym Chem* **2012,** *50*, 860-873.

[34] N. H. Nguyen; V. Percec, *J Pol Sci, Part A: Polym Chem* **2011,** *49*, 4756-4765.

[35] W. Jakubowski; L. Mueller; K. Matyjaszewski, *Abstracts of Papers of the American Chemical Society* **2007,** *234*.

[36] L. Mueller; W. Jakubowski; W. Tang; K. Matyjaszewski, *Macromolecules* **2007,** *40*, 6464-6472.

[37] L. Mueller; K. Matyjaszewski, *Macromol React Eng* **2010,** *4*, 180.

[38] T. Pintauer; K. Matyjaszewski, *Chem Soc Rev* **2008,** *37*, 1087.

[39] K. Mukumoto; Y. Wang; K. Matyjaszewski, *Acs Macro Letters* **2012,** *1*, 599-602.

[40] P. Shivapooja; L. K. Ista; H. E. Canavan; G. P. Lopez, *Biointerphases* **2012,** *7*.

[41] A. Simakova; S. E. Averick; D. Konkolewicz; K. Matyjaszewski, *Macromolecules* **2012,** *45*, 6371-6379.

[42] G. X. Wang; M. Lu, *E-Polymers* **2012**.

[43] G. X. Wang; M. Lu; Y. B. Liu, *Journal of Applied Polymer Science* **2012,** *126*, 381-386.

[44] D. Konkolewicz; A. J. D. Magenau; S. E. Averick; A. Simakova; H. K. He; K. Matyjaszewski, *Macromolecules* **2012,** *45*, 4461-4468.

[45] G. X. Wang; M. Lu; H. Wu, *Polymer* **2012,** *53*, 1093-1097.

[46] D. R. D'Hooge; D. Konkolewicz; M. F. Reyniers; G. B. Marin; K. Matyjaszewski, *Macromol Theory Sim* **2012,** *21*, 52.

[47] B. Li; B. Yu; W. T. S. Huck; F. Zhou; W. M. Liu, *Angewandte Chemie-International Edition* **2012,** *51*, 5092-5095.

[48] P. H. M. Van Steenberge; D. R. D'hooge; Y. Wang; M. Zhong; M.-F. Reyniers; D. Konkolewicz; K. Matyjaszewski; G. B. Marin, *Macromolecules* **2012**.

[49] D. T. Gillespie, *Journal of Physical Chemistry* **1977,** *81*, 2340-2361.

[50] D. R. D'Hooge; M. F. Reyniers; F. J. Stadler; B. Dervaux; C. Bailly; F. E. Du Prez; G. B. Marin, *Macromolecules* **2010,** *43*, 8766.

[51] N. M. Ahmad; B. Charleux; C. Farcet; C. J. Ferguson; S. G. Gaynor; B. S. Hawkett; F. Heatley; B. Klumperman; D. Konkolewicz; P. A. Lovell; K. Matyjaszewski; R. Venkatesh, *Macrom Rapid Commun* **2009,** *30*, 2002.

[52] D. Konkolewicz; S. Sosnowski; D. R. D'Hooge; R. Szymanski; M. F. Reyniers; G. B. Marin; K. Matyjaszewski, *Macromolecules* **2011,** *44*, 8361.

[53] L. Hlalele; B. Klumperman, *Macromolecules* **2011,** *44*, 6683-6690.

[54] A. Nabifar; N. T. McManus; E. Vivaldo-Lima; L. M. F. Lona; A. Penlidis, *Chemical Engineering Science* **2009,** *64*, 304-312.

[55] J. Gao; A. Penlidis, *Journal of Macromolecular Science, Part C* **1996,** *36*, 199-404.

[56] L. Bentein; D. R. D'Hooge; M. F. Reyniers; G. B. Marin, *Macromol Theory Sim* **2011,** *20*, 238.

[57] J. D. Woloszyn; K. B. McAuley, *Macromol React Eng* **2011,** *5*, 453-466.

[58] G. Moad; D. H. Solomon, *The Chemistry of Free Radical poylmerization*. Elsevier Science Ltd: Oxford, **1995**.

[59] J. M. Asua, *Polymer Reaction Engineering*. Blackwell Publishing Ltd: Oxford, **2007**.

[60] B. Dervaux; T. Junkers; M. Schneider-Baumann; F. E. Du Prez; C. Barner-Kowollik, *Journal of Polymer Science Part a-Polymer Chemistry* **2009,** *47*, 6641-6654.

[61] M. Buback; R. G. Gilbert; R. A. Hutchinson; B. Klumperman; F. D. Kuchta; B. G. Manders; K. F. Odriscoll; G. T. Russell; J. Schweer, *Macromolecular Chemistry and Physics* **1995,** *196*, 3267-3280.

[62] A. Nobel http://www.akzonobel.com/polymer

[63] F. Seeliger; K. Matyjaszewski, *Macromolecules* **2009,** *42*, 6050.

[64] Y. Fu; A. Mirzaei; M. F. Cunningham; R. A. Hutchinson, *Macromolecular Reaction Engineering* **2007,** *1*, 425-439.

[65] C. Toloza Porras; D. R. D'Hooge; M. F. Reyniers; G. B. Marin, *Macromolecular Theory and Simulations* **2012**.

[66] P. B. Zetterlund, *Macromolecules* **2010,** *43*, 1387.

[67] A. R. Wang; S. P. Zhu, *Abstracts of Papers of the American Chemical Society* **2002,** *224*, U363-U363.

[68] A. D. Peklak; A. Butte; G. Storti; M. Morbidelli, *Journal of Polymer Science Part a-Polymer Chemistry* **2006,** *44*, 1071-1085.

[69] O. Delgadillo-Velazquez; E. Vivaldo-Lima; I. A. Quintero-Ortega; S. P. Zhu, *Aiche Journal* **2002,** *48*, 2597-2608.

[70] J. Wieme; D. R. D'Hooge; M. F. Reyniers; G. B. Marin, *Macromol React Eng* **2009,** *3*, 16.

[71] D. R. D'Hooge; M. F. Reyniers; G. B. Marin, *Macromol React Eng* **2009,** *3*, 185.

[72] G. Johnston-Hall; M. J. Monteiro, *Journal of Polymer Science Part a-Polymer Chemistry* **2008,** *46*, 3155-3173.

[73] P. H. M. Van Steenberge; J. Vandenbergh; D. R. D'Hooge; M. F. Reyniers; P. J. Adriaensens; L. Lutsen; D. J. M. Vanderzande; G. B. Marin, *Macromolecules* **2011,** *44*, 8716-8726.

[74] P. B. Zetterlund; Y. Kagawa; M. Okubo, *Chemical Reviews* **2008,** *108*, 3747-3794.

Chapter 5: General conclusions and future prospects

5.1 General Conclusions

In this PhD thesis, kinetic modeling was successfully applied to optimize ICAR ATRP, an important controlled radical polymerization (CRP) technique, at laboratory scale in the frame of its possible industrial realization for the production of well-defined polymers. Contrary to reversible addition-fragmentation chain transfer (RAFT) polymerization and nitroxide mediated polymerization (NMP), in ATRP processes a catalyst is present (Chapter 1) as mediating agent. Since a broad range of ATRP catalysts is available, a high number of monomers can polymerized with ATRP. However, for the industrial application of ATRP ppm levels of catalyst need to be utilized, which only after careful selection of the other polymerization conditions allow to obtain a well-defined ATRP product.

The optimization of the ICAR ATRP technique was therefore focused on the identification of the lowest copper ppm level which can be employed to obtain a fast ICAR ATRP while at the same time, achieving a good control over chain length and end-group functionality (EGF). Both homopolymerizations and block copolymerizations were considered with styrene (S), *n*-butyl acrylate (*n*BuA) and isobornyl acrylate (iBoA) as model monomers. For the homopolymerization kinetic studies, a deterministic model was used, whereas for the copolymerizations an advanced kinetic Monte Carlo (kMC) modeling approach was selected, which allows the derivation of polymer microstructural information based on the individual tracking of a sufficiently high number of macrospecies. As ligands, the commercially available, tris(2-pyridylmethyl)amine) (TPMA) and N,N,N',N'',N''- pentamethyl diethylenetriamine (PMDETA) were chosen.

In Chapter 2, it was demonstrated that ICAR ATRP can be used for the determination of intrinsic kinetic activation/deactivation parameters of ATRP initiator and macrospecies, since a broad variety of polymerization rates and levels of control over

chain length is available by this technique, which allows parameter determination. Moreover, contrary to normal ATRP, no air-sensitive activator species are initially present and the inherent low ATRP catalyst amount ensures that no solubility limits for the transition metal complexes have to be considered in the kinetic model. In addition, the extra intrinsic activation/deactivation parameters involving conventional radical initiator fragments are shown to be insignificant under polymerization conditions allowing a reliable parameter assessment. However, the initial conventional radical initiator concentration has a crucial role. Too high initial concentrations lead to free radical polymerization characteristics and thus a loss over control, whereas too low initial concentrations are accompanied by a too low ICAR ATRP rate. For ATRP processes with styrene and CuBr/TPMA as catalyst, the ICAR ATRP technique allowed to validate the relatively high activity of this catalyst based on an extensive set of experimental data covering a significant variation of the polymerization temperature and initial catalyst, conventional radical initiator, and ATRP initiator concentration. The simulations reveal that in contrast to activation, deactivation is rather temperature independent and the same intrinsic kinetic activation/deactivation parameters for ATRP initiator and macrospecies can be used to describe the ICAR ATRP process. In addition, the simulations revealed that Cu levels above 10 ppm should be considered to guarantee a high control over chain length.

For the homopolymerization of *n*BuA (Chapter 3), kinetic modeling was applied to explore the potential of ICAR ATRP for the production of well-defined polymers characterized by a high targeted chain length (TCL), i.e. a high initial molar ratio of monomer to ATRP initiator, while using CuBr/PMDETA as ATRP catalyst. A sufficiently high temperature (105°C) was selected to ensure a high polymerization rate and to promote the formation of short chain branches. A more complex reaction scheme was considered including a differentiation between secondary and tertiary macroradicals, since secondary acrylate macroradicals can undergo backbiting reactions. Based on experimental ATRP literature data, activation and deactivation of the secondary and tertiary species were assessed. The obtained kinetic parameters allow to confirm the higher stability of tertiary macroradicals, i.e these species disappear slower via deactivation and are formed faster through activation compared

their secondary counterparts. Furthermore, the simulations show that the ICAR ATRP of *n*BuA can be carried out to obtain well-defined poly(*n*BuA) materials using relatively low Cu ppm levels (≤ 50 ppm), in case a sufficiently high TCL (> 600) is selected. For moderated TCLs, however, somewhat higher ppm levels are necessary. In all cases, the amount of branches per chain is relatively low (e.g. ~5; TCL~300) and the control over EGF is sufficiently high. This indicates that polyacrylate ATRP macroinitiators can be used for the design of more complex macromolecular architectures, such as the synthesis of well-defined block copolymers.

In particular, in Chapter 4 it was shown that the copolymerization of S and iBoA via ICAR ATRP allows to produce tailored diblock(-like) copolymers using again CuBr/PMDETA as ATRP catalyst. A block deviation value (<BD>), which allows to evaluate the block copolymer quality, was introduced based on the calculation of the explicit copolymer composition. For <BD> values lower than 0.3, the block copolymer is good, i.e. the contribution of unwanted homopolymer and triblock copolymer chains is sufficiently low. For the same overall Cu level, a one-pot semi-batch approach, in which the second monomer is added at a high conversion of the first block, is more suited for the production of well-defined poly(iBoA-*b*-S) block copolymers. Besides the avoiding of the intensive separation step for the isolation of the ATRP macroinitiator, this approach allows to synthesize diblock-like copolymers in a reasonable time period with a similar <BD> value as the block-copolymers obtained under analogous polymerization conditions via a two-pot batch approach, in which a too slow ICAR ATRP results. In both approaches, the best <BD> values result in case iBoA is polymerized first and a step-wise temperature profile is selected while applying the temperature step after the addition of the second monomer.

5.2 Future prospects

In the future, the applied modeling strategy can be extended to optimize other or even more advanced macromolecular architectures, such as gradient, graft and star copolymers, at laboratory scale and to other CRP techniques considering a broader range of monomers. Such optimization will contribute to answer the challenging

question which CRP technique is most suited for the production of CRP products under industrially relevant conditions.

In particular, for ICAR ATRP a further optimization is possible toward non-Cu based catalysts which will allow to increase the environmental friendliness of the ATRP concept. Required activation/deactivation kinetic parameters can again be obtained based on a systematic set of experimental polymerization data.

At the same time the modeling approach can be extended so that CRP processes can be described at industrial scale including both homogeneous and heterogeneous polymerization techniques.

Appendix A: Temperature control

The temperature inside the reaction flask was controlled by a proportional–integral–derivative controller (PID controller). For that purpose a thermocouple connected to the PID controlled was placed in the reactor flask. Water was employed as coolant and was pumped through a cold finger, which was put in contact with the reaction mixture to generate a localized cold surface. The temperature of the oil bath was set at a constant value and a magnetic stirrer was placed both in the reaction mixture and in the oil bath. A second thermocouple was placed in the oil bath for comparison with the one in the oil bath. Figure A.1 shows the two profiles for one experiment (entry 7, Table 2.1, Chapter 2), i.e. the temperature in the reaction flask and the temperature in the oil bath.

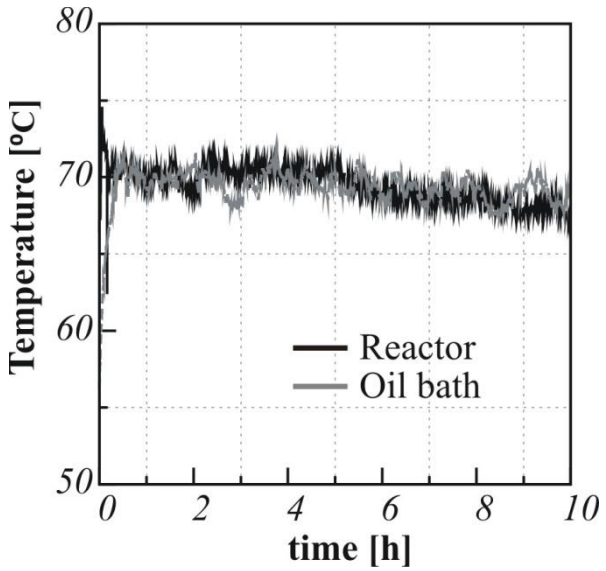

Figure A.1: Temperature profiles for the oil bath and the reaction mixture in the ICAR ATRP of styrene mediated by $CuBr_2$/TPMA. (entry 7, Table 2.1, Chapter 2, set point: 70°C).

Appendix B: Analytical techniques

The samples of polymer which were taken from the reaction flask were divided in three aliquots for the purpose of polymer characterization. The monomer conversion (equation B1: volume change neglected) was determined gravimetrically and chromatographically for a few samples in order to check the reproducibility and reliability of the analysis. On the other hand, the number-average molar mass and polydispersity index (PDI) were measured by size exclusion chromatography (GPC).

$$x_M(t) = 1 - \frac{[M]_t}{[M]_0} \qquad \text{B1}$$

B.1. Determination of monomer conversion by gravimetric analysis

In order to perform a gravimetric analysis a 1-mL sample was employed. This sample contains polymer, a negligible group of non-volatile solids ($CuBr/CuBr_2$, ligand and AIBN), and a group of volatile liquids (monomer, traces of ATRP initiator and GC standard). A glass-petri plate was weighted, the sample was placed on the glass-petri plate and weighted immediately, then ~2mL of toluene were added in order to enhance the evaporation of the monomer. After the addition of toluene the sample was dried in the oven at 80°C until a constant mass was reached. At the end, the dried mass is weighed and the monomer conversion was determined as follows:

$$x_M(t) = \frac{(plate + sample)_{after\ drying} - empty\ plate}{(plate + sample)_{before\ drying} - empty\ plate} \qquad \text{B2}$$

B.2. Determination of monomer conversion by gas chromatography (GC)

Gas chromatography (GC), is a widely used chromatographic technique for the separation and quantitative analysis of volatile multi-component mixtures. Particularly, in the field of polymer reaction engineering, residual concentrations of monomer in a polymerization mixture can be quantified depending on the suitable selection of a substance that can act as internal standard (*IS*). Furthermore, the relative amounts of

initiator, mediating agent or solvent can be also determined by GC depending on the interaction of such components with the stationary phase.

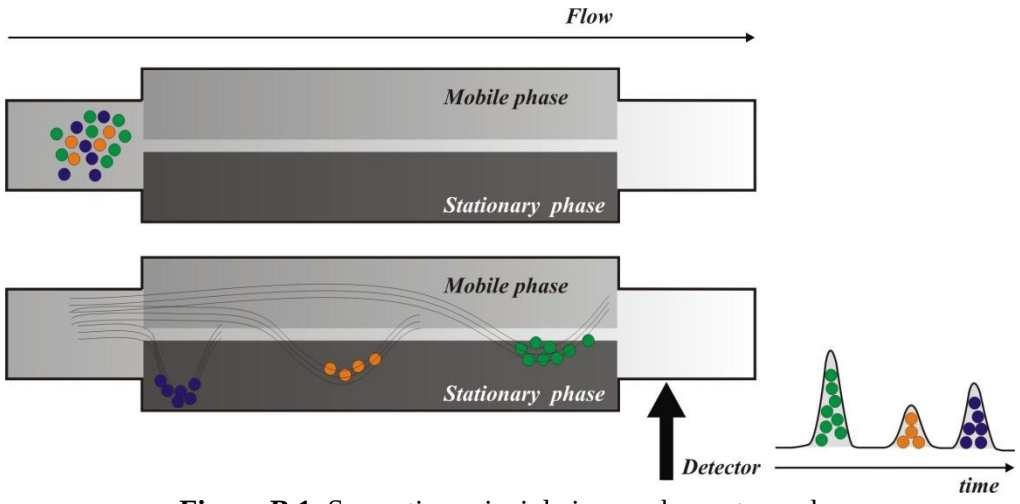

Figure B.1: Separation principle in gas chromatography

In GC, a small sample (~0.01µL) is vaporized, carried by a mobile phase and directed towards a stationary phase, in which the separation takes place (Figure B.1). The mobile phase is a carrier gas, which does not interact with the molecules of analyte, commonly an inert gas such as helium or an unreactive gas such as nitrogen is employed for this purpose. The stationary phase is a microscopic layer of an inert solid support, inside a piece of glass or metal tubing, i.e. GC column. Due to the different interaction of each vaporized compounds being analyzed with the stationary phase contained in the GC column, a different elution time for each component results. This elution time is known as the retention time of each compound and is determined at the outlet of the GC column, where a detector is placed in order to track the elution of the compounds. This is shown in a graphic, i.e. chromatogram, containing peaks as a function of retention time and as explained below the concentration of the compound can be quantified based on the calculation of the area under each peak.

The temperature at which the GC column is operated, is an important variable to optimize the separation of the compounds in the sample. Therefore, the GC column is normally contained in an oven. The optimal temperature of the column depends on the boiling points (Table B.1) of the compounds contained in the mixture and the desired degree of separation. For samples characterized by a broad range of boiling points, a

stepwise temperature program is commonly selected in order to reduce extremely long retention times while optimizing the separation.

Table B.1: Boiling point of the compounds separated via GC analysis

Compound		Boiling point (ºC)
Styrene (S)	Monomer	145
Ethyl α-bromoisobutyrate (EtBriB)	Initiator	160
N,N-Dimethylformamide (DMF)	Internal standard	153

The conversion is determined relative to the internal standard, which is an stable compound contained in the reaction mixture. The concentration of *IS* remains constant along the polymerization due to its inert character and can therefore be used to determine the concentration of monomer at any time in the reaction (equation B.3).

$$x_M(t) = 1 - \frac{\left(\frac{A_M}{A_{IS}}\right)_t}{\left(\frac{A_M}{A_{IS}}\right)_0} \qquad \text{B.3}$$

Importantly, the monomer conversion at time t (equation B.3) is not absolute, but relative to the reference, being the ratio of monomer to internal standard a time t_0. Therefore any error in the determination of the ratio $(A_M/A_{IS})_0$ propagates to all $x_M(t)$ values, independent of the accuracy in the determination of $(A_M/A_{IS})_t$.

B.3. Determination of molar mass distribution by size exclusion chromatography (GPC)

The principle of size exclusion chromatography is the separation of molecules on the basis of their size. The separation process takes place in a column which is packed with porous, micro particulate gel material. Because of their size, larger particles

cannot penetrate the gel and are excluded. Due to the shorter trajectory that larger particles have to follow, they elute sooner than the smaller particles (Figure B.2). Depending on the application, different types and number of columns can be combined to obtain an optimal separation.

In order to monitor the time and concentration of polymer eluting from the GPC columns, a detector is placed at the outlet of the column(s). There are many types of detectors, which can be considered as concentration sensitive detectors, e.g. a refractive index (RI) detector, or molar mass sensitive detectors, e.g. a low angle light scattering detector. When a single concentration detector is employed, calibration of the column(s) is necessary in order to determine the molar mass from a concentration measurement, i.e. conventional calibration. Consequently, a relative molar mass and molar mass distribution (MMD) are obtained when using a single detector.

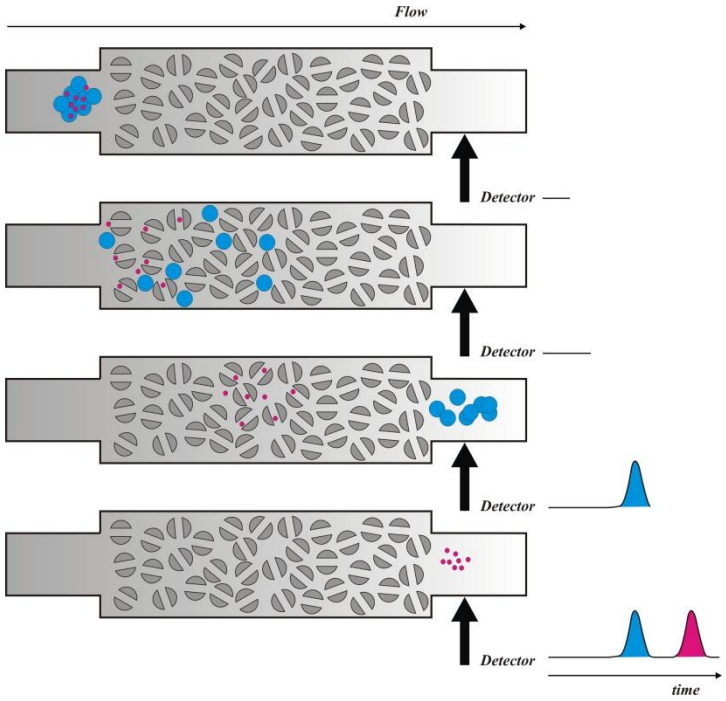

Figure B.2: Principle of gel permeation chromatography

Appendix C: Encounter pair model for diffusional limitations in the ATRP of *n*BuA termination

C.1 Calculation of apparent rate coefficient via the encounter pair model

The apparent rate coefficient for a reaction step *l* is calculated using the encounter pair model:[1-6]

$$\frac{1}{k_{l,app}} = \frac{1}{k_{l,chem}} + \frac{1}{k_{l,diff}} \quad \text{(C1)}$$

where $k_{l,chem}$ and $k_{l,diff}$ are the intrinsic chemical and diffusional rate coefficient for the reaction step l. The diffusional rate coefficient is calculated using the Smoluchowski model:[7, 8]

$$k_{l,diff} = 4\pi\sigma N_A D_{AB} \quad \text{(C2)}$$

where σ is the collision radius (6.54×10^{-10}m),[9] N_A the Avogadro number and D_{AB} the mutual diffusion coefficient of *A* and *B*, calculated as the sum of the individual center-of-mass-diffusion coefficients. For termination,[7, 10] this assumption is only valid in a first approximation, but sufficient for the present kinetic study in which general guidelines are formulated for the optimization of the ICAR ATRP of *n*-butyl acrylate. For the calculation of the individual center-of-mass diffusion coefficients a differentiation is made between non-macromolecules and macromolecules.

C.2 Calculation of the center-of-mass diffusion coefficient of a non-macromolecule

The center-of-mass diffusion coefficient of a non-macromolecule (D_A) is calculated using the Vrentas and Duda free-volume theory:[10-15]

$$D_A = D^{av}{}_{0,A} \exp\left(-V_A^* M_{j,A} \frac{\frac{w_1}{M_{j,1}} + \frac{w_2}{M_{j,2}} + \ldots \frac{w_N}{M_{j,N}}}{w_1 \frac{V_{FH,1}}{\gamma_1} + w_2 \frac{V_{FH,2}}{\gamma_2} + \ldots w_N \frac{V_{FH,N}}{\gamma_N}} \right) \quad \text{(C3)}$$

where $D^{av}{}_{0,A}$ is an average pre-exponencial factor, V_A^* the specific critical hole free volume required for a diffusional jump of A, $M_{j,N}$ the molar mass of a jumping unit of the component N in the reaction mixture, w_N its mass fraction, $V_{FH,N}$ its specific hole free volume and γ_N an overage overlap factor introduced to account for the same free volume being available for several jumping units. The ratio of $V_{FH,N}$ and γ_N can be calculated from:

$$\frac{V_{FH,N}}{\gamma_N} = K_{1N}\left(K_{2N} - T_{g,N} + T_{pol}\right) \quad \text{(C4)}$$

where K_{1N} and $K_{2N} - T_{g,N}$ are parameters to be estimated from experimental measurements of dynamic viscosity as a function of temperature; for the polymer $T_{g,N}$ corresponds to its glass transition temperature. Tables C1 and C2 summarize the Vrentas and Duda free-volume parameters used in this work. For more details the reader is referred to D'hooge et al.[16]

Table C.1: Parameters for the diffusion coefficients of the non-macromolecules (Equation C3)

Component (A)	$D^{av}{}_{0,A}$ [$m^2 \cdot s^{-1}$]	V_A^* [$m^3 \cdot kg^{-1}$]	$M_{j,A}$ [$kg \cdot mol^{-1}$]
$CuBr_2$/PMDETA	4.7×10^{-7} a)	0.608×10^{-3} a)	0.3966
*n*BuA	1.0×10^{-8} b)	0.894×10^{-3} c)	0.128

a) Taken from lterature.[2] b) Calculated based on the correlation proposed by Kobuchi et al.[17] with parameters from literature.[17, 18] c) Calculated via group contribution methods.[19-21]

Table C.2: Parameters for the specific hole free volume of pure monomer and pure polymer. (Equation C4)

Component (z)	K_{1z} [$cm^3 \cdot g^{-1} \cdot K^{-1}$]	$K_{2z} - T_{g,z}$ [K]
*n*BuA	3.0×10^{-3} a)	120 a)
Poly(*n*BuA)	5.1 b)	170 b)

a)Calculations based on the work of D'hooge et al.[16, 22] b)Taken form literature[23]

C.3 Calculation of the center-of-mass diffusion coefficient of a macromolecule

For the macromolecules, the calculation of its center-of-mass diffusion coefficient ($D^{com}_{p,i}$) is done via the scaling law proposed by Griffiths et al.[24] (equation C5), where i is chain length w_p refers to the mass fraction of polymer and D^{com}_m is the center-of-mass diffusion coefficient of the monomer.

$$D_{R_i}^{com} = \frac{D_m^{com}}{i^{0.664+2.02w_p}} \qquad \text{(C5)}$$

Again it should be emphasized that this equation is only valid in a first approximation to account for possible diffusional limitations on termination.[7, 10]

C.4 Influence of diffusional limitations on the reaction probabilities of termination

The influence of diffusional limitations on the reaction probabilities of termination is shown in Figure C1. A distinction is made between self-termination and cross-termination,[25, 26] the former occurring between two similar type of radicals, for instance termination of two secondary macroradicals, and the latter involving two different type of macroradicals, i.e. secondary and tertiary. In a first approximation, the contribution of termination can be neglected as derived from a comparison of the obtained probabilities for termination with the probabilities of deactivation, propagation and backbiting presented in Chapter 3 (Figure 3.4).

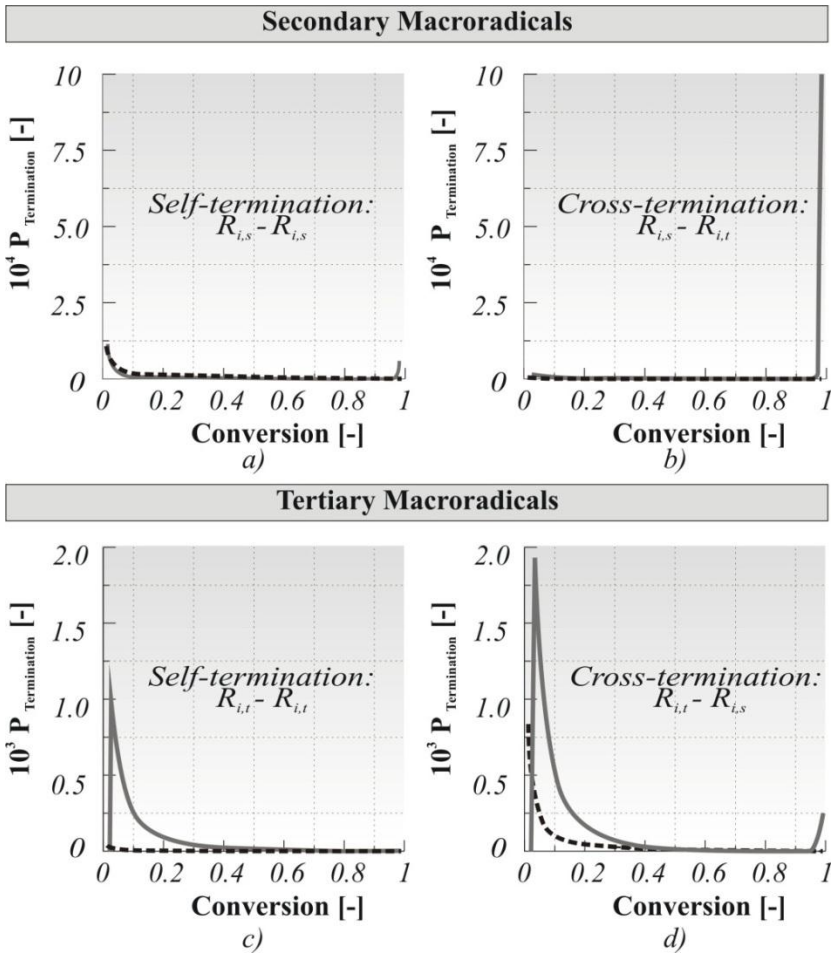

Figure C1: Effect of diffusional limitations on the reaction probabilities of a) self-termination and b) cross-termination of secondary macroradicals, and c) self-termination and d) cross-termination of tertiary macroradicals. Diffusional limitations considered (full lines) and neglected (dashed lines). Conditions as in Figure 3.4, results section.

Appendix D: Calculation of the average block deviation value, <BD>, to evaluate the diblock quality of block copolymers.

In this appendix, first the reason for using four normalized block deviations (BD_{BA}, $BD_{A\,B,}$ $BD'_{B\,A}$ and $BD'_{A\,B}$) to characterize the block copolymer quality is given. For several (theoretical) copolymers, it is shown that simpler criteria lead to incorrect <BD> values. Furthermore, the functional form of each block evaluation is discussed focusing on both symmetric and asymmetric diblocks. Additionally, the normalization to ensure a ranging between 0 and 1 for the <BD> value is discussed as a function of the average chain length of the copolymer selected.

D.1 Necessity of the calculation of the minimum of $BD_{B\ to\ A}$, $BD_{A\ to\ B,}$ $BD'_{B\ to\ A}$ and $BD'_{A\ to\ B}$ per chain explained for symmetric diblocks as ideal copolymer

For every polymer chain *z*, four normalized diblock deviations ($BD_{B\ to\ A}$, $BD_{A\ to\ B,}$ $BD'_{B\ to\ A}$ and $BD'_{A\ to\ B}$) have to be calculated:

$$BD_{BA} = \sum_{y=1}^{i} \frac{1}{2} \frac{\left|S_A - S_{A,ideal,BA}\right| + \left|S_B - S_{B,ideal,BA}\right|}{i^2} \qquad \text{(D1)}$$

$$BD_{AB} = \sum_{y=1}^{i} \frac{1}{2} \frac{\left|S_A - S_{A,ideal,AB}\right| + \left|S_B - S_{B,ideal,AB}\right|}{i^2} \qquad \text{(D2)}$$

$$BD'_{BA} = \sum_{y=1}^{i} \frac{1}{2} \frac{\left|S'_A - S'_{A,ideal,BA}\right| + \left|S'_B - S'_{B,ideal,BA}\right|}{i^2} \qquad \text{(D3)}$$

$$BD'_{AB} = \sum_{y=1}^{i} \frac{1}{2} \frac{\left|S'_A - S'_{A,ideal,AB}\right| + \left|S'_B - S'_{B,ideal,AB}\right|}{i^2} \qquad \text{(D4)}$$

In each equation, a comparison is made between the actual amount of A and B ($S_{A/B}$) as a function of (chain) position *y* and the theoretical amount needed to have a perfect diblock copolymer ($S_{A/B,ideal,AB}$; Figure 4.4 in the main text (Equation 1 in Chapter 4 corresponds here to Equation D2)). The first two equations relate to an evaluation from

'left to right', whereas the last two relate to an evaluation from 'right to left'. A further distinction is made whether (from 'left to right') a 'A to B' or 'B to A' reference symmetric diblock is used. In this way, as explained below, the block copolymer quality of the considered copolymer chain *z* can be calculated by selecting the minimum value of these four values.

To illustrate the necessity of the calculation of the minimum of four block deviation values (BD_{BA}, $BD_{AB,}$ BD'_{BA} and BD'_{AB}; Equation D1-D4) a comparison is made between following five methods:

$$BD_1 = BD_{BA} \quad \text{(D5)}$$

$$BD_2 = BD_{AB} \quad \text{(D6)}$$

$$BD_3 = BD'_{BA} \quad \text{(D7)}$$

$$BD_4 = BD'_{AB} \quad \text{(D8)}$$

$$BD_5 = \min\left\{BD_{BA}, \quad BD_{AB}, BD'_{BA}, \quad BD'_{AB}\right\} \quad \text{(D9)}$$

The first four methods (D5-D8) correspond to a single evaluation per chain *z*, whereas the last method (D9) is the one used in the main text, i.e. the minimal value of BD_{BA}, $BD_{AB,}$ BD'_{BA} and BD'_{AB} is used per chain. For all five methods the average value is obtained by:

$$< BD_k^* >= \sum_{z=1}^{z_{max}} \frac{BD_k(z)}{z_{max}} \quad \text{(D10)}$$

Note that $<BD_5^*>$ is the same as <BD*> of Chapter 4 (Equation 3), i.e. no rescaling with the <BD> value for the homopolymer with PDI of 1 is performed. The merit of each of the four evaluations separately becomes apparent when inspecting Table D1, which corresponds to the *asymmetric* diblock copolymers shown in Figure D1, all of which are assumed to possess the same *symmetric* diblock quality and which all have a transition point for the monomer type at 25%.

It can be seen from the first four entries in Table D1 that each evaluation method (D5-D8) gives a different evaluation for a fixed (asymmetric) diblock copolymer. Moreover, close inspection of the table shows that the criterion takes into account all symmetry effects, since the $<BD_k^*>$ (k = 1,…,4) values are permuted per column, indicating that using more than four evaluations will not add any information. The minimum value BD_5 is then by definition unique, hence reflecting the real block copolymer quality.

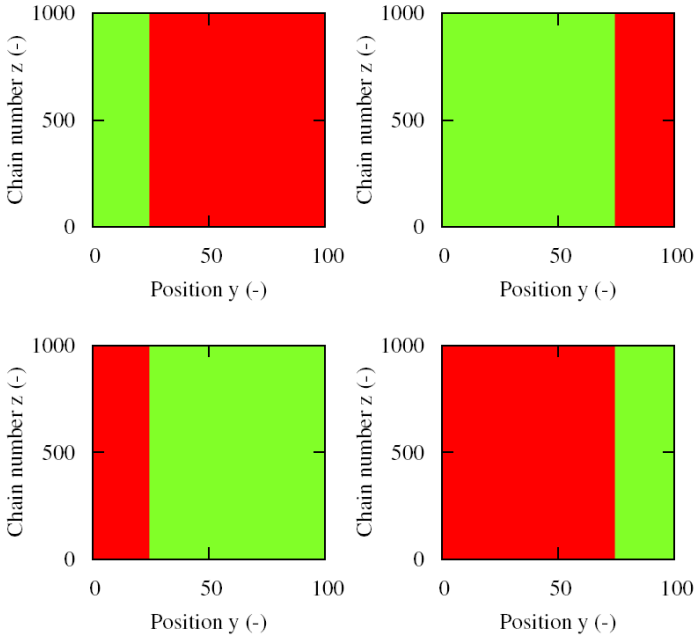

Figure D1: red: monomer B, green: monomer A; these asymmetric copolymers have the same symmetric diblock quality.

Table D1: Number average diblock deviation (<BD*>) for copolymers of Figure D1 for different criteria; k is case number; k=5: criterion used in Chapter 4 (Equation 2) without rescaling

	$<BD_k^*>$			
Case	top left	top right	bottom left	bottom right
1	0.158	0.344	0.155	**0.094**
2	0.155	**0.094**	0.158	0.344
3	0.344	0.155	**0.094**	0.158
4	**0.094**	0.158	0.344	0.155

5	**0.094**	**0.094**	**0.094**	**0.094**

D.2 Functional form for diblock evaluation (Relates to Equation 1 and 2 in Chapter 4)

As explained above, for the diblock evaluation of a copolymer chain *z* the equations D1-D4 are used. For example, Equation D2 allows to calculate per polymer chain the symmetric block deviation in case a AB diblock is the reference and a 'left to right' evaluation is performed. In what follows the functional form of Equation D2 (also Equation 1 in Chapter 5) is explained making a difference for symmetric and asymmetric diblock copolymers. A similar explanation can be given for all the other equations (D1, D3 and D4).

First, both the cumulative amount of A and B ($S_{A/B}$) are compared with the corresponding ideal reference amount (here $S_{A/B\ ideal,AB}$) for a given position *y* in the polymer chain, which are subsequently used to calculate the average:

$$\left|S_A(y,z)-S_{A,ideal,AB}(y,z)\right|+\left|S_B(y,z)-S_{B,ideal,AB}(y,z)\right| \quad \text{(D11)}$$

in which the ideal profiles are given by:

$$\begin{aligned} S_{A,ideal,AB} &= y \quad (1 \le y \le i/a) \\ S_{A,ideal,AB} &= i/a \quad (i/a \le y \le i) \\ S_{B,ideal,AB} &= 0 \quad (1 \le y \le i/a) \\ S_{B,ideal,AB} &= y - i/a \quad (i/a \le y \le i) \end{aligned} \quad \text{(D12)}$$

in which i/a is the length of the first block and thus a symmetric diblock is obtained for a=2. Note that for equal block lengths and a chain length of 100 the ideal profiles in Figure 1 are obtained. Furthermore, after summation over all positions for that polymer chain, this value is divided by the chain length *i* to express the deviation per monomer unit for the considered polymer chain (similar as was done for the calculation of the <GD> value):[27]

$$\sum_{y=1}^{i}\frac{1}{2}\frac{\left(\left|S_A(y,z)-S_{A,ideal,AB}(y,z)\right|+\left|S_B(y,z)-S_{B,ideal,AB}(y,z)\right|\right)}{i} \quad \text{(D13)}$$

However, a second deviation by *i* is necessary since $S_{A/B}$ scales with *i* (see also Van Steenberge et al. [27]):

$$\sum_{y=1}^{i} \frac{1}{2} \frac{\left(\left|S_A(y,z) - S_{A,ideal,AB}(y,z)\right| + \left|S_B(y,z) - S_{B,ideal,AB}(y,z)\right|\right)}{i^2} \quad \text{(D14)}$$

In such way, it is avoided that polymer chains with a high chain length but good diblock quality are badly evaluated.

D.3 Effect of average chain length on the evaluation of the block copolymer quality of a homopolymer (relates to Equation 4 and 5 in Chapter 4)

Figure D2 shows the <BD*> value for homopolymers obtained based on Equation D2 for different average chain lengths (PDI=1). The asymptotic value of 0.125 can be derived from Figure D3, in which the analogous figure for Figure 4.4 in Chapter 4 is given for a homopolymer chain with a chain length of 100 and monomer A units. Clearly, Equation D2 corresponds here to the surface area of a triangle. However, in the limit for average chain length as low as 2, application of Equation D2 leads a value of 0.250, since the surface area of the triangle cannot be approximated by Equation D2.

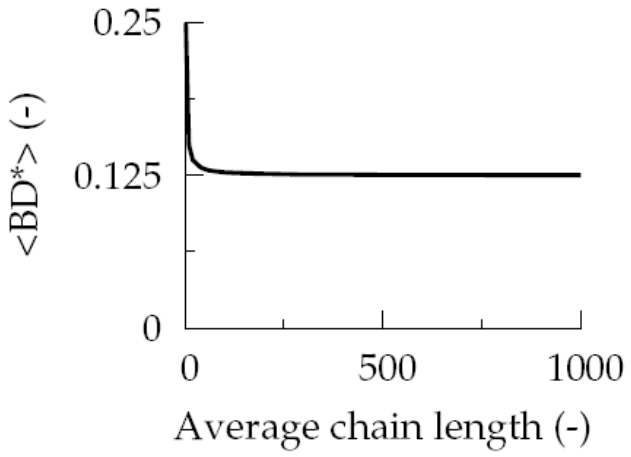

Figure D2: Block copolymer quality (<BD*>) for homopolymers (PDI=1) obtained based on Equation D2 for different average chain lengths; asymptotic value of 0.125 for average chain length higher or equal to 100

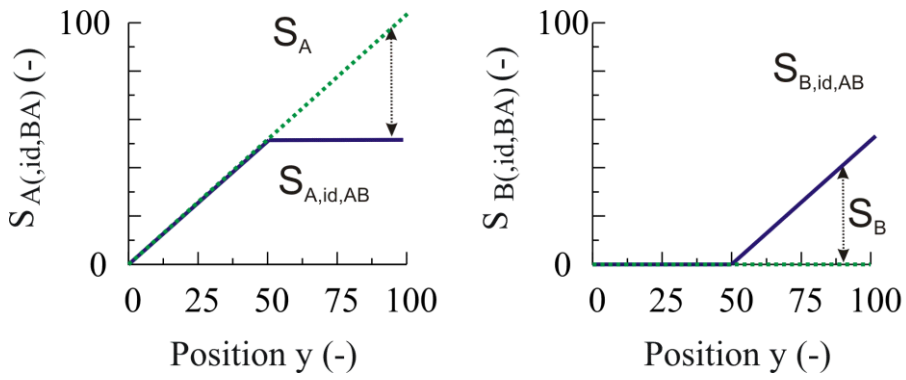

Figure D3: 'A to B' block deviation evaluation ('left to right') applied to a single homopolymer chain with a chain length i of 100 and monomer A units; here asymmetric block copolymer is assumed as the reference case, i.e. both blocks should possess the same length of 50.

Appendix E: Importance of monomer order and Cu level for the synthesis of styrene and isobornyl acrylate based diblock copolymers by ICAR ATRP using a two-pot batch procedure

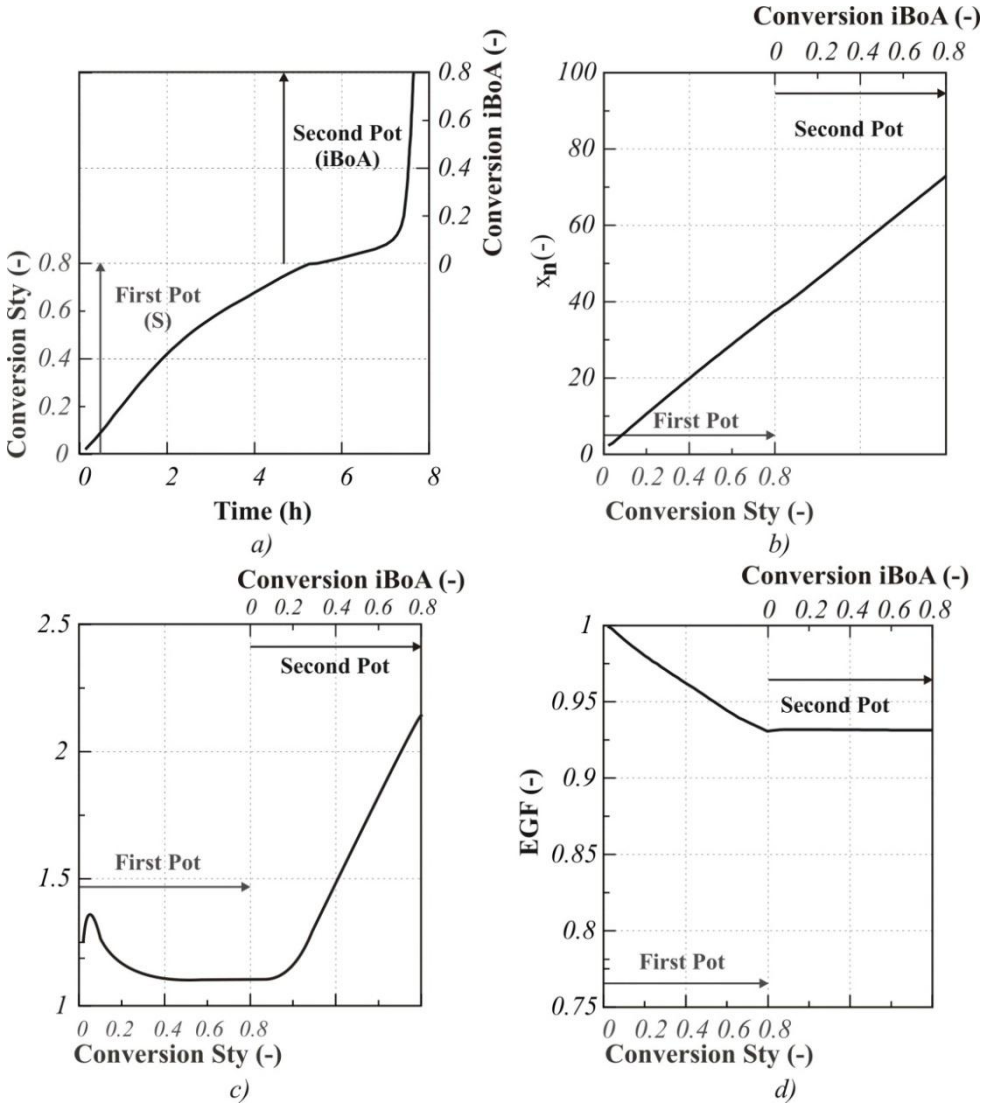

Figure E.1: Two-pot batch ICAR ATRP of styrene and iBoA: a) conversion of the Sty and iBoA block as a function of time; b) number-average chain length (x_n) c) polydispersity index (PDI) and d) end-group functionality (EGF) as a function of the conversion of the Sty/ iBoA block; first block: $[Sty]_0/[R_0X]_0/[CuBr_2/PMDETA]_0/[LPO]_0$ = 50/1/0.01/0.1; second block: $[iBoA]_0/[\sum_{i=0} R_iX\ ]_0/[CuBr_2]_0/[PMDETA]_0/[LPO]_0$ = 50/1/0.01/0.02; reference temperature of 80^0C.

Figure E.1 shows the conversion profile of the two-pot batch ICAR ATRP of styrene and iBoA with styrene being polymerized in the first pot and iBoA in the second pot as

a function of polymerization time, and the evolution of the number average chain length, polydispersity index (PDI) and end-group functionality (EGF) with conversion in both pots. In the first pot a molar ratio of: $[Sty]_0/[R0X]_0/[CuBr_2/PMDETA]_0/[LPO]_0$ = 50/1/0.02/0.1 is used while in the second pot: $[iBoA]_0/[\ \sum_{i=0} R_i X\ ]_0/[CuBr_2]_0/[PMDETA]_0/[LPO]_0$ = 50/1/0.02/0.02. The polymerization is performed at the reference temperature of 80^0C. Overall, it can be concluded that polymerizing iBoA in the first block and styrene in the second under the same conditions than the reverse order (Figure 4.4 in Chapter 4) results in better control over chain length and livingness although similar polymerization times are required to reach a conversion of 0.8. This, as mentioned in the main text, is expected since the excellent livingness of the poly(iBoA) block allows a successful chain length extension with a second monomer, e.g. styrene. In contrast, if styrene is polymerized first a higher PDI (~2) and lower EGF (~0.93) is obtained.

On the other hand, from Figure E.2 it follows that the initial amount of Cu influences to a higher extent the control over average polymer properties and the block copolymer quality of poly(iBoA-*b*-S) compared to the one-pot semi-batch ICAR ATRP in bulk (Figure 4.10 middle column, in the main text).

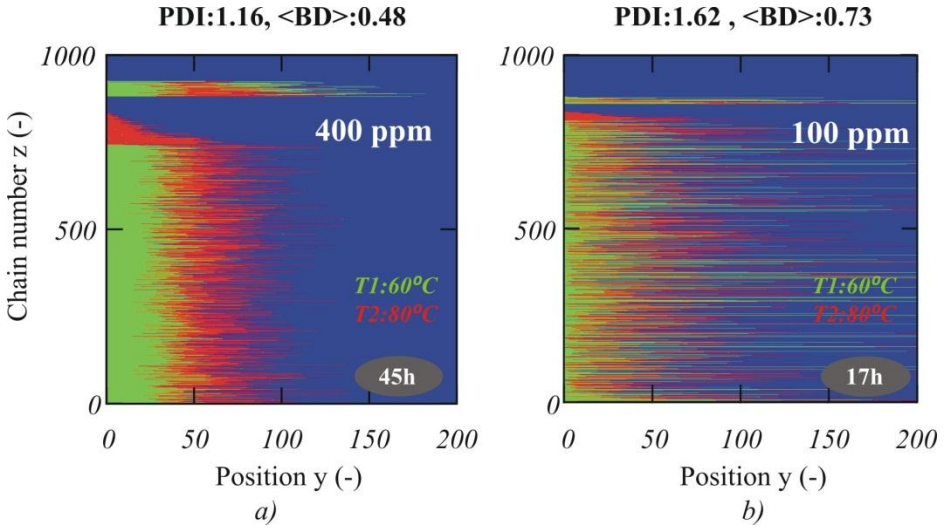

Figure E.2. Copolymer composition for the two-pot batch ICAR ATRP of iBoA and S at an overall conversion of 0.8; first block: $[iBoA]_0/[MBP]_0/[CuBr_2/\ PMDETA]_0/[LPO]_0$= 50/1/v/0.02 and second block: $[Sty]_0/[\ \sum_{i=0} R_i X\ ]_0/[CuBr_2]_0/[PMDETA]_0/[LPO]_0$ = 50/1/v/0.1 with v = 0.01 (a) and 0.0025 (b) ; profile temperature: 60^0C in the first pot and 80^0C in the second pot.

Appendix F: Deterministic model

The deterministic model applied in this work while assuming perfect mixing at the micro-scale is based on an extension of the method of moments in which population weighted apparent rate coefficients are calculated using a convergence test while applying the quasi-steady state approximation for the macroradicals.[2]

Figure F.1 summarizes the methodology employed to model the evolution of the conversion and the averaged polymer properties with time. As mentioned in Chapter 3 and similar to the stochastic model (see Appendix G), the influence of diffusional limitations is accounted for by calculating (chain length) dependent apparent rate coefficients, which are function of the intrinsic chemical rate coefficients and diffusion parameters (see Appendix C). At the beginning of the simulation initial population weighted apparent rate coefficients corresponding to a well-guessed CLD are calculated. The integration of the continuity equations for each non-macromolecular species and the moment equations for each macromolecular type, i.e. macroradicals, dormant and dead polymers, is simultaneously performed in order to calculate the moments (x_s; s=0,1,…,3) for each macromolecular type and thus the evolution of the conversion and the averaged polymer properties with time. These continuity equations and moment equations are integrated numerically using the LSODA solver (i.e. Livermore Solver for Ordinary Differential equations (ODE) with Automatic switching for stiff and nonstiff ODEs).[28]

The computer code runs the mentioned integration until the desired ending time/conversion is reached. Per time step an iterative cycle is used in which an initial guess of a CLD at the previous time step is used as an input to update the population weighted apparent/averaged rate coefficients in the moment equations. For this purpose algebraic equations resulting from the application of the quasi-steady state approximation (QSSA) for the macroradicals, which are intermediate reactive species, and differential equations corresponding to the continuity equations for the dormant species are combined to approximate the individual concentrations of the macroradicals and dormant polymer molecules. The final values for these apparent

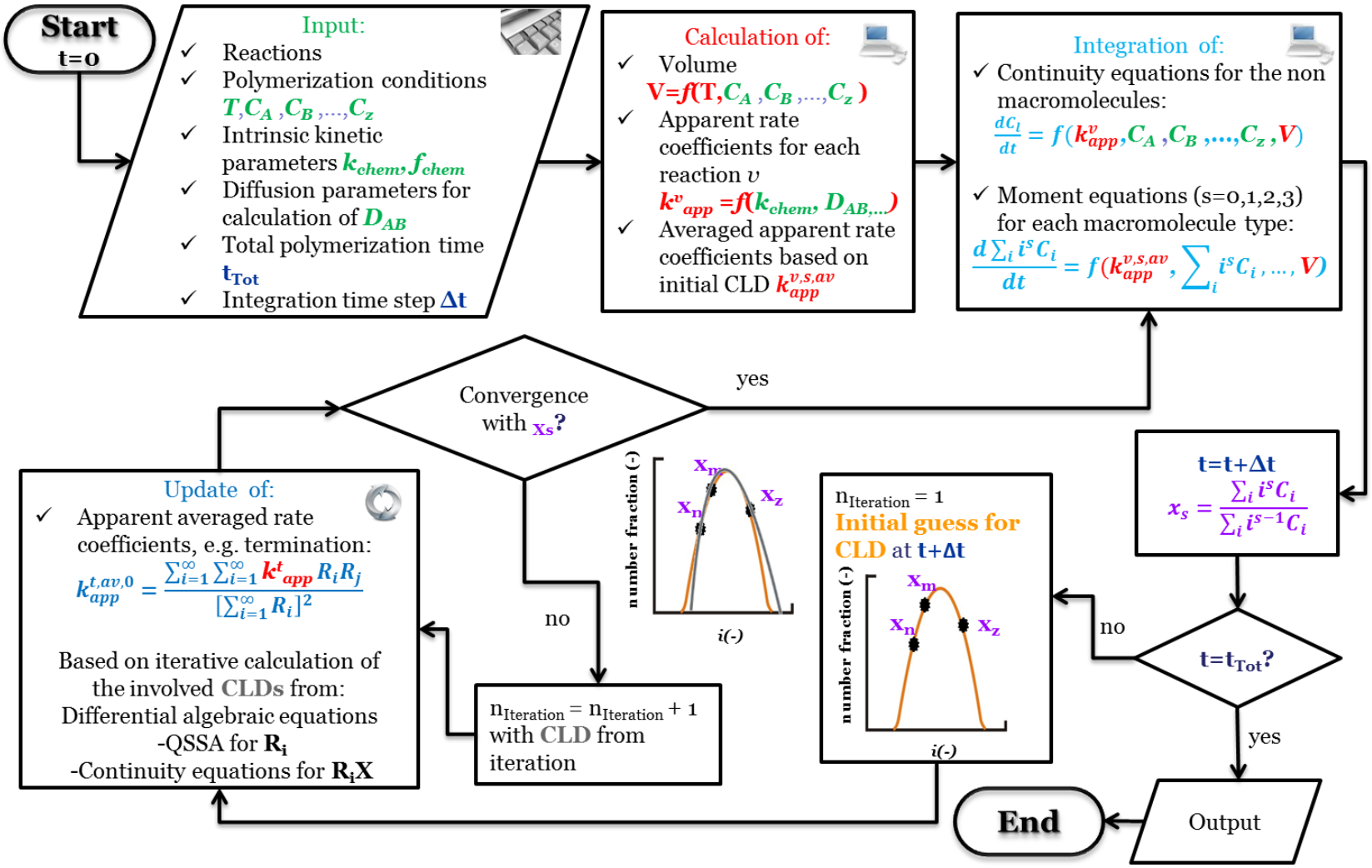

Figure F.1. Flowchart for the deterministic model; QSSA: quasi-steady state approximation; C_l with $l=A, B, \ldots Z$ corresponds to the concentration of the different l species involved in the polymerization.

averaged rate coefficients are obtained when convergence between the calculated moments from the previous time step (x_s) and the values calculated from the iterated CLD is reached.

Appendix G: Kinetic Monte Carlo model

Monte Carlo (MC) methods are based on the generation of random numbers from which reaction events are selected. In this work it is used to calculate the time evolution of the conversion and the averaged polymer properties as well as the explicit monomer sequences of the individual chains. A kinetic Monte Carlo (kMC) model previously developed for ATRP processes on the basis of the stochastic simulation algorithm developed by Gillespie[29] was adapted for modeling ICAR ATRP processes assuming perfect mixing at the micro-scale.

Instead of species concentrations, these kMC models track discrete molecules in a microscopic-scale (10^{-18} L) homogeneous reaction volume V representative of the complete system. Additionally, these models are based on a simple iterative procedure that does not involve the integration of coupled differential equations. Figure G.1 illustrates a flowchart with the general structure of the kMC algorithm employed in this work. Similar to the deterministic model, the kinetic parameters involved in the process are inputs to the kMC algorithm.

In this kMC algorithm, reactions are described using reaction events. Hence, all concentrations must be converted to numbers of molecules:

$$n_A = C_A \cdot V \cdot N_A \qquad \text{(G1)}$$

where n_A is the number of molecules of molecule A, C_A is the concentration of molecule A, V is the reaction volume and N_A is the Avogadro number. In order to calculate the rates and the reaction probabilities, the intrinsic rate coefficients k_{chem} of the considered reactions are converted to apparent "Monte Carlo rate coefficients" as follows:

$$\frac{1}{k_{app}} = \frac{1}{k_{chem}} + \frac{1}{k_{diff}} \qquad \text{(G2)}$$

in which k_{diff} corresponds to the diffusional rate coefficient calculated with the Smoluchowski model,[7, 8] as explained in Appendix C. Alternatively, for termination, the composite k_t model mentioned in Chapter 2 can be used. In a next step, the

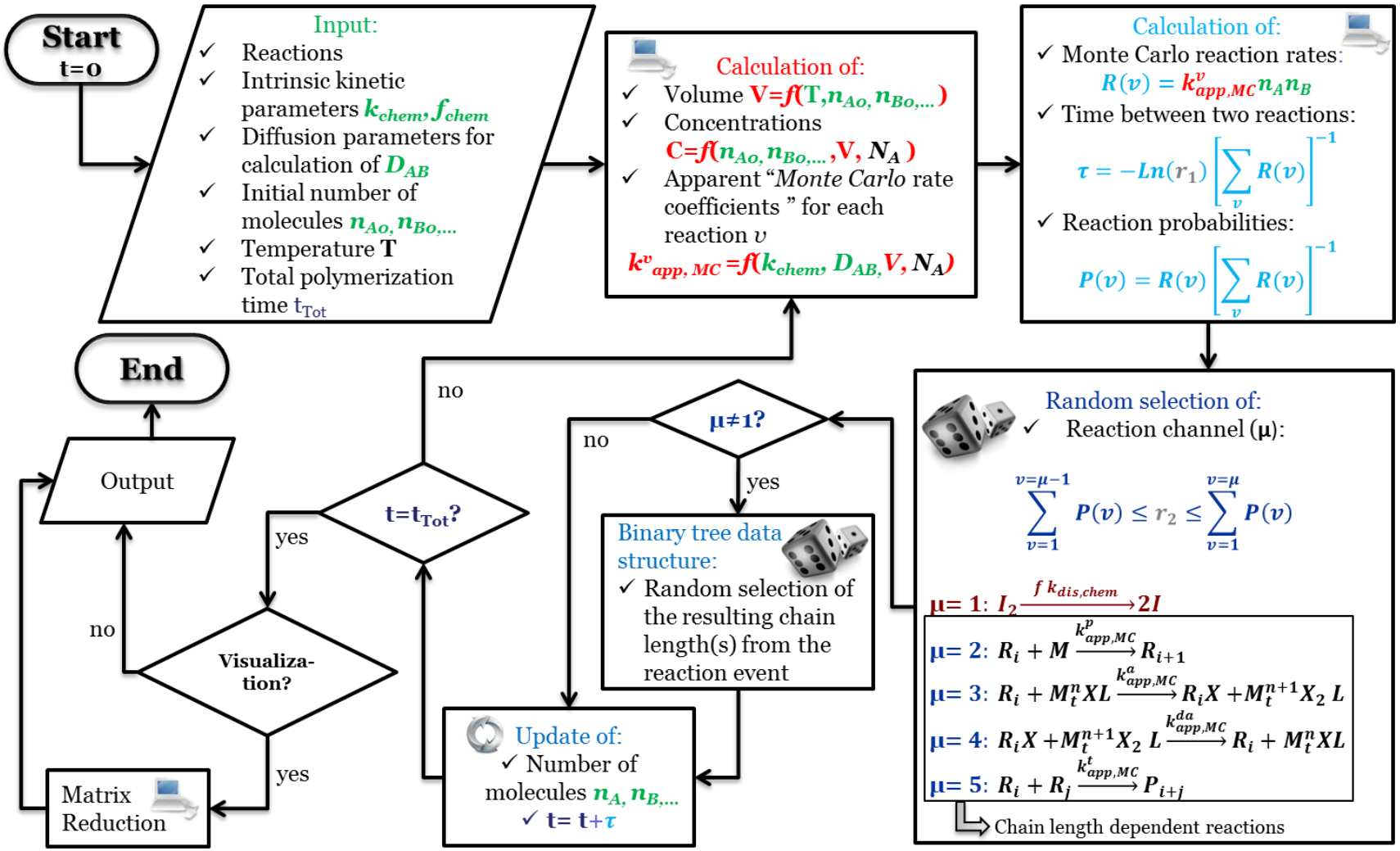

Figure G.1. Flowchart of the stochastic algorithm used in the kinetic Monte Carlo model; based on Gillespie[29] and Van Steenberge et al.[30, 31]

apparent rate coefficients are converted intto the apparent "Monte Carlo rate coefficient", i.e. depending on the molecularity of the reaction, as follows:

For unimolecular reactions: $k_{MC} = k_{app}$

For bimolecular reactions between distinguishable species: $k_{MC} = \frac{k_{app}}{V \cdot N_A}$

For bimolecular reactions between indistinguishable species: $k_{MC} = \frac{2 \cdot k_{app}}{V \cdot N_A}$

In order to calculate a reaction rate and its probability in a next step, the number of combinations of molecules h leading to that particular reaction is calculated as follows:

For unimolecular reactions: $h = n_A$

For bimolecular reactions between distinguishable species: $h = n_A n_B$

For bimolecular reactions between indistinguishable species: $h = \frac{n_A(n_A-1)}{2}$

The Monte Carlo rate R(v) (s^{-1}) of a reaction v is then calculated as:

$$R(v) = h \cdot k_{MC} \qquad \text{(G3)}$$

and represents the number of reaction events occurring per second in the volume V. This is done for every reaction ν. The calculation of the reaction rates is based on the reactions listed in Table 4.1 in Chapter 4.

For well-mixed reaction volumes, it has been proven[1,2] that the time τ between two reaction events (not necessarily of the same reaction) is exponentially distributed. A sample from this distribution can be calculated as follows:

$$\boldsymbol{\tau} = -Ln(r_1)\left[\sum_{v} R(v)\right]^{-1} \qquad \text{(G4)}$$

Where r_1 is a random number uniformly distributed between 0 and 1. Hence, if the simulation starts at t = 0, the time of the first event is given by τ. Note that the time between two reaction events (τ) decreases with the total MC reaction rate.

To determine which reaction is taking place at the selected time, the reaction rates are rescaled to obtain probabilities $P(v)$:

$$P(v) = R(v)\left[\sum_{v} R(v)\right]^{-1} \qquad \text{(G5)}$$

In case five reactions are considered, a typical distribution of reaction probabilities with respect to ν is depicted in Figure G.2 (left).

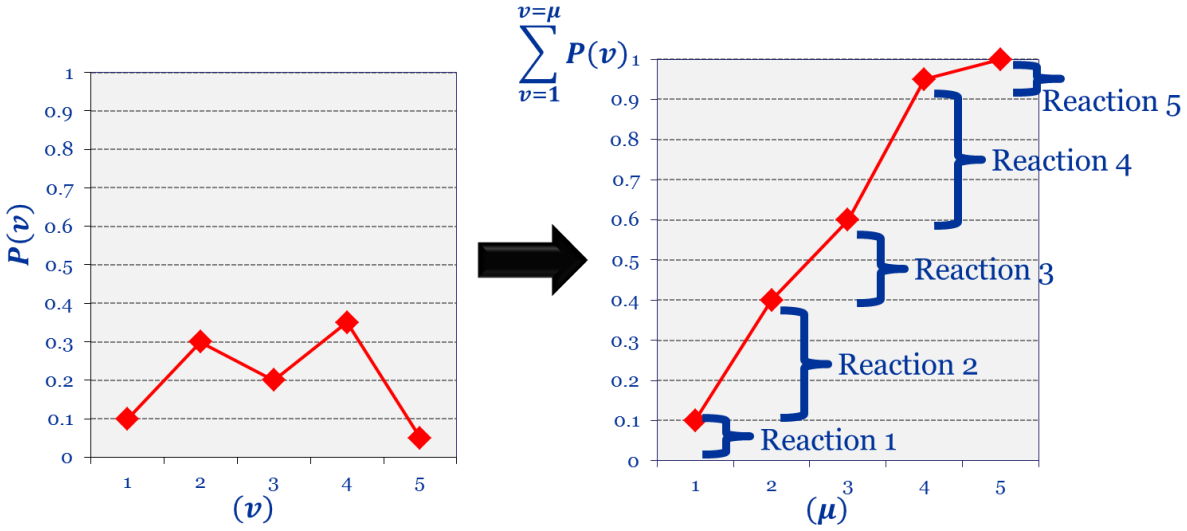

Figure G.2. Selection of reaction channel (μ) in the kinetic Monte Carlo algorithm; left: distribution of reaction probabilities: right: cumulative distribution of reaction probabilities.

Depending on the nature of the species involved in the reaction, i.e. chain length independent or chain length dependent two different methods are used to select a reaction based on these probabilities, respectively the "direct method" and the "logarithmic direct" method. These two methods are discussed in the next subsections.

G.1. Direct method for chain length independent reactions

The direct method is suitable for reactions between species which are not distributed, i.e. chain length independent reactions. According to the direct method, in order to sample a reaction event from $P(v)$ at a time t+τ, one option is to calculate the cumulative probability function $\sum_{v=1}^{v=\mu} P(v)$ (Figure G.2 (right)). If a random value (r_2) between 0 and 1 is chosen on the y-axis, the blue brackets indicate which reaction occurs. Thus, a value for v obtained by such approach is a sample originating from a stochastic variable with distribution $P(v)$. Hence, Figure G.2 illustrates the following criterion for the sampling of a reaction event:

$$\sum_{v=1}^{v=\mu-1} \boldsymbol{P(v)} \leq \boldsymbol{r_2} \leq \sum_{v=1}^{v=\mu} \boldsymbol{P(v)} \qquad \text{(G6)}$$

in which r_2 is a second random number also uniformly distributed between 0 and 1, μ is the number designating the reaction from which an event was sampled. Practically, μ is determined with a linear search on the cumulative reaction probability distribution (Equation G6).

Once the reaction event (μ) taking place at time t+τ is determined, the number of molecules related to that particular reaction are updated, e.g. for the dissociation reaction of conventional radical initiator $I_2 \xrightarrow{f\, k_{dis,chem}} 2I$

before the reaction event (μ=1): $n_{I2} = 10$ $n_I = 0$

after the reaction event (μ=1): $n_{I2} = 9$ $n_I = 2$

At this point, the first event has been finalized and the second event begins by updating the number of combinations of molecules h and recalculating the probabilities, the timestep τ, and so on. The stochastic simulation algorithm ends at predefined time ($t=t_{TOT}$) or when all reaction rates are 0.

G.2. Logarithmic direct method for chain length dependent reactions

If the reaction event to be sampled involves distributed species, such as polymer chains, binary searches using partial sums of probabilities (logarithmic method) are more suitable[4-5] than linear searches on the cumulative probabilities (direct method).

For example, consider recombination reactions between two macroradicals, in the logarithmic method a single overall recombination reaction rate is defined according to:

$$R(1) = k_{MC}^{tc} \cdot \frac{n_{Rtot} \cdot (n_{Rtot} - 1)}{2} \qquad \text{(G7)}$$

$$k_{MC}^{tc} = \frac{2 \cdot k_{app}^{tc}}{V \cdot N_A}$$

which is the total recombination rate of all the macroradicals. If this reaction channel is selected by the algorithm, then in an additional step two macroradicals should be sampled from a binary tree to calculate the resulting CLD of the macroradicals using their chain lengths. If the chain lengths of the recombining macroradicals are i and j, then the numbers of macroradicals of chain length i and j in the binary tree are decreased by unity. From the selected chain lengths of the two sampled (recombining) macroradicals, the number of dead polymers with a chain length $i + j$ is increased in a *new* binary tree for the dead polymer molecules. A similar approach is applied for the propagation, activation and deactivation chain length dependent reaction events.

Finally, after the conditions for ending the kinetic Monte Carlo algorithm are fulfilled, i.e. a predefined time is reached or all reaction rates equal to 0, an extra operation is performed in case the visualization of polymer chains is desired. In this additional operation, every n-th chain is selected from the representative kMC sample (e.g. 15000 chains, sufficiently large control volume) for visualization only (n=15 in this work) to generate a new matrix (e.g. 1000 chains). The order in which the chains are stored in the representative kMC sample is defined based on the formation of R_1 radicals, i.e. a radical is only stored in the matrix when it first propagates.

Appendix H: Synthetic schemes

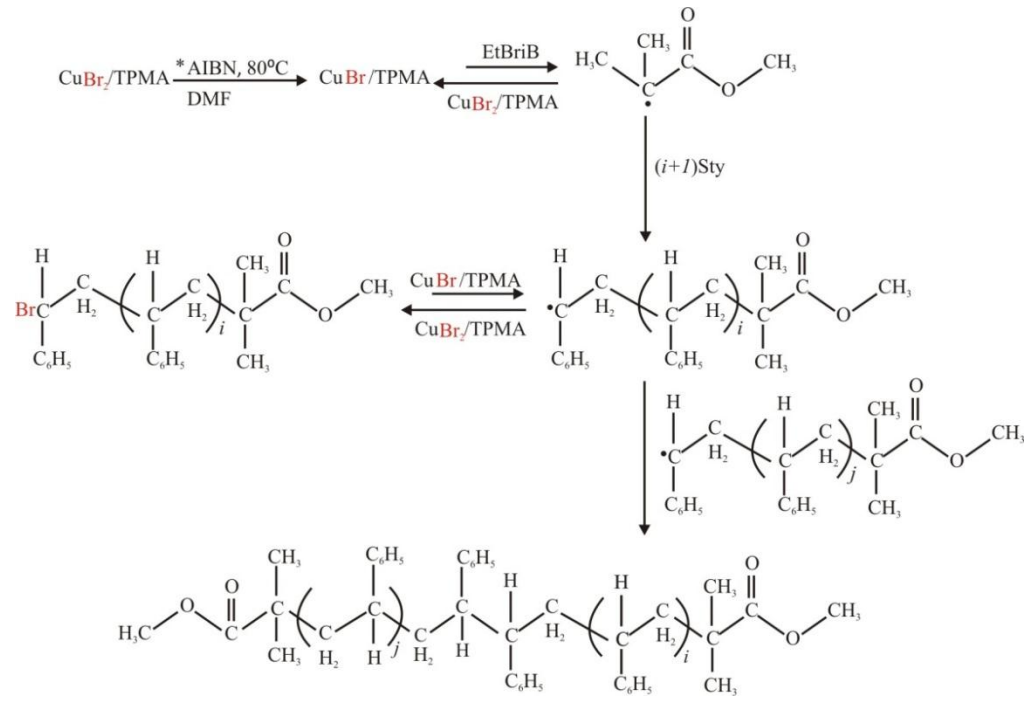

Figure H.1. General synthetic reaction scheme for the isothermal ICAR ATRP of styrene mediated by $CuBr_2$/TPMA with AIBN and EtBriB as conventional radical initiator and ATRP initiator; *the dissociation of the conventiona radical initiator is not shown.

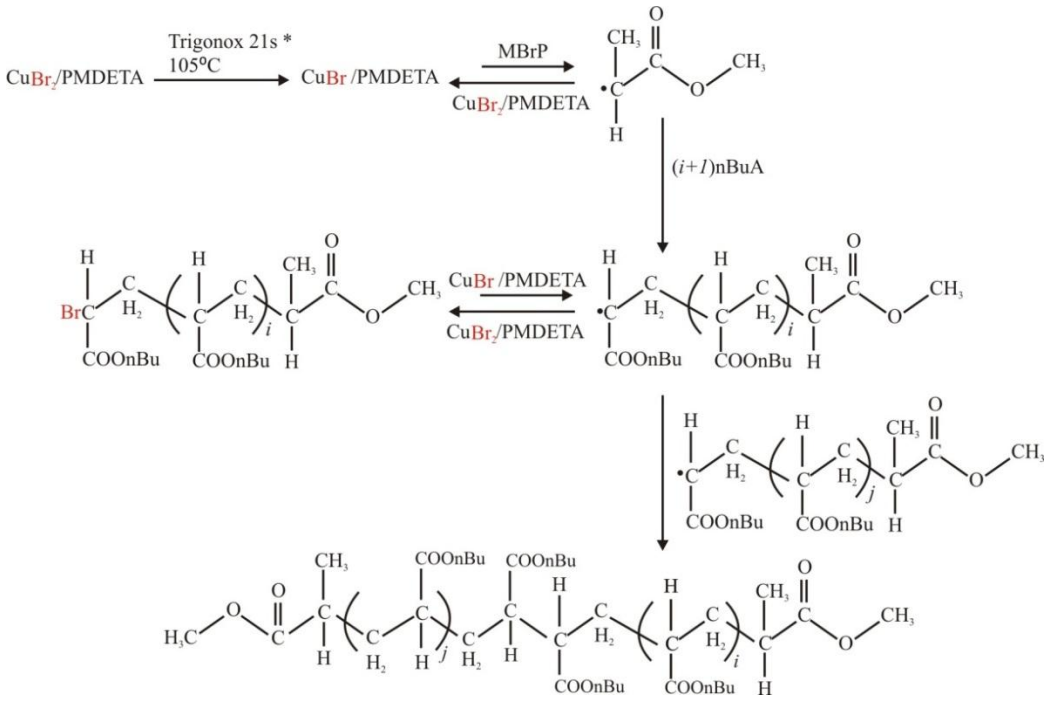

Figure H.2. General synthetic reaction scheme for the isothermal ICAR ATRP of *n*-butyl acrylate mediated by $CuBr_2$/PMDETA with *tert*-butyl peroxy-2-ethylhexanoate (Trigonox21s) and MBrP as conventional radical initiator and ATRP initiator respectively; *the dissociation of the conventiona radical initiator is not shown.

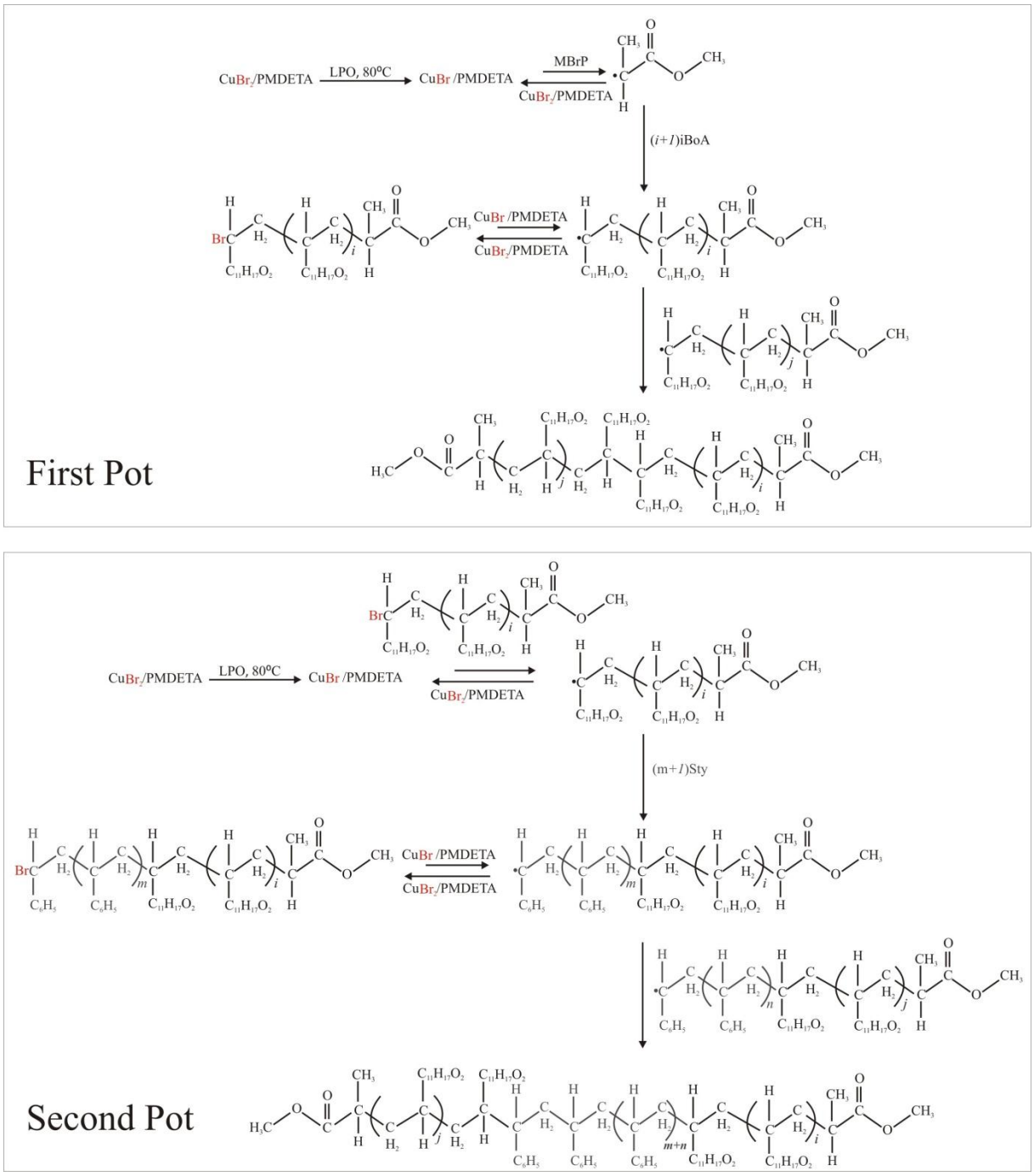

Figure H.3. General synthetic reaction scheme for the two-pot batch block copolymerization of isobornyl acrylate and styrene by ICAR ATRP mediated by $CuBr_2$/PMDETA with lauryl peroxide (LPO) MBrP as conventional radical initiator and ATRP initiator respectively; the resulting polymer from the first pot is employed in the second pot as a macroinitiator; *the dissociation of the conventiona radical initiator is not shown.

References

[1] J. B. L. de Kock; A. M. Van Herk; A. L. German, *J Macromol Sci Pol R* **2001,** *C41*, 199.

[2] D. R. D'Hooge; M. F. Reyniers; G. B. Marin, *Macromol React Eng* **2009,** *3*, 185.

[3] R. G. Gilbert, *Pure Appl Chem* **1992,** *64*, 1563.

[4] E. Vivaldolima; A. E. Hamielec; P. E. Wood, *Polym Reac Eng* **1994,** *2*, 17.

[5] J. Wieme; T. De Roo; G. B. Marin; G. J. Heynderickx, *Ind Eng Chem Res* **2007,** *46*, 1179.

[6] J. Wieme; D. R. D'Hooge; M. F. Reyniers; G. B. Marin, *Macromolecular Reaction Engineering* **2009,** *3*, 16-35.

[7] D. S. Achilias, *Macromol Theory Sim* **2007,** *16*, 319.

[8] M. Z. Smoluchowski, *Phys Chem* **1917,** *92*, 129.

[9] G. T. N. Russell, D. H.; Gilbert, R. G., *Macromolecules* **1998,** *21*, 2133.

[10] C. Barner-Kowollik; G. T. Russell, *Prog Polym Sci* **2009,** *34*, 1211.

[11] J. S. Vrentas; J. L. Duda, *J Pol Sci, Part B: Polym Phys* **1977,** *15*, 403.

[12] J. S. Vrentas; J. L. Duda, *J Pol Sci, Part B: Polym Phys* **1977,** *15*, 417.

[13] J. S. Vrentas; J. L. Duda; H. C. Ling, *J Pol Sci, Part B: Polym Phys* **1984,** *22*, 459.

[14] J. S. Vrentas; C. M. Vrentas, *E Polym J* **1998,** *34*, 797.

[15] J. S. Vrentas; C. M. Vrentas, *J Pol Sci, Part B: Polym Phys* **2003,** *41*, 501.

[16] D. R. D'Hooge; M. F. Reyniers; F. J. Stadler; B. Dervaux; C. Bailly; F. E. Du Prez; G. B. Marin, *Macromolecules* **2010,** *43*, 8766.

[17] S. Kobuchi; Y. Arai, *Prog Polym Sci* **2002,** *27*, 811.

[18] D. W. Van Krevelen, *Properties of Polymers*. Elsevier Science B.V.: Amsterdam, **1997**.

[19] W. Blitz, *IRaumchemie der Festen Stoffe*. Voss Leipzig, Berlin, **1934**.

[20] R. N. Haward, *J Macrom Sci Rev Maromol Chem* **1970,** *C 4*, 191.

[21] S. Sudgen, *J Chem Soc* **1927**, 1786.

[22] R. W. Y. Gallant, C. L. , *Physical Properties of hydrocarbons* Gulf Publishing: Houston, TX, **1993**.

[23] T. Yamaguchi; B. G. Wang; E. Matsuda; S. Suzuki; S. I. Nakao, *J Pol Sci, Part B: Polym Phys* **2003,** *41*, 1393.

[24] M. C. Griffiths; J. Strauch; M. J. Monteiro; R. G. Gilbert, *Macromolecules* **1998,** *31*, 7835.

[25] J. Barth; M. Buback; P. Hesse; T. Sergeeva, *Macromolecules* **2010,** *43*, 4023.

[26] A. N. Nikitin; R. A. Hutchinson, *Macromol Theory Sim* **2006,** *15*, 128.

[27] P. H. M. Van Steenberge; D. R. D'hooge; Y. Wang; M. Zhong; M.-F. Reyniers; D. Konkolewicz; K. Matyjaszewski; G. B. Marin, *Macromolecules* **2012**.

[28] L. R. Petzold, *SIAM, J Sci Stat Comp* **1983,** *4*, 136.

[29] D. T. Gillespie, *J Phys Chem* **1977,** *81*, 2340-2361.

[30] P. H. M. Van Steenberge; D. R. D'Hooge; Y. Wang; M. J. Zhong; M. F. Reyniers; D. Konkolewicz; K. Matyjaszewski; G. B. Marin, *Macromolecules* **2012,** *45*, 8519-8531.

[31] P. H. M. Van Steenberge; J. Vandenbergh; D. R. D'Hooge; M. F. Reyniers; P. J. Adriaensens; L. Lutsen; D. J. M. Vanderzande; G. B. Marin, *Macromolecules* **2011,** *44*, 8716-8726.

Glossary

Activation of dormant species

CRP specific reaction in which a radical center is formed.

Anionic living polymerization

a living polymerization technique involving an anionic propagating species and no termination.

Asymmetric block copolymer

block copolymer in which the length of each block is not identical.

Apparent rate coefficient

rate coefficient related to the observed kinetics, i.e. rate coefficient determined by the intrinsic chemical rate coefficient and transport phenomena.

Arrhenius coefficient

$k = A\ exp(-E_A/RT)$ with k the rate coefficient of the reaction step, R the universal gas constant, T the temperature, A the pre-exponential factor and E_A the Arrhenius activation energy.

Atom transfer radical polymerization (ATRP)

a polymerization technique allowing ’controlled’ polymer properties, i.e. a low value for the polydispersity index and a high livingness. ATRP is based on an atom transfer of the end-group functionality via a transition metal complex, i.e., the ATRP catalyst.

ATRP catalyst

a transition metal complex which is regenerated at the end of a closed reaction sequence during ATRP.

Backbiting

unimolecular reaction in which tipically a 1,5 hydrogen abstraction occurs leading to the formation of tertiary macroradicals.

βC-scission

unimolecular reaction in which a tertiary macroradical forms a macromonomer molecule and a propagating macroradical.

Block copolymer

a special kind of copolymer which are made up of blocks of different polymerized monomers.

Block deviation:

a deviation (with respect to the theoretical ideal block profile) of the cumulative monomer composition of a single chain.

Branch

defined for non-networked polymers; a linear part of a polymer chain formed by a branching reaction, such as transfer to polymer or backbiting.

Bulk polymerization

a copolymer performed in absence of solvent, i.e. in the presence of pure monomer.

Chain-growth polymerization

a polymerization technique where unsaturated monomer molecules add onto a limited number of active sites on growing polymer chains one at a time.

Chain length of a polymer molecule

the number of repeating units (coming from the (co)monomer(s)) in a polymer molecule.

Chain transfer

reaction leading to transfer of the radical center between two species.

Composite termination model

model to calculate apparent termination coefficients using power laws of which the powers are fitted based on controlled reversible addition fragmentation transfer polymerizations.

Comproportionation

a chemical reaction where two reactants, each containing the same element but with a different oxidation number, will form a product with an oxidation number intermediate of the two reactants.

Controlled radical polymerization

a polymerization technique in which the growth of the polymeric chains occurs in a controlled manner thanks to the presence of a mediating agent.

Coordination polymerization

a type of addition polymerization in which monomer adds to a growing macromolecule through an organometallic active center and an insertion mechanism.

Copolymerization

denoting the polymerization of multiple monomers. However, often the term is used to denote the polymerization of two monomers.

Deactivation of a radical

controlled specific reaction leading to incorporation of end-group functionality and the disappearance of a radical center.

Dead polymer molecule

polymer molecule without end-group functionality X

Diblock-like copolymers

a block copolymer which contains a gradient segment in the second block

Disproportionation

a specific type of redox reaction in which a species is simultaneously reduced and oxidized to form two different products; also used for termination in which an unsaturation is formed.

Dormant polymer molecule

polymer molecule possessing end-group functionality X.

Elementary reaction step

the irreducible act of reaction in which reactants are transformed into products directly, i.e., without passing through an intermediate that is susceptible to isolation.

End-group functionality

functional group allowing further chemical modification (mostly a halogen atom in atom transfer radical polymerization); part allowing livingness.

Glass transition temperature

a second-order phase transition through which a strong restriction of mobility of the polymer molecules is obtained. Below this temperature a glassy amorphous solid is obtained. Above this temperature a rubbery amorphous solid is obtained. Gradient copolymers are characterized by broad glass transition temperature range.

Gradient copolymer

mostly pertaining to linear polymer chains, denoting a gradual change in the monomer composition along the polymer chain.

Graft copolymer

a special type of branched copolymer in which the side chains are structurally distinct from the main chain.

Homo-polymer

a polymer composed of a single type of monomer.

Homo-termination

denoting the termination of similar species. For homopolymerization, it refers to an equal chain length of the recombining species. In the case of copolymerization of two monomers A and B, the termination between macroradicals ending in the same monomer unit is often termed “homo-termination”, as opposed to cross-termination denoting the termination a macroradical ending in A and a macroradical ending in B.

Ideal block copolymer chain

chain obtained by sampling from the probabilities dictated by the theoretical ideal block profile.

Kinetic Monte Carlo (kMC)

Monte Carlo method to simulate the time evolution of processes occurring in nature. The kMC method is essentially the same as the dynamic Monte Carlo method and the Gillespie algorithm, the difference is in terminology and application area. The kMC algorithm is also known as the residence-time algorithm, the *n*-fold way or the Bortz-Kalos-Lebowitz (BKL) algorithm.

Ligand

an ion or molecule that binds to a central metal atom to form a coordination complex.

Macroradical

polymer molecule possessing a radical center.

Mediating agent

a chemical compound able to trap macroradicals; also called controlling agent.

Microstructure

the entirety of structural characteristics of a polymer on the molecular level. They determine the morphological, rheological, thermal and physical properties of polymers.

Monomer conversion

monomer consumed with respect to initial amount.

Monomer sequence

A fixed-order series of monomers of arbitrary number and identity.

One-pot polymerization

a polymerization involving a single purification process. It implies that the two comonomers are coexisting at one point of the polymerization.

Overall conversion

in the one-pot approach, it refers to the conversion calculated with respect to the total amount of monomer that would be present if both monomers were added at the start of the polymerization.

Persistent radical effect

an effect in which the depletion of radicals by termination reactions increases the concentration of deactivator species therefore favoring the deactivation step.

Plasticity

refers to capability of a material to undergo deformation of shape in response to an applied force.

Polydispersity index

for polydispersity indices equal to unity, there is a unique chain length and the number, mass and z average chain length coincide. For polydispersity indices higher than unity, the polymer chains are distributed with respect to their chain length and the averages of the CLD do not coincide.

Polymer molecule

a molecule built from many monomer units.

Polymer strength

a mechanical property that quantifies how much stress the polymeric material will endure before suffering a permanent deformation.

Propagation of a radical

Reaction leading to chain growth, i.e. addition to monomer.

Rate coefficient

Coefficient of proportionality for the calculation of a reaction rate.

Reversible Addition Fragmentation chain Transfer-Chain Length Dependent-Termination (RAFT-CLD-T)'- technique

an accurate method for measuring apparent termination rate coefficients as a function of chain length and conversion using reversible addition-fragmentation chain transfer polymerization.

Segment

a monomer sequence consisting of a single type of monomer unit (either A or B but not both), also called a block.

Solution polymerization

a polymerization performed in the presence of solvent.

Star copolymer

a kind of copolymer consisting of several linear polymer chains connected at one point.

Stochastic process

as opposed to a deterministic process, describing a process which can only evolve in one way. In a stochastic process, there are several (often infinitely many) directions in which the process may evolve.

Symmetric block copolymer

block copolymer in which the length of each block is identical.

Targeted chain length

for ATRP it corresponds to the initial molar ratio of monomer to ATRP initiator

Termination of radicals

reaction leading to the formation of (a) dead polymer molecule(s) with the disappearance of two radical reactive centers.

Thermoplastic elastomer

a class of copolymers or a physical mix of polymers which consist of materials with both thermoplastic and elastomeric properties.

Topology

specifically for polymers, topology is closely related to polymer architecture and includes linear, short chain branched, long chain branched, networked, armed/star, brush, comb-like, grafted and dendritic polymers.

Triblock copolymer

a kind of copolymer containing three blocks ABA or BAB

Two-pot polymerization

a polymerization involving two purification steps and possibility different initial polymerization conditions, e.g. performed for block copolymerization